Process Intensification and Improvement of Functional Yield for Lentiviral Vectors

Michelle Yen Tran

Department of Bioengineering
McGill University, Montreal

March 2023

A thesis submitted to McGill University in partial fulfillment
of the requirements of the degree of Doctor of Philosophy

Table of Contents

Abstract

Lentiviral vectors (LVs) are a popular gene delivery tool in cell and gene therapy, mainly in *ex vivo* modifications and gaining traction in *in vivo* applications. Most notably, LVs are the primary tool for *ex vivo* transduction of T cells for expression of chimeric antigen receptor in CAR-T cell therapies, in which a patient's extracted T cells are modified to target and destroy cancer cells. Despite all the advancements in LV production over the last three decades, the persisting challenge is to produce sufficient vectors at large-scale to meet the demand for treatment beyond early clinical trials. An additional challenge is the inherently labile nature of LVs, as they are known to lose functionality throughout the production steps and process hold times, impairing their ability and efficiency in transferring genetic material to the patient's cells. As such, this work aims to implement process intensification strategies that contribute to producing sufficient LV material at large-scale while diminishing the loss of LV functionality.

Considerable efforts have been dedicated to improving the LV system and production. The review chapter highlights advances in vector design, upstream and downstream processing, as well as quantification methods to assess process efficiency and for product characterization. In fact, characterization poses an obstacle in the field, as existing analytical tools often have low throughput, low robustness, and high variability. To contribute to developing more robust tools, a high-performance liquid chromatography method for routine in-process monitoring is presented. Additionally, the gene transfer and digital droplet polymerase chain reaction assays to quantify functional and total vector particles, respectively, are optimized. Furthermore, the feasibility of qualitatively monitoring LV transduction effectiveness using confocal microscopy is illustrated.

Using a producer cell line that generates LVs with green fluorescent protein as the transgene, culturing parameters are explored at shake flask scale and the highest yielding conditions are implemented at bioreactor scale. Successful operations in perfusion mode for continuous harvesting of LVs using a scalable cell retention device with a 3L bioreactor is demonstrated, resulting in increased yield and improved quality. Next, a scalable capture step of the downstream process is investigated and implemented in a semi-continuous mode, resulting in reduced processing time and increased product recovery. In establishing an integrated semi-continuous process that connects the upstream to the downstream, process hold times are minimized and thus further contribute to maintaining a higher proportion of produced functional vector particles.

In conclusion, this work builds on analytical tools and establishes process intensification strategies that increase yield and improve product quality, advancing the large-scale manufacturing of LVs intended for gene delivery that can be applied to both *ex vivo* and *in vivo* applications.

Résumé

Les vecteurs lentiviraux (LVs) sont un outil populaire d'administration de gènes en thérapie cellulaire et génique, principalement pour les modifications *ex vivo* et qui gagne en popularité pour les applications *in vivo*. Plus particulièrement, les LVs sont le principal outil de transduction *ex vivo* des cellules T pour l'expression des récepteurs antigéniques chimériques dans les thérapies cellulaires CAR-T, dans lesquelles les cellules T extraites d'un patient sont modifiées pour cibler et détruire des cellules cancéreuses. Malgré tous les progrès réalisés dans la production de LV au cours des trois dernières décennies, le défi persistant est de produire suffisamment de vecteurs à grande échelle pour répondre à la demande de traitement au-delà des premiers essais cliniques. Un autre défi est la nature intrinsèquement labile des LVs, qui sont connus pour perdre leur fonctionnalité au cours des étapes de production et des délais de maintien du processus, ce qui nuit à leur capacité et à leur efficacité à transférer du matériel génétique aux cellules du patient. En tant que tel, ce travail vise à mettre en œuvre des stratégies d'intensification de procédés qui contribuent à produire suffisamment de matériel de LVs à grande échelle tout en diminuant la perte de fonctionnalité des LVs.

Des efforts considérables ont été consacrés à l'amélioration du système et du production de LVs. Le chapitre d'introduction souligne les progrès réalisés dans la conception des vecteurs, le traitement en amont et en aval, ainsi que les méthodes de quantification permettant d'évaluer l'efficacité du processus et de caractériser le produit. En fait, la caractérisation constitue un obstacle dans le domaine, car les outils analytiques existants ont souvent un faible débit, une faible robustesse, et une grande variabilité. Pour contribuer au développement d'outils plus robustes, une méthode de chromatographie liquide à haute performance pour le suivi de routine en cours de développement de procédés est présentée. En outre, les essais de quantification de transfert de gènes et de réaction en chaîne par polymérase en gouttelettes digitalisées pour quantifier les particules virales fonctionnelles et totales, respectivement, sont optimisés. De plus, la faisabilité d'un suivi qualitatif du processus de transduction des LVs à l'aide de la microscopie confocale est illustrée.

En utilisant une lignée cellulaire productrice qui génère des LVs avec une protéine fluorescente verte comme transgène, les paramètres de culture sont explorés à l'échelle de flacon de cultures cellulaires et les conditions produisant les rendements les plus élevées sont mises en œuvre à l'échelle de bioréacteurs. Le succès des opérations en mode perfusion pour la récolte

continue des LVs en utilisant un dispositif de rétention cellulaire évolutif avec un bioréacteur de 3L est démontré, ce qui entraîne un rendement accru et une meilleure qualité du produit final. Ensuite, une étape de capture évolutive pour le traitement en aval est étudiée et la mettons en œuvre dans un mode d'opération semi-continu. En établissant un processus semi-continu intégré qui relie les opérations en amont à en aval, les délais de réalisation du procédé sont réduits et en conséquence, contribuent ainsi à maintenir une proportion plus élevée de particules vectorielles fonctionnelles.

En conclusion, ce travail s'appuie sur des outils analytiques et établit des stratégies d'intensification de procédés qui augmentent le rendement et améliorent la qualité du produit final, faisant ainsi progresser la fabrication à grande échelle de LVs destinés à l'administration de gènes et pouvant être utilisés pour des applications *ex vivo* et *in vivo*.

Acknowledgements

I am extremely grateful to be writing these words nearing the end of my experience as a graduate student. The last five years have been a significant period of growth and development for me, both as a scientist-engineer and as a person. I had suspected that grad school would be difficult, but I had not expected it to challenge me beyond the academic context. I am leaving the program as a more well-rounded person and I have many people to thank for helping me along this journey.

First and foremost, I would like to express my sincerest gratitude to my angel of a supervisor and mentor, Dr. Amine Kamen. Thank you for welcoming me to your team, for challenging me with this project, for your unwavering support, and for offering me grace through my rough phases. It has been a privilege to be trained by you; I have learned to think about the big picture, to question the value of the work, and to strategize mitigation plans. I have always been able to count on your expertise in the field and your feedback, even when it is on short notice since I still have not managed to let go of all my perfectionistic tendencies and often need more time than I think. Your dedication towards helping patients worldwide is an inspiration and it encourages me to apply my training and knowledge in the field after graduating to make a difference. You have been a great role model and I really could not have asked for a better mentor.

Next, I would like to thank the people that made my research possible. Dr. Aziza Manceur, thank you for your work with the producer cell line, it became the springboard for my work and allowed me to move quickly to implementing my experiments. Julia Transfiguration, thank you for the opportunity to collaborate on the HPLC work, which led to our co-authored manuscript that is included in my thesis. Dr. Phil Yuen, Dr. Michael Bransby, and Dr. Rene Gantier from Repligen, thank you for lending me the TFDF system and supplying consumables as well as providing me support during the perfusion runs and some feedback during the manuscript writing process for my upstream work. Dr. Angel Varela-Rohena from Cytiva, thank you for providing me the prototype media to support my perfusion runs during the period of media shortage caused by the pandemic, which allowed me to move forward with my experiments without further delays. Dr. Shantoshini Dash, thank you for your expertise and collaboration, the microscopy project would not have come to fruition without your help. Dr. Zeyu Yang, thank you for your help with executing the semi-continuous downstream runs and general discussion during that time. Dr. Alina Venereo-Sanchez, thank you for the discussions and guidance during the experiments for my perfusion manuscript, and especially for believing in me and encouraging me to finish the Ph.D.

I would also like to thank Dr. J. Matt Kinsella and Dr. Gergely Lukacs for being my Ph.D. thesis advisory committee members. Thank you for your guidance and support over the years. One of the things I learned from being a graduate student is how to receive feedback gracefully. Thank you for your patience as I worked through my defensiveness in responding to questions.

I would like to thank Dr. Adam Hendricks for allowing me to use his team's microscope as well as Dr. Abdullah Chaudhary and Dr. Linda Balabanian for their help when I was trying to embark on the microscopy project on my own. I would like to thank Dr. Dan Nicolau for allowing Dr. Shantoshini Dash to use his team's microscope to help me with my work. I am also grateful for the access to UQAM facilities. I would like to thank all faculty and staff from the Department of Bioengineering and the Department of Biomedical Engineering, especially Pina Sorrini, who kept track of my milestones and cheered me on every step of the way.

My research would not have been possible without the financial support provided by Fonds de recherche du Québec Nature et technologies (FRQNT), McGill Engineering Doctoral Award (MEDA), and Graduate Excellence Fellowship (GEF) from the Bioengineering Department.

To the Kamen lab, thank you for all the memories and support throughout the years. The friendships that were made and maintained from what I consider the first cohort in the lab – Dr. Aline Do Minh, Dr. Sascha Kiesslich, Dr. David Sharon, Dr. Alina Venereo-Sanchez, and Dr. Omar Farnós. I will never forget the fun we had at the conference held at Mont Tremblant and our regular *cinq-à sept* gatherings. The lab dynamics changed over the many long months of pandemic lockdowns, with minimized in-person interactions and colleagues graduating from the program, but I was glad to find a new cohort for camaraderie and support towards the end of my Ph.D. The self-proclaimed perfusion girls, Julia Fulber and Cristina Silva, I am so grateful for the sanity checks during those long perfusion bioreactor runs, and also the "cats and tea" hangouts that blossomed into meaningful and loving friendships. Pablo Moço, I really relied on you during my last push with the Ph.D., thank you for solving many of my problems, from small favors in the lab to more catastrophic problems such as acquiring the data analysis software. Julia, Cristina, and Pablo, you guys were my pillars of support during the thesis writing and oral defense prepping stages, I really could not have done it without you. Xingge Xu and Sean Nesdoly, thank you for your kindness, encouragement, and thoughtful feedback. Barbara Paes, the functioning of our lab has improved tremendously with your presence, thank you for being our lab mother and being our voice of reason when we fall into rabbit holes. It has been a pleasure working and being with all members from the lab, past and present, thank you all for making an unforgettable mark in my life.

I am grateful to have worked with everyone who served on the BBME Student Society council from years 2018 through 2021, especially Michael Yitayew and Molly Shen (my favorite M&Ms) who were my pillars of strength as we supported our peers during the thick of the coronavirus pandemic.

I am incredibly lucky to have developed so many friendships in Montreal over the years. A big thank you to everyone who have supported me throughout different seasons of life – Molly Shen, Jackie Kort Mascort, Julia Fulber, Michael Yitayew, Caitlin Fowler, Victoria Madge, Cristina Silva, Carolina del Real Mata, Kyle Kavaseri, Léah Pollet, Pouria Tirgar. Also, an enormous thank you to the lifelong friends, who became my chosen family, that kept rooting for me from afar – Kelly Pratt, Sophia Li, Yeangshin Phay, Patrick Li, Andy Tran, Neressa D'Souza. I am grateful for Tila Wei, my confidante and dearest friend of nineteen years, for celebrating with me through the good times and comforting me through the rough times. I am grateful for my big sister Celine, who is also one of my best friends, for always showering me with love and sending me home with huge amounts of food when I visit her in Ottawa. I am also grateful for my other big sister Nina for loving me from the moment I was born and for raising me like her own child. Last, but not least, I would like to express my deepest gratitude for my spouse Pier-Luc Journault. Thank you, from the bottom of my heart, for your immense love, care, and support in the past two years, especially during the challenging and long thesis writing process.

Contribution to Original Knowledge

In respect to the optimization of analytical methods to support the quality assessment of LVs, there are several contributions to original knowledge. First is the optimization of the gene transfer assay (GTA), which is a cell-based analytical method that measures the transgene expression of LVs in transduced host cells to report the functional vector titer. The assay was successfully adapted to and optimized for suspension HEK293SF cells in a 24-well plate format. Building on an assay that traditionally uses adherent cells, the optimization increased assay throughput by using 5-fold higher cell density, eliminating the cell attachment and detachment steps, and cutting down the assay preparation and incubation times significantly. In my literature search and in discussions with colleagues and collaborators, I have only observed the use of adherent cells for this assay. Disseminating the knowledge gained on the optimization of this assay can help others in the field to simplify their analytical workload, which leads to accelerating the time of process development.

Second is the optimization of the droplet digital polymerase chain reaction (ddPCR) assay, which is a newer technique of PCR that is used as a physical-based direct method that quantifies the viral genome in LV samples to report total vector titer. Although the ddPCR is more robust and has higher throughput than the gold standard qPCR, it was observed that the additional sample preparations, RNA extraction and cDNA synthesis, before executing the ddPCR pose as sources of variability. Through investigating and troubleshooting, it was determined that the amount of RNA used in cDNA synthesis has an effect on the viral genome titer obtained from the ddPCR. This important finding led to the establishment of a normalization step to target the same amount of RNA used in cDNA synthesis to minimize assay variability and increase confidence in making comparisons between samples. To the best of my knowledge, this phenomenon has not been reported in the literature, especially since the ddPCR is a newer method used only in the recent years. Both of these optimized protocols are included in the published manuscript enclosed in Chapter 4.

Third is the collaborative work with the National Research Council of Canada on validating a high-throughput and robust physico-chemical characterization method that directly assesses total vector particles, as presented in the published manuscript enclosed in Chapter 3. This high-performance liquid chromatography (HPLC) method is suitable for all in-process samples from LV supernatants to final purified products, which is ideal for routine in-process monitoring of LV

quality. With simple sample preparation and fast elution time, this method is extremely useful in accelerating the development of LV processes. In addition, the HPLC has the potential to be an in-line monitoring method that can be implemented at large-scale and eventually support the realization of integrated continuous manufacturing. While the method itself was developed by my collaborators, my contribution includes analyzing samples with my optimized ddPCR method, interpreting and synthesizing all assay results to draw critical conclusions, and elucidating certain nontrivial topics that reinforced the discussion. Ultimately, I played a large role in publishing this method, which has the potential to make an impact on the large-scale manufacturing of LVs.

Fourth is the in-vitro validation of the product quality of the Mustang Q purified LV using confocal microscopy to view the LV transduction process in HEK293SF cells, as presented in the submitted manuscript enclosed in Chapter 5. This adds value to the field by demonstrating the feasibility of leveraging imaging techniques as additional analytical tools for assessing the quality of LVs.

In respect to the improvement of LV productivity through process intensification of the upstream process, the contribution to original knowledge is the successful demonstration of a scalable technology that can be used as a cell retention device that does not retain the product in perfusion mode for LV production, as presented in the published manuscript enclosed in Chapter 4. This adds tremendous value to the field since enveloped viruses tend to stick to available commercial cell retention devices or the device is not scalable. In addition, using a producer cell line for my development work contributes to the efforts of shifting to a more scalable, reproducible, and robust method for producing LVs as the field is progressing towards large-scale manufacturing. Furthermore, investigating a producer cell line that has been previously tested with another cell retention device allows for a direct comparison between the two technologies, since typically the production and bioprocessing steps can differ based on the cell line or the LV transgene.

In respect to the improvement of LV functional yield through integrated semi-continuous manufacturing, there are two contributions to original knowledge, as presented in the submitted manuscript enclosed in Chapter 5. First is the implementation of the first few steps of a downstream process in semi-continuous mode. By combining the clarification and loading of the capture step as well as operating those steps in parallel to the purification of the capture step expedite the processing time greatly as compared to processing the same volume in batch mode. In addition, loading the capture membranes in series in this semi-continuous operation improves the LV

product recovery. Second is the demonstration of integrating the upstream to the downstream, showing a substantial reduction in the total processing time and an improvement in LV product recovery. This adds tremendous value to the field by demonstrating the feasibility and practicality of implementing an integrated process in a semi-continuous manner that is advantageous in addressing the instability of LVs.

Contribution of Authors

This thesis consists of three manuscripts – two published (Chapters 3 and 4) and one submitted for publication (Chapter 5). I am the co-first author of the first manuscript and the first author of the last two manuscripts. The contributions of authors to each manuscript are listed below.

Chapter 3: **Rapid In-Process Monitoring of Lentiviral Vector Particles by High-Performance Liquid Chromatography**

Published in: *Molecular Therapy – Methods & Clinical Development* 2020, 18 (Cell Press)

Authors: Julia Transfiguracion, **Michelle Yen Tran**, Stéphane Lanthier, Sonia Tremblay, Nathalie Coulombe, Mauro Acchione, and Amine A. Kamen

Contributions: JT and **MYT** contributed equally (co-first authors). Conceptualization, JT, **MYT**, and AAK.; Methodology, JT, **MYT**, SL, ST, and NC; Execution, JT, **MYT**, SL, ST, and NC; Writing – Original Draft, JT and **MYT**; Writing – Review & Editing, JT, **MYT**, MA, and AAK; Funding Acquisition & Resources, MA and AAK.

Contribution details: The High-Performance Liquid Chromatography (HPLC) method was developed by Julia Transfiguration. Lentiviral vector production and purification as well as all analytical assays *except* for the droplet digital polymerase chain reaction (ddPCR) were completed by Julia and the other authors or arranged by them to be outsourced. The ddPCR assay was optimized and executed by Michelle Yen Tran. A preliminary draft with the abstract, introduction, materials and methods (except for ddPCR), and results sections was written by Julia. Michelle wrote the discussion and conclusion sections as well as worked heavily on transforming and fine-tuning the preliminary draft into a manuscript suitable for submission to the journal. Michelle's notable contributions were interpreting and synthesizing assay results to draw critical conclusions, generating charts for Figures 10 and 11, elucidating certain nontrivial topics that reinforced the discussion, addressing reviewer comments, most of the editing, and preparing the manuscript from the initial submission to the final publication stages.

Chapter 4:	**Production of Lentiviral Vectors Using a HEK-293 Producer Cell Line and Advanced Perfusion Processing**
Published in:	*Frontiers in Bioengineering and Biotechnology – Bioprocess Engineering* 2022, 10 (Frontiers)
Authors:	**Michelle Yen Tran** and Amine A. Kamen
Contributions:	Conceptualization, **MYT** and AAK; Methodology, **MYT**; Execution, **MYT**, Writing – Original Draft, **MYT**; Writing – Review & Editing, **MYT** and AAK; Funding Acquisition & Resources, **MYT** and AAK.

Chapter 5:	**Integrated Semi-Continuous Manufacturing of Lentiviral Vectors Using a HEK-293 Producer Cell Line**
Submitted to:	*Molecular Therapy – Methods & Clinical Development* (Cell Press)
Authors:	**Michelle Yen Tran**, Shantoshini Dash, Zeyu Yang, and Amine A. Kamen
Contributions:	Conceptualization, **MYT** and AAK; Methodology, **MYT**; Execution, **MYT**, SD, and ZY; Writing – Original Draft, **MYT**; Writing – Review & Editing, **MYT** and AAK; Funding Acquisition & Resources, AAK.
Contribution details:	Shantoshini Dash executed the microscopy experiments and analyzed the images presented in this manuscript. Zeyu Yang helped Michelle Yen Tran with the execution of semi-continuous downstream operations.

List of Figures and Tables

List of Abbreviations

CAR-T	chimeric antigen receptor T
Clone 92	stable producer cell line HEK293SF-LVP-CMVGFPq-92
CV	coefficient of variation
ddPCR	droplet digital polymerase chain reaction
DNA	deoxyribonucleic acid
dpi	days post induction
DSP	downstream processing
ELISA	enzyme-linked immunosorbent assay
EQ	equilibration
FR	flowrate
FT	flowthrough
GFP	fluorescent green protein
GMP	good manufacturing practice
GTA	gene transfer assay
HCD	high cell density
HEK293SF	serum free suspension Human Embryonic Kidney-293 cells
HIV	human immunodeficiency virus
hpi	hours post induction
HPLC	high-performance liquid chromatography
LCD	low cell density
LVs	lentiviral vectors
MV	membrane volume
PAT	process analytical technology
PBS	phosphate buffered saline
PCR	polymerase chain reaction
qPCR	quantitative polymerase chain reaction
RNA	ribonucleic acid
RPM	revolutions per minute
SC	sucrose cushion
SC LV	sucrose cushion purified LV
TFDF	Tangential Flow Depth Filtration

TFF	tangential flow filtration
TFP	total functional particles
TOI	time of induction
TU	transducing units
TVP	total vector particles
TVP/TFP	ratio of total vector particles to total functional particles
USP	upstream processing
Vg	vector (or viral) genome units
VSV-G	vesicular stomatitis virus glycoprotein
VVD	vessel volume per day
WPRE	woodchuck hepatitis virus posttranscriptional regulatory element

Chapter 1: Introduction

Background

Cancer is the leading cause of death worldwide, responsible for almost 10 million deaths and account for one in six deaths in 2020 (World Health Organization, 2022). The global cancer burden is expected to rise 47% between 2020 and 2040, bringing the number of projected cases to 28.4 million in 2040 (Sung et al, 2021). Traditional cancer treatments include surgery, chemotherapy, and radiation therapy. Since the 2000s, targeted therapies that kill cancer cells by detecting specific molecular changes became an additional tool for cancer treatment. In the past decade, a new technique called immunotherapy emerged, where the patient's immune system is recruited to attack the tumors. An example of immunotherapy is a type of drugs known as immune checkpoint inhibitors. The checkpoints refer to proteins that are made by immune cells, such as T cells, and some cancer cells that prevent huge immune responses, which sometimes can keep the T cells from killing the cancer cells. (National Cancer Institute, 2022, CAR T Cells)

CAR-T cell therapy is another form of immunotherapy that has received a lot of attention in the past five years. Typically, CAR-T cell therapy is employed when the cancer has not been responding to other types of cancer therapy. In this type of therapy, T cells are modified in the laboratory to make a type of protein known as CAR (chimeric antigen receptor) that binds to a certain protein on the surface of the patient's cancer cells, which improves the ability of the T cells to attack the cancer cells. (National Cancer Institute, 2022, T-Cell Transfer Therapy) The receptors are chimeric since they combine both antigen-binding and T cell activating functions into a single receptor. Lentiviral vectors (LVs) are the primary tool for the *ex vivo* transduction of T cells for this therapy. Prior to the transduction, T cells are extracted from the patient and LVs are produced in the laboratory to carry a gene of interest. During the transduction, the LVs add the gene of interest to the T cells to be integrated for the expression of the special receptor. Then, the T cells are re-infused into the patient for treatment. (Castella et al., 2020)

There are six CAR-T cell therapies approved by the Food and Drug Administration for treatment of blood cancers such as lymphoma, some forms of leukemia, and multiple myeloma (OHSU Knight Cancer Institute, 2022). The first approval was Kymriah in August 2017 and the most recent approval was Carvykti in February 2022. There are currently 90 CAR-T cell trials that utilize LVs as the gene delivery tool. Overall, there are 4673 LV clinical trials as well as significant

ongoing research activities using LVs for treatments for various conditions that are steadily progressing toward clinical applications. (ClinicalTrials.gov, accessed on 13 December 2022)

Rationale

With the current state of LV production, although the amount of produced vectors is adequate to support early phase clinical trials that enroll between a few dozens to under a hundred patients, manufacturing sufficient vectors at large scale to support later phase clinical trials of several hundred patients, as well as prolonged treatments, remains to be a huge challenge (Milone and O'Doherty 2018; Ansorge et al., 2010; Escors et al., 2012). The number of LVs required to effectively modify T cells is especially high, in part due to the fact that only a small percentage of the total LVs produced is functional. The LV's functionality refers to its ability and efficiency in transferring the genetic material to the patient's cells to be integrated into the host cell genome. The rest of the produced LVs is comprised of other populations, such as defective or low-transferring vectors (Do Minh et al., 2021), which renders dosing for treatment inefficient. In the field, it is well known that LVs are unstable, and the produced functional vectors are diminished throughout the production process (Ansorge et al., 2010; McCarron et al., 2016).

Furthermore, another challenge lies in the analytical tools required to assess the quality of the produced LVs. Extensive process and product characterization are required in manufacturing virus-based gene vectors in a good manufacturing practice (GMP) environment to better control batch-to-batch variability and to develop a product suitable for human use (McCarron et al., 2016). However, it has been an on-going challenge to make accurate assessments of LV product quality since different analytical tools provide only pieces of information, characterization methods often have low throughput and robustness, and standardized methods do not exist.

Hypothesis and Objectives

The two challenges that I am interested in examining are increasing the LV product yield to support the treatment of patients beyond early phase clinical trials and improving the LV functional yield by mitigating their instability throughout the production process. Specifically, I am most interested in investigating practical and scalable methods that can be implemented at large-scale manufacturing in the context of mass production of LVs. The hypothesis of my thesis is that an integrated semi-continuous manufacturing process can increase LV production and improve functional yield for LVs by slowing down the loss of functionality that is typically caused

during processing times and process hold times of the production and purification processes. To support my investigations, I also contribute to optimizing analytical methods for making assessment of LV product quality.

Based on this, the three main research objectives of my Ph.D. thesis are to 1) optimize analytical methods to support the quality assessment of LVs, 2) improve LV productivity through process intensification of the upstream process, and 3) improve LV functional yield through integrated semi-continuous manufacturing.

Chapter 2: Literature Review

Gene and Cell Therapy

Gene transfer became an area of interest starting in the 1970s. The retroviral system was the most promising since gamma-retroviral vectors showed a low extent of gene transfer into hematopoietic stem cells. The major breakthrough clinical trial conducted in 2000 using retroviral vectors based on the mouse leukemia virus corrected X-linked severe combined immunodeficiency in children. However, a large number of the children developed leukemia due to insertional mutagenesis (Escors et al., 2012). Retroviral vectors tend to insert their transgenes near oncogene promoters, which in the event of gene mis-regulation could cause normal cells to become cancerous (Wu et al., 2003). In search of a better viral system to overcome oncogenic development, researchers turned to optimizing the human immunodeficiency virus for gene and cell therapy, which serves as a backbone to lentiviral vectors.

Lentiviral vectors (LVs) are from the family *Retroviridae*. Like retroviral vectors, LVs offer high transduction efficiency, can stably integrate their genome into the host cell's chromosome, and provide long-term transgene expression. An advantage that LVs has over retroviral vectors is the ability to transduce non-dividing cells in addition to dividing cells. LVs can deliver large amounts of genetic information, around 10 kb, into host cell DNA and they have low mutagenicity as compared to other viral systems (Escors et al., 2012; Sharon and Kamen, 2018). For example, LVs have a random integration profile, where they prefer to integrate the genetic material into actively transcribed genes as opposed to the preference for integration around transcription start sites like retroviral vectors (Mitchell et al., 2004).

Due to the advantages that LVs offer, they quickly became a popular gene delivery tool to treat diseases, as supported by a review by Arabi et al. (2022) that reported the makeup of viral and non-viral vectors in gene therapy clinical trials conducted from 2010 to 2020. Figure 1A shows that LVs, adenovirus, adeno-associated virus (AAV), and retrovirus are the most commonly used viral vectors in these clinical trials. Figure 1B shows that there has been a significant increase in the use of LVs, adenovirus, and AAVs in the 10 year span of the review, with a heavy uptrend of LVs especially due to their use in the *ex vivo* transduction of T-cells for expression of chimeric antigen receptor in CAR-T cell therapies. While LVs dominate the *ex vivo* applications, adenoviral vectors are known for their use as oncolytic viruses and viral vaccines, and AAVs are promising candidates for *in vivo* applications. Figure 1A also shows other viral vectors that are less frequently

used, such as herpes simplex virus (HSV), vaccinia, vesicular stomatitis virus (VSV), measles virus, and poxvirus.

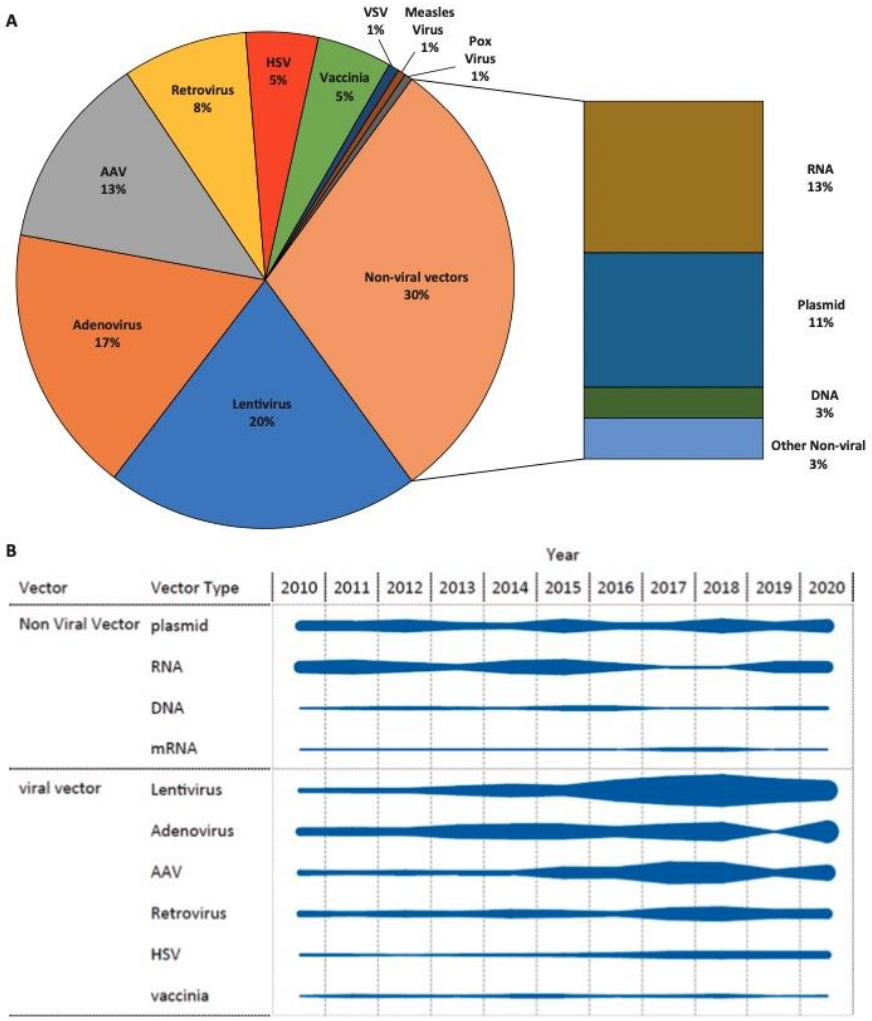

Figure 1. Viral and non-viral vectors used in gene therapy clinical trials conducted from 2010 to 2020. (A) Percentage of clinical trials for each viral and non-viral vector. (B) Time trend of clinical trials using different viral and non-viral vector. (Arabi et al., 2022)

LVs are approximately 80 to 100 nm in diameter and their genome consists of two copies of positive-sense single-stranded RNA inside a conical capsid, which is surrounded by a lipid bilayer (Tolmachov et al., 2011). The capsid also contains viral reverse transcriptase, integrase, and other viral enzymes. The lipid envelope contains protruding viral glycoproteins that determine tropism. Some examples of lentiviruses are human (HIV), simian (SIV), feline (FIV), and equine infectious anemia (EIAV) immunodeficiency viruses and the most widely used LVs are derived from the HIV-1 virus. It is important to note that viral vectors used for gene delivery are non-replicating, especially in the case of LVs. After the LV enters the cell, it will go through reverse transcription and integration, but it will stop after mRNA synthesis because it does not have the

necessary genes to assemble a new virus for a subsequent infection. The term "transduction" is used, as opposed to "infection," to describe the delivery of genetic material through the introduction of recombinant viral vector particles to the host cell for integration to eventually express the transgene. While LVs are also used for *in vivo* applications and vaccines, this Ph.D. thesis focuses on their use in *ex vivo* applications, specifically for gene delivery in CAR-T cell therapies.

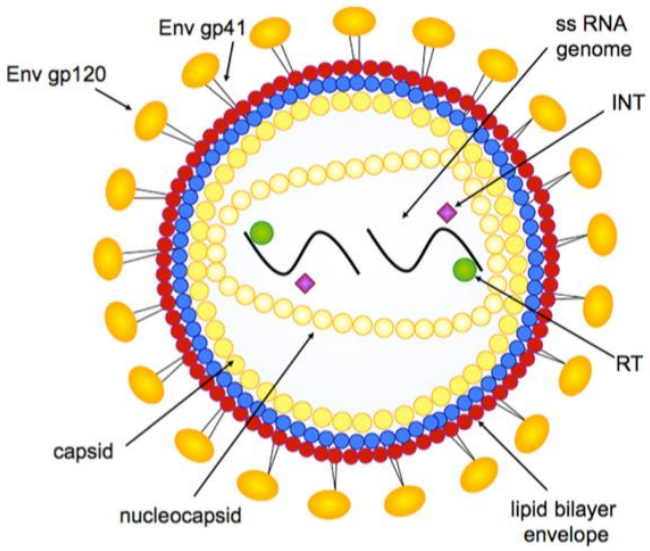

Figure 2: Schematic representation of an HIV-1 virus. (Escors et al., 2012)

Lentiviral Vector System and Envelope Protein

The third generation of LVs is currently the most widely used system because it provides the most biosafety features. It does not include any viral accessory genes (*vif*, *vpr*, *vpu*, and *nef*) and essential genes are separated into four different plasmids, which means that four recombination events would be necessary to constitute a replication-competent lentivirus (RCL). The two regulatory genes *tat* and *rev*, which are included in the same plasmid in the first and second generation of LV systems, are treated differently in the third generation. *Tat*, a positive regulator of transcription, is omitted to further ensure biosafety. Since the HIV promoter in the 5' long terminal repeat (LTR) depends on *tat*, this wildtype promoter is replaced with a constitutively active promoter sequence such as cytomegalovirus (CMV) or Rous sarcoma virus (RSV) plus an optional enhancer or an inducible/repressible promoter sequence (Merten et al., 2016). *Rev*, a gene important for synthesis of major viral proteins and essential for viral replication, is included in one of the two packaging plasmids.

The other packaging plasmid includes *gag-pol*, which encodes for structural proteins and viral enzymes. The transfer vector plasmid includes the genetic material of interest and consists of the LV backbone containing the transgene expression cassette flanked by *cis*-acting elements required for encapsidation, reverse transcription, and integration. In addition, the transfer vector plasmid includes the packaging signal ψ (Merten et al., 2016). As an additional safety feature in the third-generation LV system, the promoter-enhancer sequences in the LTR of the integrated transgene (i.e. provirus) were deleted through a self-inactivating (SIN) design, which further minimizes the chance of RCL.

The envelope plasmid includes *env*, an envelope glycoprotein. A foreign viral envelope protein is typically used for the LV system to target specific cell types and it is combined through a process called pseudotyping. Vesicular Stomatitis Virus Glycoprotein (VSV-G) is a heterologous envelop protein commonly used for pseudotyping of LVs because it allows gene transfer to a broad array of cell types and species (Tolmachov et al., 2011). Another benefit that VSV-G provides is improved stability during downstream processing, since these particular pseudotyped LVs can withstand higher ultracentrifugation speeds (Naldini et al., 2016).

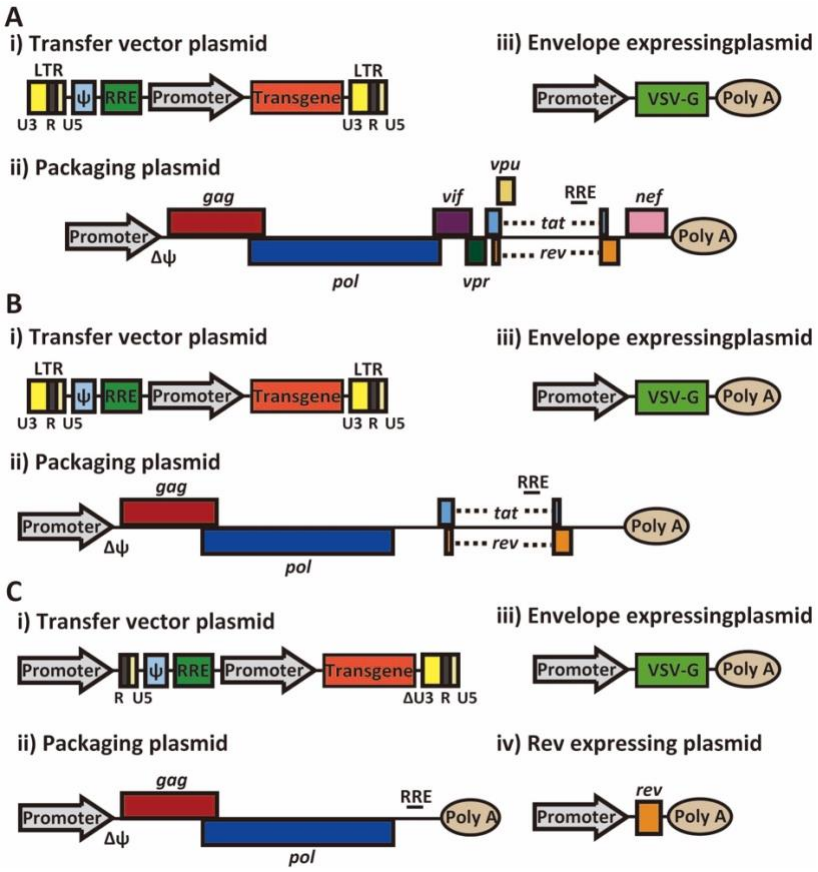

Figure 3: Schematic representation of HIV-1-derived lentiviral vector (LV) packaging constructs. (A) First-generation LVs. (B) Second-generation LVs. (C) Third-generation LVs. (Suzuki and Suzuki, 2011)

Lentiviral Vector Production

The HEK293 cell line, derived from human embryonic kidney cells, is a well-established system for the production of viral vectors since they are easy to transfect and they provide the suitable glycosylation pattern required for efficient viral production (Petiot et al., 2015). There has been a shift from adherent to suspension cells as cell culture in large bioreactors is the best approach for industrial manufacturing. HEK293SF is a suspension adapted variant (Broussau et al., 2008) of HEK293 that can achieve high cell densities in the absence of bovine serum and animal origin components in cell culture media, which is suitable for clinical manufacturing by eliminating lot-to-lot variability and decreasing the risk of contamination by adventitious agents (Merten et al., 2016).

The production of LVs can be achieved by three methods – transient transfection, transient transfection of the transgene plasmid in stable packaging cell lines, and induction of stable producer cell lines. Traditionally, LVs are produced by transient transfection, using 3 to 4 plasmids. Due to manufacturing scalability challenges, packaging cell lines have been developed by stably integrating necessary genetic elements for the assembly and functioning of the vectors, leaving only the transgene plasmid to transfect. In addition, to address cytotoxicity issues that arise from the viral proteins (e.g. Gag, Rev, VSV-G), the expression of these elements is often regulated by an inducible promoter that is activated only at the time of LV production (Broussau et al., 2008). To further facilitate the scalability, producer cell lines have been developed to integrate the remaining transgene plasmid, making the process more reproducible for clinical applications (Manceur et al., 2017).

The most frequently used inducible systems are the Tet-on and Tet-off systems, which are based on the addition or removal, respectively, of the tetracycline/doxycycline antibiotic in the culture medium to trigger gene transcription through the tetracycline response element (TRE) (Broussau et al., 2008). Another inducible system involves the cumate switch. The absence of cumate prevents transcription since the copper oxide (CuO) promoter is inhibited by the cumate repressor (CymR). Therefore, the addition of cumate releases CymR from the CuO operator, allowing for transcription (Broussau et al., 2008). The combination of the Tet-on system and cumate switch provides tighter transcription regulation, which can mitigate the cytotoxic effects from viral proteins and, thus, increasing the LV yield.

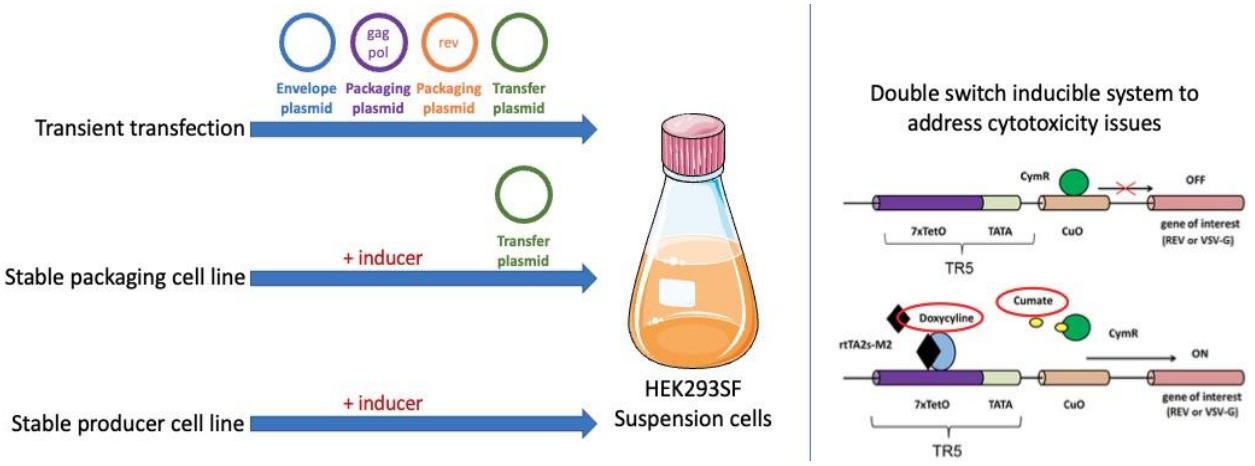

Figure 4: Three methods of LV production (left) and the double switch inducible system (right, figure from Manceur et al., 2017).

There are different types of cell culture methods, such as batch, fed-batch, and perfusion. In batch mode, all nutrients are supplied in an initial base medium. Typically, these cells will reach a peak viable cell density before declining sharply due to complete consumption of glucose. In fed-batch mode, nutrients are added once they are depleted. Typically, these cells will achieve a higher viable cell density and they survive longer than in batch mode. In perfusion mode, the medium circulates through a growing culture, which allows for simultaneous removal of waste, supply of nutrients, and harvesting of the product. Typically, these cells reach the highest peak viable cell density and survive the longest out of the three culture methods (Tapia et al., 2016).

Although there has been a shift from adherent to suspension cells (Bauler et al., 2020) as well as a shift from transient transfection to utilizing packaging (Broussau et al., 2008; Sanber et al., 2015) and producing cell lines (Manceur et al., 2017; Powers et al., 2020), LV production is still predominantly carried out by transient transfection with adherent cells. Most materials for clinical studies are produced using PEI or calcium phosphate transfection with LV functional vector titers in the 10^6-10^7 transducing units per milliliter (TU/mL) range (Schweizer and Merten, 2010). LV production using adherent cells can generate enough material for small scale clinical trials, however, they often are difficult to scale. There was study using suspension cells for transient transfection in perfusion mode for cell culture, which achieved titers in the 10^8 TU/mL range (Ansorge et al., 2009). However, transfection reagents and plasmid DNA are costly, and requires the clearing of DNA plasmids in the purification steps. Some studies have used producer cell lines based on adherent HEK293T cells (Greene et al., 2012; Sanber et al., 2015), which reduced toxicity caused by VSV-G since the cells produce LVs under an inducible promoter.

However, the functional titers are still in the 10^5-10^8 TU/mL range and, again, the adherent cells are difficult to scale. In a review, it was reported that transient transfection yield titers of 10^6-10^8 TU/mL and stable cell lines are producing in the order of 10^6-10^7 TU/mL (Gutierrez-Granados et al., 2018).

Searching the literature with the perspective of generating enough LVs for later stage clinical trials and prolonged treatments, I was most interested in finding scalable methods that can be implemented at large scale. The study conducted by Manceur et al. (2017) using a stable producer cell line that was adapted to be in suspension (abbreviated as Clone 92) that was cultured using the perfusion method gave me the inspiration for my work, which is explained more in detail in the Preface to Chapter 4. Then, Chapter 4 discusses the experiments I conducted using the same Clone 92 producer cell line to support Objective 2 of my thesis, which is to *improve LV productivity through process intensification of the upstream process*.

Bioprocessing

The bioprocessing workflow usually separates the upstream and the downstream processes (Figure 5). The upstream process typically refers to the production and harvesting of LVs. The downstream process includes nuclease treatment, clarification, purification, polishing, and formulation. Changes made in the upstream have implications for the downstream process. For example, using the perfusion culturing method, where a large of volume of harvest is collected, can pose as a challenge for the downstream steps.

At lab scale, centrifugation and filtration are typically used for harvest and clarification to remove cells and cell debris, followed by ultracentrifugation of the purification step of LVs. A popular method is ultracentrifugation using a sucrose cushion, which offers some purification along with concentration of the material (Merten et al., 2016). However, ultracentrifugation is not a scalable process, and it is known for concentrating impurities from the bioprocess and reducing the transducibility of the LVs given the stress conditions (Moreira, Cavaco et al., 2021). The field has shifted to more scalable methods over the years, and a recently published work discussed about the benefits of purified LVs as compared to ultracentrifuged LVs (Soldi et al., 2020).

For large-scale downstream processing of LVs, a mixture of process steps such as ultracentrifugation, membrane filtration, ultrafiltration/diafiltration using tangential flow filtration (TFF), membrane based chromatography, and column chromatography are used. In terms of column chromatography, anion-exchange and size exclusion chromatography are most commonly used. The low recovery from chromatography matrix is attributed to the restrictive process

conditions that are imposed by LV fragility. LV vectors are very sensitive to pH variations and high salt concentrations, which are the two parameters normally altered to optimize binding and elution in ion-exchange chromatography. It has been shown that affinity chromatography based on heparin column can be used; however, this type of chromatography media is not suitable for industry where components of animal origin such as heparin should be excluded (Moreira, Cavaco et al., 2021).

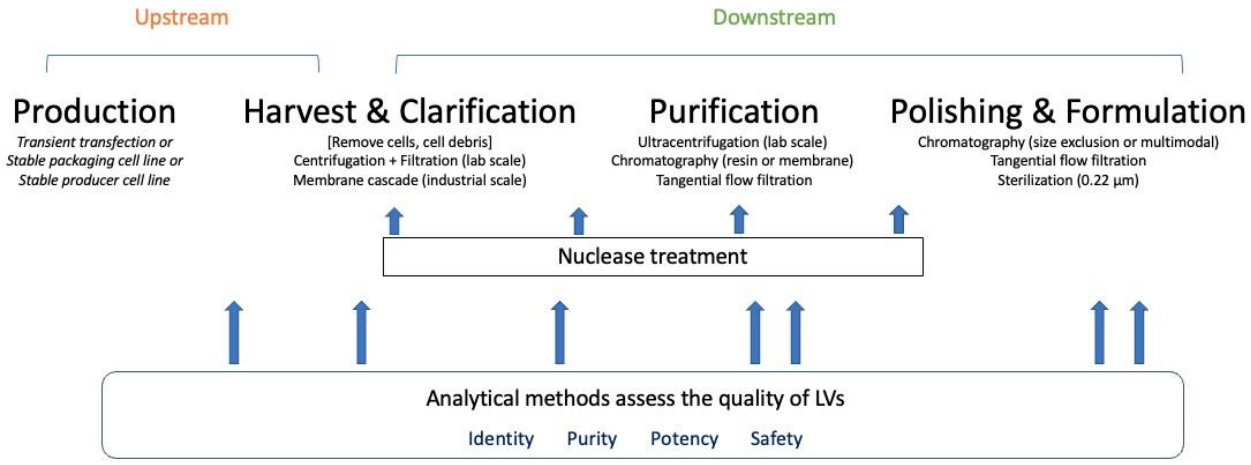

Figure 5: Bioprocessing workflow for LV production and purification.

Analytical methods are needed to assess the quality of the produced LVs at different stages of the bioprocess. The main aspects that contribute to the LV product quality are identity, purity, potency, and safety. Figure 6 summarizes the assays that have been used in the literature to assess the different aspects of LV product quality (Moreira, Cavaco et al., 2021). Typically, the identity is characterized early in the development process to confirm the product of interest before moving onto the bulk of the development and safety is addressed later in the process to confirm the purified material. Potency and purity are typically assessed at every step of the process to use as feedback for how to proceed with designing the purification, polishing, and formulating the final product.

Chapter 3 of this Ph.D. thesis discusses some analytical methods used for assessing the potency aspect – gene transfer assay (GTA), p24 enzyme-linked immunosorbent assay (ELISA), droplet digital polymerase chain reaction (ddPCR). The work presented in Chapter 3 also used the same Clone 92 producer cell line used, therefore the confirmation of identity for the produced LVs are presented with data from SDS-PAGE, western blot, and negative stain electron microscopy.

Target	Assay(s)	Ref.
Identity		
Confirm identity	Western Blot, vector sequencing, restriction enzyme mapping, reverse phase HPLC, SDS-PAGE	[100]
Purity		
Total protein	Bradford, BCA protein assay	[24,68]
Host cell protein	ELISA	[24]
Residual endonuclease	ELISA	[24]
Residual BSA	ELISA	[24]
Total DNA	Fluorimetry (PicoGreen)	[24]
Host cell DNA	qPCR, fluorimetry	[36,121]
DNA size distribution	Agarose gel eletrophoresis, capillary electrophoresis	[69,122]
E1A and SV40 LTA sequences in the vector	qPCR, Southern blot	[24]
Transfer of plasmid (vsv-g and gag-pol), and host-cell (EIA and SV40 LTA) sequences to target cells	qPCR, Southern blot	[4,24]
Potency		
Total viral particles	p24 ELISA, PERT, RT qPCR	[24,69,100]
Functional viral particles (analysis of transduced cells)	Flow cytometry, qPCR, ddPCR	[24,69,100]
Safety		
Recombinant competent lentiviruses (RCL)	RCL amplification in suitable cell line by serial passages followed by quantitation assay (e.g., PCR, p24 ELISA)	[4,24]
Adventitious agents	In vitro testing, PCR-based methods	[4,69]
Mycoplasma	Culture-based methods, PCR-based methods	[4]
Endotoxins/pyrogens	LAL test, rabbit pyrogen test	[4]
Sterility	Bacterial and fungal sterility	[4]

Ref., reference; BCA, bicinchoninic acid; ELISA, enzyme-linked immunosorbent assay; PCR, polymerase chain reaction; qPCR, quantitative polymerase chain reaction; PERT, product-enhanced reverse transcriptase; RT qPCR, quantitative reverse transcription-polymerase chain reaction; ddPCR, droplet digital polymerase chain reaction; LAL, Limulus amebocyte lysate.

Figure 6: Analytical methods to assess the quality of LVs. (Moreira, Cavaco et al., 2021)

Integrated Continuous Bioprocessing

The trend in bioprocessing started with large fed-batch or batch systems in the 1990s that produced >10,000 L in upstream processing (USP) and > 100 L in downstream processing (DSP). For example, stable protein production was done in 10-20 kL stainless steel bioreactors with larger volumes to process in the DSP. A decade later, the trend shifted to smaller bioreactors, around 2 kL, and columns that operate at higher frequency with smaller processing lots. The changes, which have been brought on by process intensification, have shown to provide benefits such as increasing viral vector yield per unit culture volume, lowering production costs, and providing the possibility of scale up and/or adaptation of smaller single-use bioreactors to have a reduced footprint. Since around 2011, there has been a shift to continuous operations with smaller equipment and processing lots (Croughan 2015).

The strategy of continuous bioprocessing has been successfully implemented for certain industries, such as oil refining, chemicals, and food. There has been an increase of activities in the continuous bioprocessing space for biological products since the release of a Strategic Plan for Regulatory Science by the U.S. Food and Drug Administration in August 2011. In supporting new

approaches to improve product manufacturing and quality, the FDA included investigating the effects of continuous manufacturing on product quality. Continuous bioprocessing has the potential to address the current challenges of biomanufacturing technology, such as reducing cost, increasing flexibility and standardization, accelerating development and scaling times, and improving product quality. The impact of both continuous bioprocessing and integrated continuous manufacturing have been thoroughly discussed (Konstantinov 2014, Croughan 2015, Zydney 2015, Walther 2015).

The two highly discussed drivers behind the current interest in continuous bioprocessing are cost and improvements in product quality. In terms of cost, an article discussing the LV bioprocess economics for cell and gene therapy reported high treatment costs for gene-modifying cell therapy products that use LVs as the gene delivery method; $473k USD for Kymriah approved in 2017 to treat acute lymphoblastic leukemia and $1.8M USD projected for Zynteglo approved in 2022 to treat beta-thalassemia (Comisel et al., 2020). There is an increased interest in reducing the price, especially in the effort to make life saving therapies to patients in developing countries. In terms of product quality, continuous processing has the potential to provide improvements through enhanced control of the manufacturing process.

In the context of LVs, the main motivation for an integrated continuous process is the instability of LVs, which is explained more in detail in the Preface to Chapter 4 and Preface to Chapter 5. Chapter 4 focuses on the process intensification of the upstream process. Chapter 5 focuses on the intensification of the downstream as well as the integration of the upstream and downstream in a semi-continuous manner.

While increasing the total vector yield through process intensification in the upstream process contributes to the scalability and mass production of LVs, improving the functional yield will improve the transducibility ratio, which means less LVs are needed for an effective treatment. Together, increasing vector yield and improving functional yield will lead to higher quantity and quality of viral vectors, contributing to improved process performance and robustness. Overall, these improvements will lead to lower drug prices for consumers and allows manufacturers to respond much quicker to changes in demand, contributing to the prevention of drug shortages. In addition, establishing reliable analytical methods to characterize LVs will be critical at all development steps and will contribute to generating more knowledge in the fields of LVs and cell and gene therapy.

Research hypothesis:

An integrated semi-continuous manufacturing process can increase LV production and improve functional yield for LVs by slowing down the loss of functionality that is typically caused during processing times and process hold times of the production and purification processes.

Research objectives:

1) Optimize analytical methods to support the quality assessment of LVs
2) Improve LV productivity through process intensification of the upstream process
3) Improve LV functional yield through integrated semi-continuous manufacturing

Preface to Chapter 3

The published manuscript enclosed in Chapter 3 is in support of Objective 1, which is to *optimize analytical methods to support the quality assessment of LVs*. Chapter 3 explains the importance of developing analytical tools to support the quality assessment of LVs, highlights the necessary advancements needed to support the process at large-scale manufacturing for clinical applications, and presents the development of a high-performance liquid chromatography (HPLC) method for assessing total vector particles.

In this chapter, the HPLC method is compared to two other methods that are also used to quantify total vector particles, the p24 ELISA and the digital droplet polymerase chain reaction (ddPCR) method. The former is applicable only for HIV-1 derived LVs and the latter includes extra sample preparation steps that lengthen the analytical time. In contrast, the sample preparation for the HPLC method is simple and the analysis time is quick. Combined with its suitability for analyzing all in-process samples from the LV production process (from LV supernatant to the final LV product), the HPLC method is an excellent candidate to be implemented as a routine in-process monitoring tool at the manufacturing scale, where decisions need to be made quickly as the process steps advance in order to preserve as high quality of the LV material as possible. This chapter contributes to the field of LVs by offering a method with an at-line capability that could support process analytical technology at large-scale manufacturing, which is fitting in the context of investigating practical methods that can be implemented to support the mass production of LVs.

In addition, this chapter demonstrates the importance of tracking both total and functional vectors in LV batches, a theme that is revisited throughout the thesis and highlights the two main challenges of LV production and purification – increasing the quantity (i.e., total vectors produced) and improving the quality (i.e., by maintaining the functional vectors produced).

The ddPCR method used to analyze samples for this chapter is the same one used for the work presented in Chapters 4 and 5. A more complete protocol for this ddPCR assay is included in the Materials and Methods section of Chapter 4 and its optimization is described in Appendix 2. On the other hand, the gene transfer assay (GTA) from this chapter is different from the one used in Chapters 4 and 5. In this chapter, the GTA was conducted by our collaborators with their own protocol using adherent HEK293A cells. In contrast, my GTA protocol was adapted to suspension HEK293SF cells.

Chapter 3: Rapid In-Process Monitoring of Lentiviral Vector Particles by High-Performance Liquid Chromatography

Authors:	Julia Transfiguracion,[1,3] **Michelle Yen Tran**,[2,3] Stéphane Lanthier,[1] Sonia Tremblay,[1] Nathalie Coulombe,[1] Mauro Acchione,[1] and Amine A. Kamen[1,2]
Author affiliation:	[1] National Research Council, Human Health Therapeutics Research Center, 6100 Royalmount Avenue, Montreal, QC H4P 2R2, Canada; [2] Viral Vectors and Vaccine Bioprocessing Group, Department of Bioengineering, McGill University, 817 Sherbrooke West #270, Montreal, QC H3A 0C3, Canada.
Author contribution	[3] These authors contributed equally to this work

Journal:	*Molecular Therapy – Methods & Clinical Development* (Cell Press)
Year:	2020
Volume:	18
DOI:	10.1016/j.omtm.2020.08.005
Status:	Published
Article History:	Received 27 March 2020; Received in revised form 02 July 2020; Accepted 31 July 2020; Available online 05 August 2020.

Written agreement: Julia Transfiguration and I (Michelle Yen Tran) are co-first authors on this manuscript. Julia Transfiguration hereby acknowledges that I, Michelle Yen Tran, will be using this manuscript in my doctoral thesis, and that she cannot use it in her own graduate thesis.

Michelle Yen Tran Signature: 07 December 2022

Julia Transfiguration Signature: Transfiguracion, Julia Digitally signed by Transfiguracion, Julia Date: 2022.12.07 07:28:15 -05'00'

Abstract

Lentiviral vectors (LVs) are a popular gene delivery tool in cell and gene therapy and they are a primary tool for *ex vivo* transduction of T cells for expression of chimeric antigen receptor (CAR) in CAR-T cell therapies. Extensive process and product characterization are required in manufacturing virus-based gene vectors to better control batch-to-batch variability. However, it has been an ongoing challenge to make quantitative assessments of LV product because current analytical tools often are low throughput and lack robustness and standardization is still required. This paper presents a high-throughput and robust physico-chemical characterization method that directly assesses total LV particles. With simple sample preparation and fast elution time (6.24 min) of the LV peak in 440 mM NaCl (in 20 mM Tris-HCl [pH 7.5]), this ion exchange high-performance liquid chromatography (IEX-HPLC) method is ideal for routine in-process monitoring to facilitate the development of scalable and robust LV manufacturing processes. Furthermore, this HPLC method is suitable for the analysis of all in-process samples, from crude samples such as LV supernatants to final purified products. The linearity range of the standard curve is 3.13 x 10^8 to 1.0 x 10^{10} total particles/mL, and both the intra- and inter-assay variabilities are less than 5%.

Keywords

High performance liquid chromatography, lentiviral vector, particle quantification.

1. Introduction

Lentiviral vectors (LVs) are approximately 80-100 nm in diameter and their genome consists of two copies of positive-sense single-stranded RNA inside a conical capsid, which is surrounded by a lipid bilayer (Tolmachov et al., 2011). In addition to LVs' ability to transduce both dividing and non-dividing cells, they offer many advantages, such as stable genome integration, long-term transgene expression, low mutagenicity, and delivery of large amounts of genetic information (~10 kb) into host cell DNA (Escors et al., 2012). Some examples of lentiviruses are human (HIV), simian (SIV), feline (FIV), and equine infectious anemia (EIAV) immunodeficiency viruses and the most widely used LVs are derived from the HIV-1 virus (Tolmachov et al., 2011).

To date, there are two approved CAR (chimeric antigen receptor)-T cell therapies (Kymriah and Yescarta) and one approved *ex vivo* therapy for monogenic immunodeficiency

(Strimvelis) that uses integrating LVs. Currently, there are 185 LV clinical trials, including 75 CAR-T cell trials that utilize LVs to transduce the T cells (ClinicalTrials.gov, accessed on March 10, 2020), as well as significant ongoing research activities using LVs for cell and gene therapy treatments for various conditions that are steadily progressing toward clinical applications (Milone and O'Doherty, 2018). To effectively support these progressions and accelerate the transition from research and development to the clinic, scalable and robust LV manufacturing processes must be developed. A key factor in speeding up process development is rapid and sensitive quantification methods of vector particles that are suitable for analyzing in-process samples, from crude supernatants to final purified products. Such methods provide the means to assess process efficiency in terms of yield and recovery at each step of the manufacturing process. In addition, extensive characterization of purified LV batches is required in a good manufacturing practice (GMP) environment to develop a product suitable for human use. In fact, in response to the growing demand of LV standardization and to ensure the delivery of safe and efficacious doses of LV products for patients, the World Health Organization recently developed and characterized the first standard for LV integration (Zhao et al., 2019).

Over the years, there has been an increase of effort in developing faster and more reliable characterization methods to measure functional and total LV particles. However, the existing analytical tools often have low throughput and robustness, there is high variability in the obtained results due to limitations of each method, and the field continues to face the persisting challenge of making quantitative assessments of LV products. Some commonly used methods are the gene transfer assay (GTA), p24 enzyme-linked immunosorbent assay (ELISA), and polymerase chain reaction (PCR) (Scherr et al., 2001; Sastry et al., 2002; Geraerts et al., 2006; Delenda and Gaillard, 2005; Barczak et al., 2015; Lizée et al., 2003).

GTA is a cell-based analytical method that measures the transgene expression in transduced target cells to report functional vector particles. This method is commonly used in process development because the transgene can include green fluorescent protein (GFP), which can be easily detected and counted by flow cytometry. However, results from this cell-based assay are generally obtained in 3 days or longer, rendering it unsuitable to be used as a routine in-process monitoring tool. p24 ELISA, which is applicable only for HIV-1-derived LVs, and PCR are physical-based direct methods that provide faster delivery of results. However, they are tedious to perform and only a limited number of samples can be analyzed at a time (Delenda and Gaillard, 2005). The droplet digital PCR (ddPCR) method is more robust and has higher throughput than

the gold standard quantitative PCR since it provides absolute quantification with higher sensitivity, omits the use of a standard, and requires less sample volume (Wang et al., 2018). However, the sample preparation steps, RNA extraction and cDNA synthesis, have been identified as sources of variability.

High-performance liquid chromatography (HPLC) methods, which are physico-chemical based, have been developed and used for the particle quantification of viral vectors, viral vaccines, and therapeutics, such as adenovirus, adeno-associated virus, baculovirus, influenza, and reovirus (Transfiguracion et al., 2011; Transfiguracion et al., 2015; Transfiguracion et al., 2008; Transfiguracion et al., 2001; Klyushnichenko et al., 2001; Kapteyn et al., 2009; Debelak et al., 2000). In fact, an ion exchange (IEX)-HPLC method was instrumental in the development of a scalable and robust process at the 100-L scale in record time, leading to the process technology transfer to a GMP contract manufacturing organization to produce clinical-trial-grade material (Transfiguracion et al., 2008). This paper presents the development of an IEX-HPLC method for the quantification of total LV particles to be used for routine in-process monitoring. In addition, the HPLC method is compared with the commonly used characterization methods (GTA, p24 ELISA, and ddPCR) described above.

2. Results

2.1 LV Standard Used for Method Development

An in-house sucrose cushion purified LV material, SC-LV, was generated to be used for the HPLC method development. The LVs were produced using a stable producer cell line, HEK293SF-LVP- CMVGFPq-92, developed by the National Research Council Canada (Manceur et al., 2017). These LVs contain GFP as the transgene and vesicular stomatitis virus-glycoprotein (VSV-G) at the membrane surface. The functional vector titer, determined by GTA, is 1.08×10^8 TU/mL (transducing units per milliliter) and the total vector titer, determined by p24 ELISA, is 1.16×10^{10} LP/mL (LV particle concentration per milliliter). Figure 7A shows the SDS-PAGE (sodium dodecyl sulfate polyacrylamide gel electrophoresis) profiles of the protein molecular weight marker and SC-LV. Based on their apparent molecular weights, p24 capsid and VSV-G envelope were the major bands detected. Figure 7B shows the western blot profiles against p24 capsid and VSV-G envelope. In lane 1 of Figure 7B, p24 was detected as a major band and precursor Pr55 was detected as a minor band, with two light bands below Pr55 that are possibly intermediate proteins released during Pr55 maturation. In lane 2 of Figure 7B, VSV-G envelope

was the only detected band. Figure 7C is an electron micrograph of SC-LV with pronounced rigid tails, which is typical of LVs when stained with phosphotungstic acid (PTA) and might underline the challenges associated with the size distribution of LV particles.

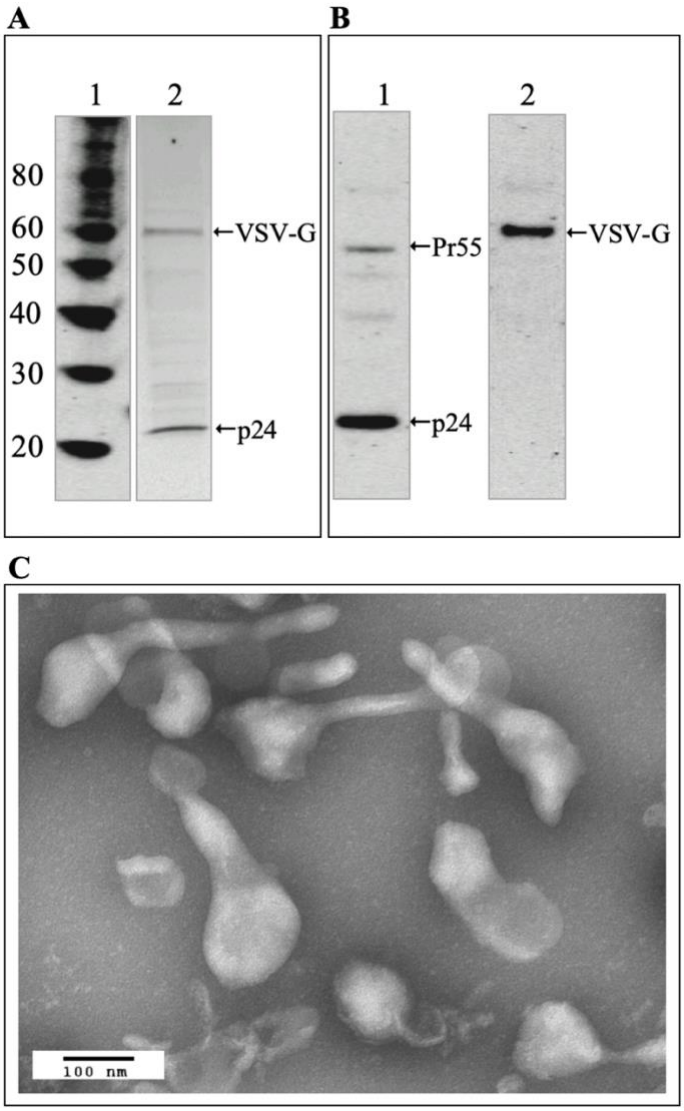

Figure 7. Characterization of Sucrose Cushion Purified LV Standard (SC-LV). (A) SDS-PAGE profiles: lane 1, protein molecular weight markers; lane 2, SC-LV, showing p24 capsid (bottom band) and VSV-G envelope (top band). (B) Western blot profiles: lane 1, against p24 capsid (bottom band) with precursor Pr55 (top band) and two light bands below Pr55 that are possibly the intermediate proteins released during Pr55 maturation; lane 2, against VSV-G envelope. (C) Negative stain electron microscopy using phosphotungstic acid staining, where the scale bar represents 100 nm at 40,000x magnification.

2.2 Resolution and Confirmation of LV Elution

An IEX-HPLC method for total LV particle quantification was developed using the LV standard (SC-LV), LV supernatant collected at 3 days post induction (3 dpi), and cell culture

supernatant without LVs (0 dpi). First, a linear NaCl gradient of 100 mM/mL in 20 mM Tris-HCl (pH 7.5) was used to analyze SC-LV. The chromatographic peaks were monitored by fluorescence (FL), absorbance at 260 nm (OD260), and absorbance at 280 nm (OD280). Figure 8A shows the chromatogram monitored by OD260, where four peaks were detected (indicated as 1, 2, 3, and 4) and eluted at NaCl concentrations of 35, 190, 508, and 777 mM, respectively. To identify and confirm LVs, the same SC-LV sample was repeatedly injected at a volume of 200 mL, and the individual peaks as shown in Figure 8A (except for peak 4) were collected, pooled, and concentrated, followed by western blot analysis against p24 capsid and VSV-G envelope. Peak 3, which eluted around 500 mM NaCl, exhibits the presence of p24 capsid and VSV-G envelope bands (inset figure of Figure 8A), whereas these bands were not detected in the other peaks (results shown in Figure S1). Thus, these results confirmed the identity of LVs in peak 3.

Peaks 1 and 2 were assumed to be residual host proteins based on their elution in low salt concentrations. Peak 4 was identified to be residual host DNA based on the analysis of double-stranded DNA standard (Figure S2A), and its area in Figure 8A suggests that the amount is insignificant in the SC-LV sample. Overall, the chromatographic profile in Figure 8A shows that LVs can be well resolved from host proteins and DNA. Chromatograms monitored by FL were used for the remainder of the method development because its detection shows superior sensitivity as compared with OD260 detection, as shown in Figure S2B.

Then, to further assess the LV separation from other components in the sample matrix, 3 and 0 dpi samples, as well as the cell culture medium used for production, were analyzed using the same linear salt gradient used for SC-LV. Figure 8B shows the chromatographic profiles of these samples detected by FL with an overlay of SC-LV. The peak eluted at 500 mM NaCl for 3 dpi is significantly higher than for SC-LV, although it is unresolved from an adjacent peak, which is eluted earlier. The 0 dpi sample shows a similar profile as 3 dpi, except with lower signal intensity. As expected, no peak was detected at 500 mM NaCl for cell culture medium. Given that 0 dpi is a cell culture supernatant with no LVs, the eluted peak at 500 mM NaCl for this sample was assumed to be extracellular vesicles (EVs) or exosomes. To confirm the presence of EVs in these samples, we performed the acetylcholinesterase (AChE) activity assay, a commonly used method for detecting the presence of exosomes in biological samples. The results showed that all three samples (SC-LV, 3 dpi, and 0 dpi) exhibited AChE activity (results shown in Table S1), which is indicative of the presence of EVs.

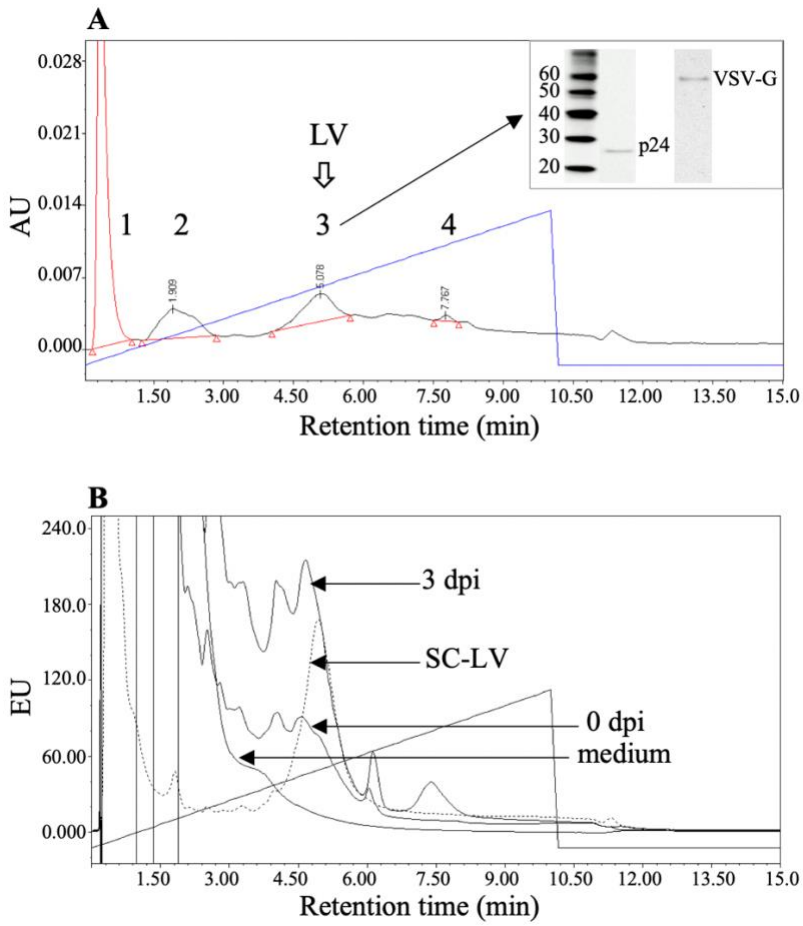

Figure 8. HPLC Chromatographic Profiles during Method Development Using a Linear NaCl Gradient of 100 mM/mL in 20 mM Tris-HCl (pH 7.5). (A) SC-LV sample detected by OD260, where LVs were confirmed to elute in peak 3 at ~500 mM NaCl based on the detection of p24 capsid and VSV-G envelope by western blot analysis (inset figure). (B) 3 dpi LV supernatant, 0 dpi cell culture supernatant, and cell culture medium samples with an overlay of the SC-LV sample, detected by FL.

2.3 Minimization of Co-eluting EVs

The method was further optimized to separate or minimize the presence of EVs in the LV peak by implementing a column wash post sample injection while maintaining the elution at 500 mM NaCl. The tested step gradients for the column wash were from 250 to 400 mM NaCl, the samples used for this optimization were SC-LV and 0 dpi, and the analysis was based on the peak area (PA) reduction of the peak eluted at 500 mM NaCl. Figure S3 shows the highest PA reduction of 85% and 94% for SC-LV and 0 dpi, respectively, with 370 mM NaCl column wash. Additionally, the OD260/280 ratio was used to evaluate the quality of the LV peak eluted at 500 mM NaCl with the varying concentrations of the NaCl wash. OD260/ 280 ratio results from Table S2 suggest that the 0 dpi sample contains only EVs, whereas the SC-LV sample contains both LVs and EVs.

2.4 Optimization of LV Peak Elution

Based on the results obtained from minimizing the presence of co-eluting EVs, the optimized conditions are a 370 mM NaCl step gradient column wash, followed by a 500 mM NaCl step gradient elution. Next, the three samples (SC-LV, 3 dpi, and 0 dpi) were analyzed to validate these conditions. Interestingly, the LV peak for 3 dpi was detected as split peaks with retention times of 6.24 and 6.68 min, whereas SC-LV showed a single peak eluted at 6.24 min and 0 dpi showed an insignificant peak also at 6.24 min (Figure S4A). To resolve the split peaks, we further optimized the LV elution using a step gradient elution lower than 500 mM NaCl, where the test range was from 410 to 450 mM NaCl. An enlarged profile of the LV peak at these varying NaCl concentrations and some of the OD260/280 ratios are shown in Figure S4B. From the evaluation of LV peak intensities and OD260/280 ratios, 440 mM NaCl was selected as the step gradient elution.

2.5 Finalized HPLC Method

SC-LV, 3 dpi, and 0 dpi samples were analyzed using the final established conditions (50-µL sample injection, 370 mM NaCl step gradient column wash post sample injection, 440 mM NaCl step gradient elution, and detection by FL at excitation and emission wave- lengths at 290 and 335 nm, respectively). Figure 9 shows overlaid chromatographic profiles of the three samples, where the LV peak in 3 dpi is now a single peak eluted at the same retention time as the LV peak in SC-LV. The 0 dpi sample shows a minor LV peak eluted at 6.24 min as compared with the SC-LV and 3 dpi samples. This was expected because the 0 dpi sample should not contain any LVs. Note that the 3 dpi sample shows a significant peak eluted at a similar retention time as DNA (as indicated in Figure 9A). This was expected because the cell viability at harvest was low (<30%) and no DNase digestion was performed prior to analysis. Because DNA alone does not exhibit FL at the wavelengths used for detection, as previously shown in Figure S2B, it was assumed that the signal can come from host proteins bound to host DNA.

A standard curve was generated using the LP per milliliter obtained by p24 ELISA of the SC-LV sample, where standards ranging from 3.13×10^8 to 1.0×10^{10} were injected in repeats. The standard curve was plotted as total particles per milliliter (TP/mL) in the x-axis and PA in the y-axis. A good correlation coefficient (R^2) of 0.9999 was obtained with a slope of 0.0077 and y-intercept of 296,992. The precision or variability of the assay, expressed as percentage relative standard deviation (RSD), was determined by the analysis of the 3 dpi LV supernatant sample for

5 days, with six injections per day. The repeat injections had a <5% RSD and were within ±20% of the linear regression line. The intra-assay (repeatability) and inter-assay (day-to-day) variabilities of the assay were found to be less than 5% RSD.

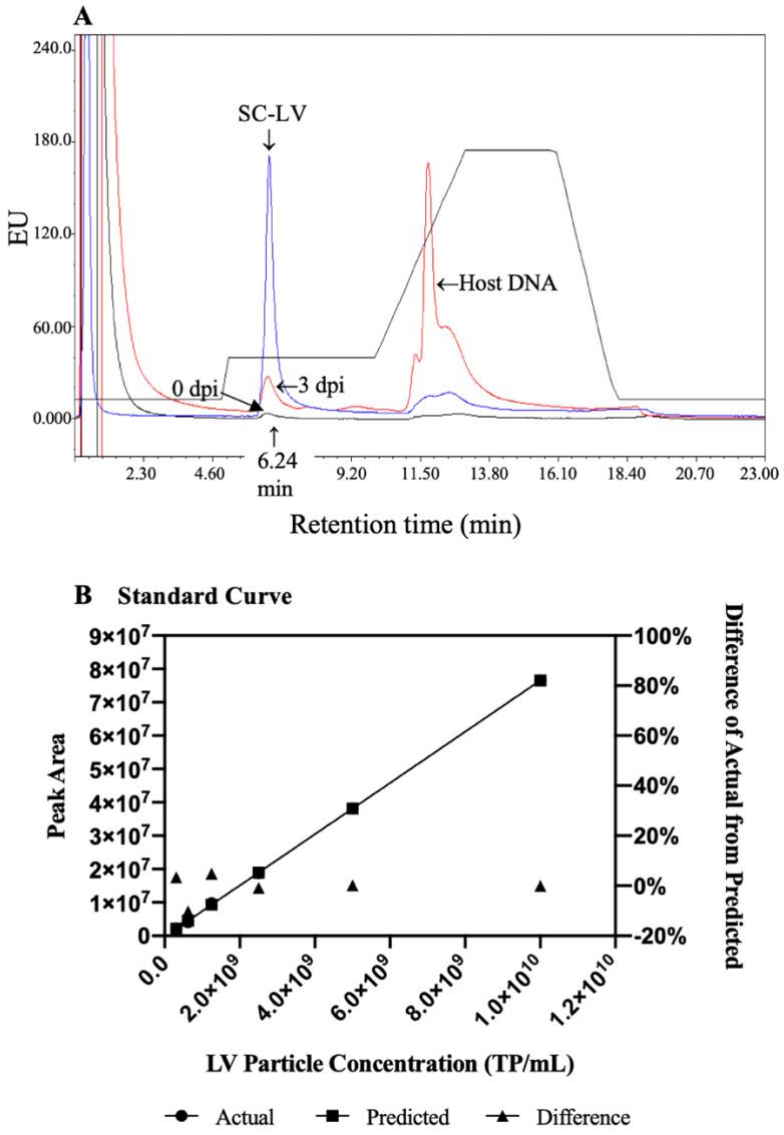

Figure 9. Final Established HPLC Method: 370 mM NaCl Step Gradient Column Wash after Sample Injection and 440 mM NaCl Step Gradient Elution of LVs in 20 mM Tris-HCl (pH 7.5). (A) HPLC chromatographic profile shows one single LV peak eluted at 6.24 min for SC-LV and 3 dpi samples. (B) A standard curve was generated using the SC-LV standard, with the linearity range of 3.13×10^8 to 1.0×10^{10} TP/mL. The intra-assay (repeatability) and inter-assay (day-to-day) variabilities are less than 5% RSD.

2.6 Monitoring LV Particles in Upstream Samples

The developed HPLC method, along with p24 ELISA and GTA, was performed on six LV supernatants (referred to as LV-1 to LV-6) that were collected at 3 days post induction during an

optimization of an upstream process with various tested conditions, such as medium, seeding density, and production method. These LVs were produced using the stable producer cell line HEK293SF-LVP-CMVGFPq-92 (Manceur et al., 2017). Figure 10A shows that the TP/mL (total particles per milliliter), measured by HPLC, is higher than LP/mL (LV particle concentration per milliliter), measured by p24 ELISA, in all crude supernatants except for LV-4. In regard to the GTA, the TU/mL (transducing units per milliliter) values, which reflect functional LV particles, for LV-1 to LV-6 are significantly lower than both TP/mL and LP/mL values, which reflect total LV particles.

In addition, LV supernatant of a 3L perfusion production was collected from 2 to 4 dpi and analyzed by HPLC, p24 ELISA, ddPCR (in vector genomes per milliliter [Vg/mL]), and GTA, as shown in Figure 10B. These LVs were also produced using the stable producer cell line HEK293SF-LVP-CMVGFPq-92 (Manceur et al., 2017). GTA, in comparison with HPLC, p24 ELISA, and ddPCR, shows a similar trend as in Figure 10A, where the number of functional LV particles is significantly lower than the number of total LV particles measured by the three different methods. The total vector particle values for the three analytical methods converge as the LV production progresses, with an average of 9.39×10^8 titer and 3.8% coefficient of variation (CV) for the 4 dpi sample.

2.7 Monitoring LV Particles in Downstream Samples

The developed HPLC method, along with p24 ELISA, GTA, and ddPCR, was also performed on downstream process (DSP) samples from a LV production by transient transfection using the third generation LV encoding a CAR using four plasmids. In brief, the DSP started with the collection of the 3 dpi supernatant, DNA digestion with endonucleases, clarification through filtration, followed by concentration and diafiltration by tangential flow filtration (UFDF). The samples collected from the DSP are referred to as supernatant, DNA digestion, clarified supernatant, and UFDF product. Figure 11A shows that HPLC and p24 ELISA values exhibit a similar pattern, with TP per milliliter higher than LP per milliliter for each sample in the DSP. The ddPCR values are similar to p24 ELISA values for supernatant (average 2.92×10^9 total particle titer, 3.1% CV) and clarified supernatant (average 3.05×10^9 total particle titer, 8.7% CV) samples, but lower for DNA digestion and UFDF product samples. The functional vector particles (TU/mL) are significantly lower than the total vector particles (TP/mL, LP/mL, and Vg/mL), which is the same trend observed in the upstream samples.

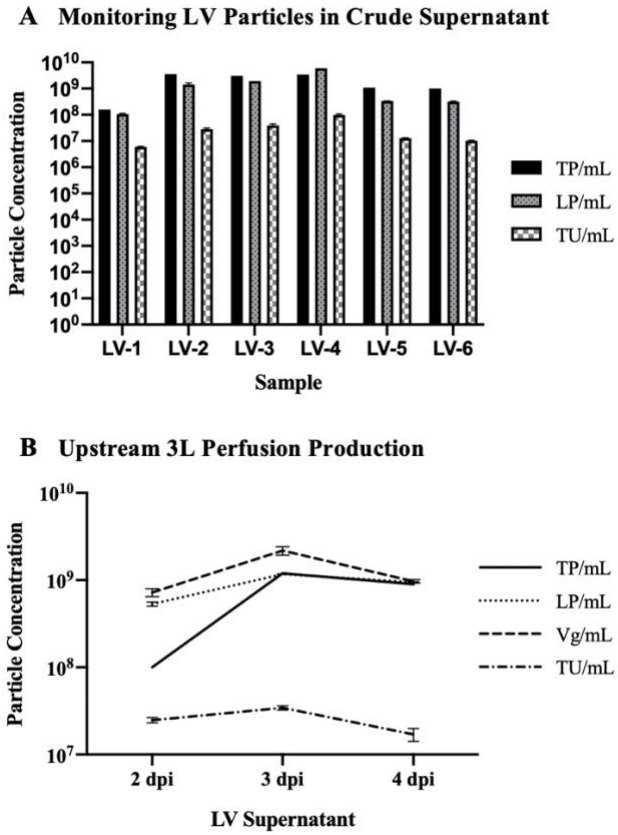

Figure 10. LV Particle Monitoring in Upstream Samples. LP/mL, Vg/mL, and TU/mL values are shown as mean + SD. (A) For six different crude supernatant samples: TP/mL (HPLC) is higher than LP/mL (p24 ELISA) for all samples, except for LV-4; TU/mL values (reflect functional particles) are significantly lower than TP/mL and LP/mL values (both reflect total particles). (B) Supernatants collected from 2 to 4 days after induction for a 3L perfusion LV production: TU/mL values are significantly lower than TP/mL, LP/mL, and Vg/mL values; total vector particle values converge as the LV production progresses.

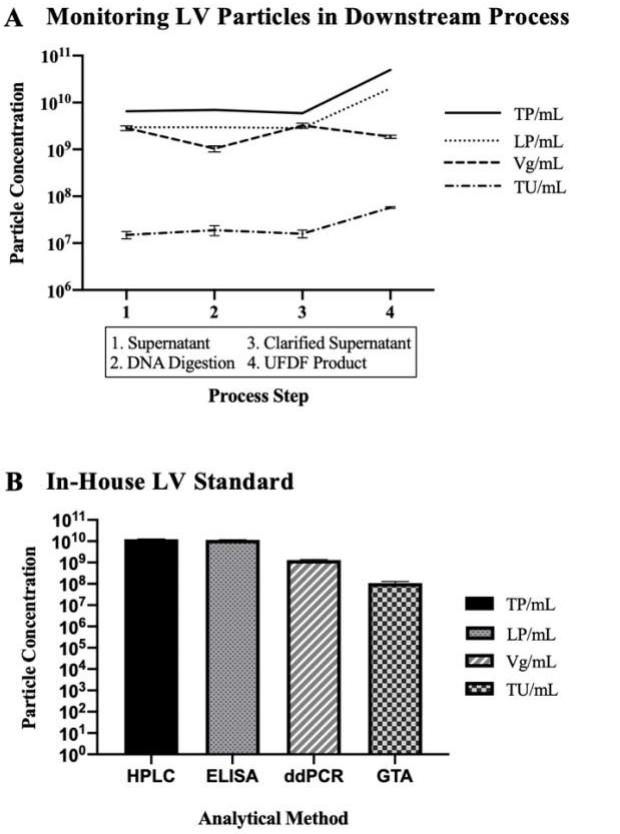

Figure 11. Total and Functional Vector Titers for Downstream Samples and the In-House LV Standard. (A) LV particle monitoring in downstream samples. HPLC and p24 ELISA values exhibit a similar pattern, with the former (TP/mL) higher than the latter (LP/mL) for each sample. ddPCR values (Vg/mL) are similar to p24 ELISA values (LP/mL) for supernatant and clarified supernatant samples, but lower for Benzonase digestion and UFDF product samples. Functional vector particles (TU/mL) are significantly lower than total vector particles (TP/mL, LP/mL, and Vg/mL). Vg/mL and TU/mL values are shown as mean + SD. (B) LV particle monitoring in the in-house LV standard (SC-LV). All values are shown as mean + SD

Figure 11B shows the total vector particles, assessed by the three different analytical methods, as well as the functional vector particles, assessed by GTA, for the in-house LV standard, SC-LV. For this sample, the HPLC and p24 ELISA values are similar (average 1.20 x 10^{10} total particle titer, 5.0% CV), the ddPCR value is 1 log lower (1.31 x 10^{9} Vg/mL), and the GTA value is 2 logs lower (1.08 x 10^{8} TU/mL). As seen in Figure 11, both SC-LV and UFDF product samples show 10^{9} Vg/mL for ddPCR and 10^{10} total particle titer for HPLC and p24 ELISA. The trend where

functional vector particles are lower than total vector particles still exists; however, the functional vector titer is 10^8 TU/mL instead of 10^7 TU/mL, as previously seen in other DSP samples and upstream samples.

3. Discussion

The linearity range of the standard curve of this HPLC method was established to be 3.13 x 10^8 to 1.0 x 10^{10} TP/mL. Taking the current state-of-the-art LV production into consideration, vector particles ranging from 10^8 to 10^{10} TP/mL can be achieved. With perfusion as the production method and ultracentrifugation as the concentration method for the in-house SC-LV, the practical higher limit of 10^{10} TP/mL was achieved and utilized as the upper limit of the linearity range. Theoretically, surpassing 10^{10} TP/mL can be achieved with process intensification and other improvements. However, currently, the ability to further concentrate beyond 10^{10} TP/mL is limited by the risk of aggregation. Thus, a higher upper limit of the linearity range cannot be proved experimentally. Until a more robust LV production process becomes a reality, this linearity range can still be utilized for characterizing viral preparations with higher total vector titers by sample dilution.

Toward the beginning of the HPLC method development, it was observed that the 3 dpi sample showed a significantly higher LV peak than SC-LV, where it was unresolved from an adjacent peak, and the 0 dpi sample exhibited a similar eluted profile as 3 dpi with lower signal intensity. Given that 0 dpi is a cell culture supernatant with no LVs, the eluted LV peak for this sample was assumed to be EVs or exosomes, because it is widely known that these particles co-produce with lentivirus/HIV production (Gluschankof et al., 1997; Ellwanger et al., 2017; Bess et al., 1997; Cantin et al., 2008). In addition, it has been shown that EVs co-purify with LVs, given their intrinsic similarities in physico-chemical properties with lentivirus/HIV (Cantin et al., 2008). Thus, it was also assumed that EVs can be present in the 3 dpi and SC-LV samples. The HPLC method was further optimized to minimize the presence of EVs in the LV peak by implementing a column wash after sample injection.

During method development, the OD260/280 ratio was used to assess the LV peak content because this ratio reflects the relationship between nucleic acids and proteins in a virus suspension (Porterfield and Zlotnick, 2010). In general, proteins typically have an OD260/280 ratio that is <1.0, which is indicative of the absence of nucleic acids (a major contribution to the OD260) and the presence of tryptophan and tyrosine residues, as well as disulfide bonds in proteins (a major

contribution to the OD280). Although the OD260/280 ratio of a purified LV has not been determined, nor is it available in the literature, this approach was utilized to monitor the eluted LV peak while different NaCl column wash gradients were implemented. An OD260/280 ratio closer to or below 1.0 indicates that there might be a significant amount of EVs present in the eluted peak. The results obtained suggest that the 0 dpi sample contains only EVs, whereas the 3 dpi and SC-LV samples contain both LVs and EVs. The presence of co-eluting EVs is a well-recognized problem in the field of LV production. Although the current state-of-the-art does not support the complete removal of EVs, this developed HPLC method can serve as a valuable tool that quantifies LVs while minimizing EV contributions to the overall detection signal of LV particles.

The applicability of the HPLC method was demonstrated with crude LV supernatants collected at 2-4 dpi and at each step of the DSP. Overall, HPLC, p24 ELISA, and ddPCR methods show comparable total vector particle values for all samples. In comparison to the p24 ELISA, the HPLC method proves to be a superior method because of the ease of sample preparation, short analysis time, and cost-effectiveness of materials and reagents. The HPLC method is also a superior method when compared to ddPCR because the latter requires extra sample preparation steps (nucleic acid extraction and cDNA synthesis), which have been identified as sources of variability, before the samples can be analyzed. Consequently, the HPLC method has the advantage of simple sample preparation while providing more consistent results. In addition, ddPCR has good precision for downstream samples, but not upstream samples. Thus, one main advantage of the HPLC method is its ability to characterize crude supernatant samples.

The data presented in Figures 10 and 11 support the important notion of tracking both total and functional vector particles because they show that only a fraction of the total produced LVs is functional. As expected, it is crucial to assess the total vector titer for each batch of produced LVs in order to assess yields and recoveries from the manufacturing process. However, any batch will include defective and non-functional particles in addition to the desired functional particles, which means not all of the produced LVs have the ability and efficiency in transducing host cells to effectively deliver genetic material to be integrated in the host cell genome. Thus, it is equally important to determine the functional vector titer for each batch of produced LVs to appropriately estimate the manufactured amount needed for an effective treatment. It is notably important to extensively characterize virus-based gene vectors because they tend to have greater variability between batches, especially when it comes to the ratio of functional to total vector particles (McCarron et al., 2016).

Reliable, rapid, and sensitive analytical methods are crucial in accelerating and transferring the process from development to manufacturing for the clinic, ultimately facilitating the development of scalable and robust LV manufacturing processes. In addition to being a high-throughput and robust method with simple sample preparation, a key advantage to this HPLC method is that it is suitable to be used routinely for analyzing all in-process samples, from crude samples such as LV supernatants to final purified products.

4. Materials and Methods

4.1 LV Production

For the in-house sucrose cushion LV standard and all crude supernatant samples, LVs were produced using the stable producer cell line HEK293SF-LVP-CMVGFPq-92, developed by the National Research Council Canada (Manceur et al., 2017), with HyClone SFM4Transfx-293 or HyClone HyCell media from Cytiva (Marlborough, MA, USA) in 3L bioreactors, both in perfusion and batch modes, as previously described (Manceur et al., 2017). For downstream samples, LVs were produced by transient transfection using the third generation LV encoding a CAR (LV-CAR) using four plasmids.

4.2 Purification of the In-House LV Standard

LV supernatant collected at 3 dpi from a 3L perfusion production was digested with 20 U/mL Benzonase from EMD Life Sciences (Darmstadt, Germany) for 1 h at room temperature, followed by clarification through a Supor membrane with double pore size of 0.8/0.45 µm from Pall Corporation (Port Washington, NY, USA) and centrifugation in 25% sucrose cushion at 37,000 x g using the A621 Sorvall rotor from Thermo Fisher Scientific (Waltham, MA, USA) for 3 h at 4ºC. The spent medium was discarded, and Tris buffer (20 mM Tris-HCl [pH 7.5]) with 5% sucrose and 2 mM $MgCl_2$ were added to the LV pellet, then kept overnight at 4ºC. The pellet was then resuspended by gentle pipetting up and down, aliquoted, and kept at 80ºC for future analyses. This in-house LV standard was characterized by SDS- PAGE, western blot, negative stain electron microscopy (NSEM), GTA, p24 ELISA, ddPCR, and HPLC.

4.3 SDS-PAGE and Western Blot

SDS-PAGE was performed using a 4% - 15% Mini-PROTEAN TGX pre-cast gel under reducing conditions, and silver staining of the protein bands was performed using Clarity Western

ECL Substrate, both from Bio-Rad (Hercules, CA, USA). Western blot was performed by transferring the protein bands onto a 0.45-µm Protran Premium nitrocellulose membrane from GE Healthcare (Chicago, IL, USA) and incubating with primary antibodies against p24 from eENZYME (Gaithersburg, MD, USA) and VSV-G from Sigma-Aldrich (St. Louis, MO, USA). The specific bands were detected by incubation with anti-mouse horseradish peroxidase conjugated antibody from Jackson ImmunoResearch Laboratories (West Grove, PA, USA).

4.4 NSEM

NSEM was performed at Institut Armand Frappier (Laval, Canada) according to a method previously described (Alain et al., 1987). Staining was performed using 3% PTA for 1 min.

4.5 AChE

AChE activity was assessed using a fluorometric AChE assay kit (ab138872) from Abcam (Cambridge, UK), following the manufacturer's protocol. This assay uses the FL of a thiol probe, reported in relative FL units, to measure AChE activity (reported in mU/mL) in samples.

4.6 GTA for Functional LV Quantification

The functional titer in transducing units per milliliter of LV samples was determined by a flow cytometry-based GTA as previously described (Manceur et al., 2017). For convenience, the protocol used was as follows: HEK293A (adherent) cells were cultured in Dulbecco's modified Eagle's medium (DMEM) containing 5% FBS and 2 mM L-glutamine; the cells were seeded at a density of 1 x 10^5 cells/well of a 24-well plate 5 h before transduction with LVs; LV samples were serially diluted in DMEM supplemented with 8 µg/mL polybrene and incubated at 37ºC for 30 min prior to transduction; transduction was performed by removing culture medium, adding 200 µL of diluted LVs to cells, and incubating overnight at 37ºC; 800 µL of culture medium was added to each well the next day, and cells were incubated for an additional 48 h prior to flow cytometry to quantify GFP-expressing cells. The titer was determined by using the following formula: (% of GFP positive cells/100) x (number of cells transduced) x (dilution factor) x (1 mL / volume transduced).

4.7 p24 ELISA for Total LV Quantification

The LV particle concentration per milliliter was quantified by the p24 ELISA kit from Cell

Biolabs (San Diego, CA, USA), following the manufacturer's protocol. All LV samples were diluted in Tris buffer (20 mM Tris-HCl [pH 7.5]), which was established to be used as a diluent because it was found that the use of cell culture medium resulted in lower titers by up to 5 logs difference (refer to Table S3 in the Supplemental Information for more details).

4.8 ddPCR for Total LV Quantification

The LV Vg (Vg/mL) was quantified by a QX200 ddPCR System from Bio-Rad (Hercules, CA, USA). Prior to running samples on the ddPCR system, sample preparation included extracting RNA from LV samples using a High Pure Viral Nucleic Acid Kit from Roche (Basel, Switzerland) and reverse transcribing into cDNA using an iScript Select cDNA Synthesis Kit from Bio-Rad (Hercules, CA, USA), both following the manufacturers' protocols. Serial dilutions of cDNA were prepared in nuclease-free water. PCRs were prepared with the QX200 ddPCR EvaGreen Supermix and the woodchuck hepatitis virus posttranscriptional regulatory element (WPRE) primer set, because WPRE is known to stabilize the transgene mRNA and therefore enhance transgene expression delivered by LVs (Zufferey et al., 1999). PCR mixtures (22 µL) were prepared for the QX200 Droplet Generator, with final primer concentration of 0.8 µM. After droplet generation, the following PCR program was run: one cycle of 95ºC for 5 min; 40 cycles of 95ºC for 30 s, 60ºC for 1 min, and 72ºC for 30 s; one cycle of 72ºC for 5 min; indefinite 12ºC hold. ddPCR results were analyzed with the QX200 Droplet Reader and QuantaSoft Program.

4.9 HPLC for Total LV Quantification

A Waters HPLC Alliance System (Milford, MA, USA) equipped with a 2695 separation module, 996 photodiode array, 2475 FL detectors, and Empower software for data acquisition and peak integration was used. The stock solutions used were as follows: stock solution A, 0.10 M Tris-HCl (pH 7.5); stock solution B, 2 M NaCl in Milli-Q purified water; and stock solution C, Milli-Q purified water. All stock solutions were filtered through a 0.22-µm membrane before use. A 4.6 x 10 µm UNO Q polishing anion exchange column from Bio-Rad (Hercules, CA, USA) was used for viral separation. The output stream was monitored by FL at excitation and emission wavelengths of 290 and 335 nm, respectively, OD260, and OD280.

All samples were filtered through a Supor membrane with a pore size of 0.45 µm from Pall Corporation (Port Washington, NY, USA) before injection. Unless otherwise specified, all samples were injected at 50 µL, all gradients were formed with 20% stock solution A (final composition:

20 mM Tris-HCl [pH 7.5]), and a flow rate of 1 mL/min was employed during the entire analysis. Prior to the first sample injection, the column was equilibrated with 18.5% stock solution B for 10 min, followed by three consecutive injections of Tris buffer (20 mM Tris-HCl [pH 7.5]) to ensure a flat baseline. After sample injection, the column was washed with the same concentration of stock solution B for 5 min, followed by a step gradient elution at 21% stock solution B for 5 min. The column was cleaned and regenerated using a linear gradient from 21% to 75% stock solution B for 3 min and was put on hold at 75% stock solution B for 3 min, followed by re-equilibration at 18.5% stock solution B for 7 min before the next sample injection.

Supplemental Information

Supplemental Information can be found online at https://doi.org/10.1016/j.omtm.2020.08.005.

Author Contributions

Conceptualization, J.T., M.Y.T., and A.A.K.; Methodology, J.T., M.Y.T., S.L., S.T., and N.C.; Execution, J.T., M.Y.T., S.L., S.T., and N.C.; Writing – Original Draft, J.T. and M.Y.T.; Writing – Review & Editing, J.T., M.Y.T., M.A., and A.A.K.; Funding Acquisition & Resources, M.A. and A.A.K.

Conflicts of Interest

The authors declare no competing interests.

Acknowledgements

M.Y.T. is financially supported by a fellowship from the Faculty of Engineering, and A.A.K. is partially funded through Canada Research Chair CRC-240394. The authors would like to thank David Sharon for help in setting up the ddPCR method and Nasha Nassoury for performing the AChE activity assay.

References

Alain, R., Nadon, F., Séguin, C., Payment, P., and Trudel, M. (1987). Rapid virus sub-unit visualization by direct sedimentation of samples on electron microscope grids. *Journal of Virology Methods, 16*(3), 209-216. https://doi.org/10.1016/0166-0934(87)90005-X

Barczak, W., Suchorska, W., Rubis, B., and Kulcenty, K. (2015). Universal real-time PCR-

based assay for lentiviral titration. *Molecular Biotechnology, 57*, 195-200. https://doi.org/10.1007/s12033-014-9815-4

Bess, J.W., Jr., Gorelick, R.J., Bosche, W.J., Henderson, L.E., and Arthur, L.O. (1997). Microvesicles are a source of contaminating cellular proteins found in purified HIV-1 preparations. *Virology, 230*(1), 134-144. https://doi.org/10.1006/viro.1997.8499

Cantin, R., Diou, J., Bélanger, D., Tremblay, A.M., and Gilbert, C. (2008). Discrimination between exosomes and HIV-1: purification of both vesicles from cell-free supernatants. *Journal of Immunology Methods, 338*(1-2), 21-30. https://doi.org/10.1016/j.jim.2008.07.007

Debelak, D., Fisher, J., Iuliano, S., Sesholtz, D., Sloane, D.L., and Atkinson, E.M. (2000). Cation-exchange high-performance liquid chromatography of recombinant adeno-associated virus type 2. *Journal of Chromatography B: Biomedical Sciences and Applications, 740*(2), 195-202. https://doi.org/10.1016/S0378-4347(00)00100-6

Delenda, C. and Gaillard, C. (2005). Real-time quantitative PCR for the design of lentiviral vector analytical assays. *Gene Therapy, 12*, S36–S50. https://doi.org/10.1038/sj.gt.3302614

Ellwanger, J.H., Veit, T.D., and Chies, J.A.B. (2017). Exosomes in HIV infection: a review and critical look. *Infection, Genetics and Evolution, 53*, 146-154. https://doi.org/10.1016/j.meegid.2017.05.021

Escors, D., Breckpot, K., Arce, F., Kochan, G., and Stephenson, H. (2012). Lentiviral Vectors and Gene Therapy. *Springer*. https://doi.org/10.1007/978-3-0348-0402-8

Geraerts, M., Willems, S., Baekelandt, V., Debyser, Z., and Gijsbers, R. (2006). Comparison of lentiviral vector titration methods. *BMC Biotechnology, 6*, 34. https://doi.org/10.1186/1472-6750-6-34

Gluschankof, P., Mondor, I., Gelderblom, H.R., and Sattentau, Q.J. (1997). Cell membrane vesicles are a major contaminant of gradient-enriched human immunodeficiency virus type-1 preparations. *Virology, 230*(1), 125-133. https://doi.org/10.1006/viro.1997.8453

Kapteyn, J.C., Porre, A.M., de Rond, E.J., Hessels, W.B., Tijms, M.A., Kessen, H., Slotboom, A.M., Oerlemans, M.A., Smit, D., van der Linden, J., Schoen, P., and Thus, J.L.G. (2009). HPLC-based quantification of haemagglutinin in the production of egg- and MDCK cell-derived influenza virus seasonal and pandemic vaccines. *Vaccine, 27*(9), 1468-1477. https://doi.org/10.1016/j.vaccine.2008.11.113

Klyushnichenko, V., Bernier, A., Kamen, A., and Harmsen, E. (2001). Improved high-performance liquid chromatographic method in the analysis of adenovirus particles. *Journal of*

Chromatography B: Biomedical Sciences and Applications, 755(1-2), 27-36. https://doi.org/10.1016/S0378-4347(00)00597-1

Lizée, G., Aerts, J.L., Gonzales, M.I., Chinnasamy, N., Morgan, R.A., and Topalian, S.L. (2003). Real-time quantitative reverse transcriptase-polymerase chain reaction as a method for determining lentiviral vector titers and measuring transgene expression. *Human Gene Therapy*, *14*(3), 497-507. https://doi.org/10.1089/104303403764539387

Manceur, A.P., Kim, H., Misic, V., Andreev, N., Dorion-Thibaudeau, J., Lanthier, S., Bernier, A., Tremblay, S., Gélinas, A.M., Broussau, S., Gilbert, R., and Ansorge, S. (2017). Scalable Lentiviral Vector Production Using Stable HEK293SF Producer Cell Lines. *Human Gene Therapy Methods, 28*(6), 330-339. https://doi.org/10.1089/hgtb.2017.086

McCarron, A., Donnelley, M., McIntyre, C., andParsons, D. (2016). Challenges of up-scaling lentivirus production and processing. *Journal of Biotechnology, 240*, 23-30. https://doi.org/10.1016/j.jbiotec.2016.10.016

Milone, M.C. and O'Doherty, U. (2018). Clinical use of lentiviral vectors. *Leukemia, 32*(7), 1529-1541. https://doi.org/10.1038/s41375-018-0106-0

Porterfield, J.Z. and Zlotnick, A. (2010). A simple and general method for determining the protein and nucleic acid content of viruses by UV absorbance. *Virology 407*(2), 281-288. https://doi.org/10.1016/j.virol.2010.08.015

Sastry, L., Johnson, T., Hobson, M.J., Smucker, B., and Cornetta, K. (2002). Titering lentiviral vectors: comparison of DNA, RNA and marker expression methods. *Gene Therapy, 9*(17), 1155-1162. https://doi.org/10.1038/sj.gt.3301731

Scherr, M., Battmer, K., Blömer, U., Ganser, A., and Grez, M. (2001). Quantitative determination of lentiviral vector particle numbers by real-time PCR. *Biotechniques, 31*(3), 520-526. https://doi.org/10.2144/01313st05

Tolmachov, O.E., Tolmachova, T., and Al-Allaf, F.A. (2011). Designing lentiviral gene vectors. *Viral Gene Therapy*, 263-284. https://doi.org/10.5772/17361

Transfiguracion, J., Bernier, A., Arcand, N., Chahal, P., and Kamen, A. (2001). Validation of a high-performance liquid chromatographic assay for the quantification of adenovirus type 5 particles. *Journal of Chromatography B: Biomedical Sciences and Applications, 761*(2), 187-194. https://doi.org/10.1016/S0378-4347(01)00330-9

Transfiguracion, J., Bernier, A., Voyer, R., Coelho, H., Coffey, M., and Kamen, A. (2008). Rapid and reliable quantification of reovirus type 3 by high performance liquid chromatography

during manufacturing of Reolysin. *Journal of Pharmaceutical and Biomedical Analysis, 48*(3), 598-605. https://doi.org/10.1016/j.jpba.2008.05.038

Transfiguracion, J., Manceur, A.P., Petiot, E., Thompson, C.M., and Kamen, A.A. (2015). Particle quantification of influenza viruses by high performance liquid chromatography. *Vaccine, 33*(1), 78-84. https://doi.org/10.1016/j.vaccine.2014.11.027

Transfiguracion, J., Mena, J.A., Aucoin, M.G., and Kamen, A.A. (2011). Development and validation of a HPLC method for the quantification of baculovirus particles. *Journal of Chromatography B, 879*(1), 61-68. https://doi.org/10.1016/j.jchromb.2010.11.011

Wang, Y., Bergelson, S., and Feschenko, M. (2018). Determination of Lentiviral Infectious Titer by a Novel Droplet Digital PCR Method. *Human Gene Therapy Methods, 29*(2), 96-103. https://doi.org/10.1089/hgtb.2017.198

Zhao, Y., Traylen, C., Rigsby, P., Atkinson, E., Satkunanathan, S., Participants, and Schneider, C.K. (2019). Report on a Collaborative Study for the Proposed WHO 1st International Reference Panel (19/158) for the Quantification of Lentiviral Vector Integration Copy Numbers. *World Health Organization*. WHO/BS/2019.2373

Zufferey, R., Donello, J.E., Trono, D., and Hope, T.J. (1999). Woodchuck hepatitis virus posttranscriptional regulatory element enhances expression of transgenes delivered by retroviral vectors. *Journal of Virology, 73*(4), 2886-2892. https://doi.org/10.1128/JVI.73.4.2886-2892.1999

Copyright

Preface to Chapter 4

The published manuscript enclosed in Chapter 4 is in support of Objective 2, which is to *improve LV productivity through process intensification of the upstream process*. Transient transfection using adherent cells to produce LVs is still the industry standard. However, in recent years, there have been considerable efforts toward improving LV production by switching to suspension cells and developing packaging and stable producer cell lines to improve scalability to industry-scale manufacturing, increase reproducibility and robustness for clinical applications, and decreasing the cost of goods to lower treatment prices. With the continual rise in successful LV clinical trials and approved *ex vivo* LV products, the need for scalable, reproducible, and robust processes are even more critical to generate sufficient and consistently high-quality material for treating patients.

With this trajectory, I believe spending effort in optimizing a process utilizing a producer cell line will make a bigger difference in the field as compared to the other two LV production methods. Therefore, of the three methods of producing LVs in upstream processing – (1) transient transfection of 3 or 4 plasmids, (2) transfecting only the transgene plasmid in a packaging cell line that includes all necessary genetic elements for the assembly and functioning of the vectors, and (3) inducing a producer cell line that incorporates the transgene along with the genetic elements for the vectors – I had chosen a producer cell line for my upstream process intensification work.

The chosen producer cell line was adapted to be in suspension, bypasses the use of plasmids, and uses serum free and chemically defined medium. Suspension cells are advantageous since they improve scalability of the process and ease of operation. Adherent production is labor intensive (e.g., cell detachment during cell passaging and cell amplification) and scales out (i.e., increasing the surface area for cell growth by adding culturing units in parallel) as compared to suspension production, which eliminates cell detachment, takes advantage of the 3D volumetric space of the bioreactor, and scales up (i.e., increasing the bioreactor volume). Omitting the use of serum in the process decreases cost, avoids implementing additional techniques in downstream processing for plasmid removal, and decreases the risk of contamination by adventitious agents. Chemically defined media is suitable for clinical manufacturing by eliminating lot-to-lot variability. While stable producer cell lines have longer process development timelines and higher upfront costs, they reduce running costs and have the potential to generate more consistent harvest titers and higher quality material.

Chapter 4 focuses on the process intensification of LV production in upstream cell culture and highlights the demonstration of a scalable cell retention device that effectively retains the cells while allowing the LV product to pass for harvesting. Implementing LV production in perfusion mode using suspension cells improves LV productivity by increasing the total amount of vectors and by improving the vector quality. Since LVs are unstable with a short half-life at 37ºC that is typical of their cell culture environment, continuously harvesting LVs reduces the residence time in the bioreactor, which limits the loss of functionality. Thus, the continuous nature of the perfusion process plays an important role in maintaining the vector quality. Furthermore, this successful proof-of-concept of the cell retention device makes a significant contribution to the field of LV production, as this device is capable of advancing LV production in large-scale manufacturing in the industry.

In addition, the work in Chapter 4 – choosing an appropriate producer cell line, implementing LV production in perfusion mode, and finding an effective cell retention device – is vital in establishing an integrated semi-continuous manufacturing process that bridges the upstream to the downstream process, which is presented and discussed in Chapter 5.

The two main analytical tools used to support the quality assessment of LVs for the conducted lab-scale experiments discussed in Chapters 4 and 5 are the gene transfer assay (GTA) for quantifying functional vector particles and the digital droplet polymerase chain reaction (ddPCR) assay for quantifying total vector particles. The detailed protocols for GTA and ddPCR are included in the Materials and Methods section of Chapter 4, the optimization of the GTA is described in Appendix 1, and the optimization of the ddPCR assay is described in Appendix 2.

Although the HPLC method, described in Chapter 3, would have been a useful analytical tool for quantifying total vector particles for the work in Chapters 4 and 5 given its high throughput aspect, it was not used to analyze these samples due to the overlap of the project aims. I had started using the ddPCR assay to characterize some samples that I produced for these chapters before transferring the HPLC method to our laboratory; therefore, I decided to continue using the ddPCR assay for consistency across all of my samples. In the Discussion section of Chapter 3, I had stated that ddPCR showed good precision for downstream samples and not upstream samples; however, this claim was refuted as I analyzed more samples from Chapters 4 and 5. Consequently, the ddPCR assay is appropriate for quantifying both upstream and downstream samples.

Chapter 4: Production of Lentiviral Vectors Using a HEK-293 Producer Cell Line and Advanced Perfusion Processing

Authors: **Michelle Yen Tran** and Amine A. Kamen

Author affiliation: Viral Vectors and Vaccine Bioprocessing Group, Bioengineering Department, McGill University, Montreal, Quebec, Canada

Journal: *Frontiers in Bioengineering and Biotechnology – Bioprocess Engineering* (Frontiers)

Year: 2022

Volume: 10

DOI: 10.3389/fbioe.2022.887716

Status: Published

Article History: Received 01 March 2022; Received in revised form 03 May 2022; Accepted 24 May 2022; Available online 14 June 2022

Abstract

The field of lentiviral vector (LV) production continues to face challenges in large-scale manufacturing, specifically regarding producing enough vectors to meet the demand for treating patients as well as producing high and consistent quality of vectors for efficient dosing. Two areas of interest are the use of stable producer cell lines, which facilitates the scalability of LV production processes as well as making the process more reproducible and robust for clinical applications, and the search of a cell retention device scalable to industrial-size bioreactors. This manuscript investigates a stable producer cell line for producing LVs with GFP as the transgene at shake flask scale and demonstrates LV production at 3L bioreactor scale using the Tangential Flow Depth Filtration (TFDF) as a cell retention device in perfusion mode. Cumulative functional yields of 3.3 x 10^{11} and 3.9 x 10^{11} transducing units were achieved; the former over 6 days of LV production with 16.3 L of perfused media and the latter over 4 days with 18 L. In comparing to a previously published value that was achieved using the same stable producer cell line and the acoustic filter as the perfusion device at the same bioreactor scale, the TFDF perfusion run produced 1.5-fold higher cumulative functional yield. Given its scale-up potential, the TFDF is an excellent candidate to be further evaluated to determine optimized conditions that can ultimately support continuous manufacturing of LVs at large scale.

Keywords

Lentiviral vector, stable producer cell line, lentiviral vector production, perfusion, cell retention device, lentiviral vector manufacturing, large-scale manufacturing, continuous manufacturing.

1. Introduction

Lentiviral vectors (LVs) are a popular gene delivery tool in cell and gene therapy and they are the primary tool for *ex vivo* transduction of T-cells for expression of chimeric antigen receptor in CAR-T cell therapies (Escors et al., 2012; Naldini et al., 2016; Milone and O'Doherty, 2018). In LV production, there have been many improvements in vector design, upstream processing, and downstream processing over the years (Tolmachov et al., 2011; Segura et al., 2013; McCarron et al., 2016; Merten et al., 2016; Sharon and Kamen, 2018; Moreira et al., 2021; Perry and Rayat, 2021). However, the field continues to face difficulties in large-scale manufacturing of LVs (Ansorge et al., 2009, 2010; Martínez-Molina et al., 2020), specifically regarding producing

enough vectors to meet the demand for treating patients as well as producing high and consistent quality of vectors for efficient dosing. Continuous processing is appealing for viral vectors, enzymes, exosomes, and cell-based therapies that are unstable (McCarron et al., 2016; Schofield, 2018). For example, the stability of LVs is relatively low, with a half-life of only 3-18 h at 37ºC (Ansorge et al., 2010), and LVs have a high sensitivity to environmental pH, salt concentration, and shear stress during harvest and downstream processing (Merten et al., 2016). In addition, LVs lose their functionality significantly in accordance with downstream processing steps (Transfiguracion et al., 2020) and process hold times.

An impactful strategy for process intensification is to establish an integrated continuous processing, where continuous harvesting in perfusion mode is combined with downstream capture, to provide benefits such as improved product quality and faster processing time, which reduces cost and increases flexibility and productivity (Gutiérrez-Granados et al., 2018; Moleirinho et al., 2020). In terms of LV production, these improvements would have a direct impact on LV product quality in two ways – first, increasing vector production by lengthening the LV production phase through the means of perfusion; second, and more importantly, increasing vector quality by slowing down the loss of functionality of LVs through reduced processing and hold times, which is achieved by continuously removing LVs from the cell culture environment and passing the LVs directly on to downstream processing steps.

To date, no such strategy has been successfully implemented for LV production, largely because commercial cell retention devices used for perfusion tend to retain the lentivirus product, rendering it difficult to remove the fragile LVs. Although a proof of principle has been demonstrated using an acoustic filter (Manceur et al., 2017), this system is not scalable to industrial-size bioreactors. This manuscript explores the possibility of utilizing the Tangential Flow Depth Filtration (TFDF) device as a cell retention device to support LV production in perfusion mode at manufacturing scale, since the device is scalable up to 2000L bioreactor scale. The TFDF combines the benefits of both tangential flow and depth filtration, where it can process high cell density cultures with minimal membrane fouling while allowing for high product recovery. The TFDF is currently commercially used for clarification to replace centrifugation or reduce depth filters and it has been shown to effectively separate cells and cell debris from LVs (Williams et al., 2020). In addition, this device has shown to be non-stressful on cells while supporting multiple harvests (Williams et al., 2020), which supports the notion that it can be used in perfusion mode during cell culture.

Traditionally, LVs are produced by transient transfection, using 3 to 4 plasmids. Due to manufacturing scalability challenges, packaging cell lines have been developed by stably integrating necessary genetic elements for the assembly and functioning of the vectors, leaving only the transgene plasmid to transfect (Kafri et al., 1999; Hu et al., 2015). To further facilitate the scalability of LV production processes, producer cell lines have been developed to integrate the remaining transgene plasmid, making the process more reproducible for clinical applications (Sanber et al., 2015; Tomás et al., 2018; Chen et al., 2020). The stable producer cell line HEK293SF-LVP- CMVGFPq-92 (Manceur et al., 2017), abbreviated as Clone 92, is utilized for the work presented in this manuscript. These producer cells contain GFP as the transgene and VSV-G at the membrane surface; and they are induced with doxycycline and cumate only during the time of LV production, which addresses cytotoxicity issues that typically arise from the viral proteins (e.g., Gag, Rev, VSV-G) (Broussau et al., 2008).

This manuscript presents LV production (1) under different culturing parameters at shake flask scale in batch and pseudo-perfusion modes to better understand Clone 92 producer cells and (2) in perfusion mode at 3L bioreactor scale with TFDF as the cell retention device to evaluate its performance. Of the main aspects that contribute to the LV product quality – identity, potency, purity, and safety – the analysis for this work mainly focuses on the potency aspect, as the identity of the LVs produced by this producer cell line has already been characterized and published (Transfiguracion et al., 2020), and purity and safety are typically addressed in downstream processing. To probe the potency of the LVs produced in this manuscript, we assess the functional vector particles and total vector particles. We use the gene transfer assay, a cell-based analytical method that measures the transgene expression in transduced target cells, to report functional vector particles in transducing units. We use the droplet digital PCR, a physical-based analytical method, to report total vector particles in vector genome units.

2. Materials and Methods

2.1 Stable Producer Cell Line

The stable producer cell line HEK293SF-LVP-CMVGFPq-92 (abbreviated as Clone 92) (Manceur et al., 2017), developed by the National Research Council Canada, was used to produce LVs that contain GFP as the transgene and VSV-G at the membrane surface by inducing with 1μg/mL final concentration of doxycycline and 10 μg/mL final concentration of cumate. The combination of the Tet-on system and the cumate switch provides tighter transcription regulation

(Broussau et al., 2008). The Tet-on system is based on the addition of the tetracycline/doxycycline antibiotic in the culture medium to trigger gene transcription through the tetracycline response element by promoting the binding of the reverse tetracycline transactivator (rtTA2s-M2) to the tetracycline promoter (TR5). The addition of cumate releases the cumate repressor from the copper oxide promoter, allowing for transcription (Broussau et al., 2008).

2.2 LV Production at Shake Flask Scale

125 ml polycarbonate shake flasks from Avantor (Phillipsburg, NJ) were used to produce LVs at shake flask scale. Clone 92 cells were inoculated at 0.35 x 10^6 cells/mL in Hyclone HyCell TransFx-H media from Cytiva (Marborough, MA), supplemented with final concentrations of 4 mM GlutaMax from life Technologies (Grand Island, NY) and 0.1% Kolliphor poloxamer 188 from Millipore Sigma (Ontario, Canada), with a working volume of 25 mL. The shake flasks were incubated at 37ºC with shaking speed of 135 RPM. After 48 h, the low cell density flasks reached 1 x 10^6 cells/mL and they were induced with 1 μg/mL final concentration of doxycycline hyclate and 10 μg/mL final concentration of 4-isopropylbenzoic acid, both from Sigma-Aldrich (Darmstadt, Germany). The high cell density flasks either went through a one-step concentration using centrifugation or daily medium exchange to reach higher cell density, before being induced for LV production.

Some flasks were subjected to medium exchange after induction to achieve "pseudo-perfusion" and some flasks had basic feeding strategies of 6 g/L glucose, prepared in-house using D-(+)-Glucose from Sigma-Aldrich (Darmstadt, Germany), and 3 mM GlutaMax from life Technologies (Grand Island, NY) from the time of induction until the time of harvest. For the flasks that underwent medium exchange after induction, the inducers doxycycline hyclate and 4-isopropylbenzoic acid were added in the medium at the values previously defined above to allow the continuation of LV production. The LVs were harvested 3 days post induction by centrifugation at 300 g for 5 min to remove the induced Clone 92 cells, then 1200 g for 10 min to collect the supernatant. Cell count was done using the Vi-Cell XR Cell Viability Analyzer from Beckman Coulter (Indianapolis, IN).

The details of the different tested parameters are well described in the results Section 3.1 as well as Table 1. The first set of shake flask experiments (M1 through M6) for parameter evaluation were run in single flasks and the second set of shake flask experiments (M17 through M25) for parameter confirmation were run in triplicate flasks.

2.3 LV Production at Bioreactor Scale – Batch Mode

Two 1L bioreactors from Applikon Biotechnology (Delft, Netherlands) were used to produce LVs in batch mode. Clone 92 cells were inoculated at 0.35 x 10^6 cells/mL in Hyclone HyCell TransFx-H media from Cytiva (Marborough, MA), supplemented with final concentrations of 4 mM GlutaMax from life Technologies (Grand Island, NY) and 0.1% Kolliphor poloxamer 188 from Millipore Sigma (Ontario, Canada), at a working volume of 700 mL. Some media was added 48 h after inoculation to target 1 x 10^6 cells/mL at the time of induction, 1 μg/mL final concentration of doxycycline hyclate and 10 μg/mL final concentration of 4-isopropylbenzoic acid, both from Sigma-Aldrich (Darmstadt, Germany), were added for induction, and the final working volume was at 850 mL. The LVs were harvested 3 days post induction by centrifugation at 300 g for 5 min to remove the induced Clone 92 cells, then 1200 g for 10 min to collect the supernatant. The set points were 7.15 for pH, 37ºC for temperature, 40% for dissolved oxygen, and 100 RPM for stirrer. Cell count was done using the Vi-Cell XR Cell Viability Analyzer from Beckman Coulter (Indianapolis, IN).

2.4 LV Production at Bioreactor Scale – Perfusion Mode

Two 3L bioreactors from Applikon Biotechnology (Delft, Netherlands) were used for LV production in perfusion mode with the Tangential Flow Depth Filtration (TFDF) cartridge from Repligen Corp (Rancho Dominguez, CA) as the cell retention device, which was operated by the KML-100 System, also from Repligen Corp. Clone 92 cells were inoculated at 0.35 x 10^6 cells/ mL at 2 L working volume and the cells were grown in batch mode until 72 h after inoculation. Then, perfusion started at 0.5 VVD (vessel volume per day) for 3 days and ramped up to 0.75 and 1 VVD, respectively, for the following 2 days to support the high cell density. At 176 h after inoculation, in which the viable cell density was 11.4 x 10^6 cells/mL for perfusion run 1 (P1) and 12.3 x 10^6 cells/mL for perfusion run 2 (P2), 1μg/ml final concentration of doxycycline hyclate and 10μg/mL final concentration of 4-isopropylbenzoic acid, both from Sigma-Aldrich (Darmstadt, Germany), were added for induction and perfusion continued at 1 VVD for P1 and ramped up to 2 VVD for P2.

The inducers and basic feeding strategies of 6 g/L glucose, prepared in-house using D-(+)-Glucose from Sigma-Aldrich (Darmstadt, Germany), and 3 mM GlutaMax from life Technologies (Grand Island, NY) were employed from the time of induction until the final harvest, which was at 6 days post induction at 3.3 x 10^6 cells/mL for P1 and 4 days post induction at 5.9 x 10^6 cells/mL

for P2. The HyClone HyCell TransFx-H modified SH31192 (referred to as "Prototype" media in the manuscript) from Cytiva (Logan, UT) was used for the cell growth phase in both perfusion runs (VVD: 0.5, 0.5, 0.75, 1). For P1, the HyCell TransFx-H medium from Cytiva (Marborough, MA) was used for the LV production phase (VVD: 1, 1, 1.25, 1.25, 1.25, 1). For P2, the HyClone HyCell TransFx-H modified SH31192 was used for the LV production phase at a constant 2 VVD rate each day. Both types of HyCell media were supplemented with final concentrations of 4 mM GlutaMax from life Technologies (Grand Island, NY) and 0.1% Kolliphor poloxamer 188 from Millipore Sigma (Ontario, Canada).

For P1, one TFDF cartridge with the surface area of 30 cm^2 was used for cell growth phase (7 days and 8 h), LV production phase (6 days), and a final harvest step (1.5 h), where the cell culture in the bioreactor was concentrated, diafiltered with 1x phosphate buffered saline (PBS) from Cytiva (Logan, UT), and concentrated again. For P2, one TFDF cartridge with the surface area of 30 cm^2 was used for cell growth phase (7 days 8 h) and LV production phase (4 days), with no final harvest step. The set points for the bioreactors were 7.15 for pH, 37^{o}C for temperature, 40% for dissolved oxygen, and 100 RPM for stirrer. Cell count was done using the Vi-Cell XR Cell Viability Analyzer from Beckman Coulter (Indianapolis, IN).

2.5 Gene Transfer Assay for Functional LV Quantification

A flow cytometry based GTA was used to determine functional vector titer in transducing units per milliliter (TU/mL). HEK293SF (Cote et al., 1998) cells were inoculated in tissue culture 24-well suspension plates from Sarstedt (Nümbrecht, Germany) at 0.5 x 10^6 cells/mL in Hyclone HyCell TransFx-H media from Cytiva (Marborough, MA) supplemented with 8 ng/µL final concentration of polybrene at a volume of 450 µL per well and then transduced with 50 µL neat or diluted LVs per well, for a final volume of 500 µL per well. LV sample dilutions were made with HyCell TransFx-H media. The plates were incubated for 72 h at 37^{o}C with shaking speed of 135 RPM.

Transduced cells were harvested by centrifugation at 500 g for 6 min to remove the supernatant. The pellet of transduced cells was resuspended in 150 µL of 2% paraformaldehyde (PFA) from Electron Microscopy Sciences (Hatfield, PA) in 1x phosphate buffered saline (PBS) from Cytiva (Logan, UT) for fixing cells for 30 min. The transduced cells were once again centrifuged at 500 g for 6 min and resuspended in 150 µL of 1x PBS before reading for GFP expression. Flow cytometry was carried out on the Accuri C6 instrument from BD Sciences

(Franklin Lakes, NJ).

All LV samples, positive control, and negative control were run in duplicates on the same assay plate. The LV samples were assayed at the same dilution in duplicates. The positive control was an LV supernatant produced in our lab that has been used as the internal control for our GTA and ddPCR work. The negative control was cells that were "transduced" with 50 µL media rather than LVs. The percent of GFP expression was used to calculate for the titer in TU/mL. The equation used for the calculation is (GFP percentage) / 100 x total cells x dilution factor x 1000 / (volume of LVs).

2.6 Droplet Digital Polymerase Chain Reaction Assay for Total LV Quantification

The LV vector genome (Vg/mL) was quantified by a QX200™ Droplet Digital PCR (ddPCR) System from Bio-Rad (Hercules, CA). Prior to running samples on the ddPCR system, sample preparation included extracting RNA from LV samples using the High Pure Viral Nucleic Acid Kit from Roche (Basel, Switzerland) and reverse transcribing into cDNA using the iScript™ Select cDNA Synthesis Kit from Bio-Rad (Hercules, CA), both following the manufacturers' protocols. Although the Select cDNA Synthesis Kit states that 1 pg to 1 µg of total RNA can be accommodated in the cDNA prep, results from our lab showed that either extreme of that range gives falsely elevated vector genome titer. Thus, to minimize variability, we included a normalization step by targeting 10 ng RNA for cDNA synthesis for every sample.

Following the RNA extraction step, the NanoDrop™ 2000 Spectrophotometer from Thermo Fisher Scientific (Waltham, MA) was used to determine the RNA content and the elution buffer from the High Pure Viral Nucleic Acid Kit was used as a buffer blank. The RNA samples were read in duplicates on the NanoDrop to ensure reliable values. Then, the RNA samples were diluted 1:100 with milli-Q water, and 10 ng RNA from that dilution was used in the cDNA synthesis step for each sample. For example, for a sample where a value of 100 ng was obtained from the NanoDrop and 1ng was obtained from the 1:100 dilution, 10 µL of the 1:100 dilution plus 3 µL milli-Q water was used for a total sample volume of 13 µL in the cDNA reaction.

Each PCR reaction was prepared with 11.1 µL of the QX200TM ddPCR™ EvaGreen Supermix, 1.1 µL of the 2 µM stock of woodchuck hepatitis virus posttranscriptional regulatory element (WPRE) primer set, 4.4 µL milli-Q water, and 5.5 µL neat or diluted cDNA samples in milli-Q water. WPRE was used because it is known to stabilize the transgene mRNA and therefore enhance transgene expression delivered by LVs (Zufferey et al., 1999). For droplet generation in

the QX200™ Droplet Generator, 20 µL of the PCR reactions were transferred to the G8™ Cartridges for QX200™. Then, the droplets were transferred to the ddPCR™ 96-Well Plate and the following PCR program was run on the thermo-cycler: one cycle of 95ºC for 5 min; 40 cycles of 95ºC for 30 s, 60ºC for 1 min, and 72ºC for 30 s; one cycle of 72ºC for 5 min; indefinite 12ºC hold. ddPCR results were analyzed with the QX200™ Droplet Reader and QuantaSoft Program.

All LV samples, positive control, and negative control were run in duplicates. LV samples were run in duplicates at two different sample dilutions. The positive control was an LV supernatant produced in our lab that has been used as the internal control for our ddPCR and GTA work. The negative control was milli-Q water that is added in place of an LV sample. Reverse transcription minus controls were tested to ensure there is no detectable genomic DNA impurity from the producer cells present in the LV production batches.

2.7 Picogreen Assay for DNA Quantification

DNA was quantified using the Quant-iT PicoGreen dsDNA Assay kit from Invitrogen (Eugene, OR). Each LV sample was serially diluted from 1:2 to 1:256 with 1x TE buffer in the CorningTM Polystyrene 96-Well Microplate from Fisher Scientific (Ontario, Canada). The λ dsDNA standard was diluted with 1x TE buffer from 0 to 500 ng/mL and the dilutions were included in duplicates on the same plate. After adding the diluted dye reagent to each well and incubating for 15 min at room temperature, the fluorescence was measured in the SYNERGY HTX multi-mode reader at 480/520 nm. The final DNA concentrations for samples were calculated based on the generated standard curve.

2.8 Statistical Analysis

Ordinary one-way ANOVA was performed to compare the effect of the selected parameters (i.e., high cell density at the time of induction, medium exchange post-induction to implement pseudo-perfusion, and feeding post-induction) on the total functional particles and total vector particles for the second set of shake flask experiments as described in Section 3.1. An unpaired t-test was performed to compare the total functional particles and total vector particles attained in perfusion mode and batch mode at bioreactor scale as described in Section 3.3. For all analysis, the alpha was set to 95%, the comparisons that resulted in p values <0.05 were considered statistically significant, and the representation of the p-values in the figures is as follows: 0.1234 (ns), 0.0332 (*), 0.0021 (**), 0.0002 (***), <0.0001 (****).

3. Results

3.1 LV Production at Shake Flask Scale

An extensive set of shake flask experiments was performed to explore different parameters to select the best ones leading to improved yields for LV production using Clone 92 producer cells. The tested parameters are low cell density (LCD) of 1 x 10^6 cells/ mL versus high cell density (HCD) of 5 x 10^6 cells/mL at the time of induction (TOI), one-step concentration versus medium exchange before induction as the method in reaching HCD, medium exchange after induction to mimic perfusion at bioreactor scale (henceforth referred to as "pseudo-perfusion," as the medium is exchanged every 24 h instead of continuously), and basic feeding strategies of 6 g/L glucose and 3 mM glutamine after induction.

Comparing to the baseline parameters of LCD at the TOI with no medium exchange (i.e., batch mode) and no feeding (baseline shake flask referred to as M1), the first set of experiments was designed to assess: whether medium exchange post-induction (i.e., pseudo-perfusion) improve LV production at the same LCD (M2), whether Clone 92 cells can produce LVs at HCD with only feeding if a one-step concentration method is employed (M3), whether there are differences in one-step concentration (M3) versus medium exchange (M4) pre-induction as a means of reaching HCD, and the effects of pseudo-perfusion and feeding (M5 and M6).

Table 1 compares the total functional particles (TFP) in transducing units (TU), determined by the gene transfer assay (GTA) with GFP as the readout signal, and the total vector particles (TVP) in vector genome copies (Vg), determined by droplet digital PCR, for the sample pools at 1 dpi (day post induction), 2 dpi, and 3 dpi, as well as final product pools. Table 1 also compares the ratio of TVP to TFP (TVP/TFP) for the final product pools, where a smaller number indicates higher LV potency since it means that a higher percentage of the produced total vector particles have effectively transduced the host cells and delivered the genetic material to be integrated in the host cell genome, thus expressing the GFP transgene.

In Table 1, Section A1 summarizes the increase or decrease of TFP, TVP, and TVP/TFP of shake flasks M2-M6 with the tested parameters, as described in the preceding paragraph, when compared to the baseline shake flask M1. These results show that the strategies of inducing at HCD, pseudo-perfusion, and feeding can increase the TFP and TVP of the final product up to 32- and 13-fold, respectively, and decrease the TVP/TFP up to 3.4-fold. Section A2 shows that one-step concentration increases the TFP of the final product by 1.3-fold and decreases the TVP/TFP by 1.5-fold when compared to medium exchange pre-induction to reach HCD, while the TVP is

comparable. Section A3 shows that pseudo-perfusion alone at HCD increases the TFP and TVP of the final product by 2.8- and 2.3-fold, respectively, and decreases the TVP/TFP by 1.2-fold. Section A4 shows that feeding alone at HCD increases the TFP and TVP of the final product by 1.9- and 2.7-fold, respectively, although the TVP/TFP is in favor of no feeding.

Shake flask	Parameters	TFP = total functional particles (in transducing units, TU)				TVP = total vector particles (in vector genome copies, Vg)				TVP/TFP
		1 dpi	2 dpi	3 dpi	Final product	1 dpi	2 dpi	3 dpi	Final product	Final product
A1. Parameter evaluation: Comparing to M1 (baseline conditions: LCD, batch, no feed)										M1: 55
M2	LCD Pseudo-perfusion	+3.4x	+15x	+3.9x	+6.1x	+5.2x	+2.5x	+5.4x	+3.1x	27 (-2.0x)
M3	HCD-C Feed	+25x	+41x	+8.4x	+15x	+7.8x	+6.6x	+3.0x	+5.1x	19 (-2.9x)
M4	HCD-ME Feed	+41x	+35x	+4.7x	+11x	+40x	+9.0x	+0.4x	+5.8x	28 (-2.0x)
M5	HCD-ME Pseudo-perfusion	+37x	+52x	+8.2x	+17x	+31x	+9.7x	+7.6x	+4.9x	16 (-3.4x)
M6	HCD-ME Pseudo-perfusion Feed	+35x	+111x	+13x	+32x	+25x	+17x	+9.6x	+13x	23 (-2.4x)
A2. Parameter evaluation: Comparing one-step concentration vs. medium exchange to reach HCD										
M3	Concentration		comparable	+1.8x	+1.3x			+7.2x	comparable	-1.5x
M4	Medium exchange	+1.6x				+5.1x	+1.4x			
A3. Parameter evaluation: Effect of pseudo-perfusion at HCD										
M4		comparable				+1.6x				
M6	Pseudo-perfusion		+3.1x	+2.8x	+2.8x		+1.9x	+23x	+2.3x	-1.2x
A4. Parameter evaluation: Effect of feed at HCD										
M5		comparable				+1.2x				-1.4x
M6	Feed		+2.2x	+1.6x	+1.9x		+1.7x	+1.3x	+2.7x	
B. Parameter confirmation: Comparing the average of two selected parameter sets vs. baseline conditions set (i.e., LCD set)										LCD: 60
HCD-C set (n = 3)	HCD-C Pseudo-perfusion, Feed	+13x	+40x	+15x	+23x	+10x	+12x	+3.6x	+8.6x	22.3 (-2.7x)
HCD-ME set (n = 3)	HCD-ME Pseudo-perfusion, Feed	+71x	+46x	+9.2x	+26x	+52x	+15x	+6.0x	+12x	29.8 (-2.0x)

Table 1. Comparison of LV production at shake flask scale. TFP, total functional particles; TVP, total vector particles; TU, transducing units; Vg, vector genome; dpi, days post induction; LCD, low cell density; HCD-C, high cell density, obtained by one-step concentration; HCD-ME, high cell density, obtained by daily medium exchange; pseudo-perfusion = daily medium exchange after induction to mimic perfusion at bioreactor scale; feed = 6 g/L glucose and 3 mM glutamine daily. Parameter evaluation was implemented in single flasks (M1 through M6) to explore different parameters (inducing at HCD, pseudo- perfusion, and feeding) to select the best ones leading to improved yields for LV production using Clone 92 producer cells. Parameter confirmation was implemented in triplicate flasks for 3 sets (LCD baseline conditions; HCD-C + pseudo-perfusion + feed; HCD-ME + pseudo-perfusion + feed) to confirm results.

For parameter evaluation in this first set of experiments (shake flasks M1-M6), Figure 12A shows a decreasing trend in both the viable cell density (VCD) and percent cell viability over the time course of LV production, and Figure 12B shows an increase of the TFP and TVP when the strategies of HCD at the TOI, pseudo- perfusion, and feeding are implemented. Overall, the results from the first set of experiments support the findings of improved yields when operating under the

parameters of HCD at the TOI, medium exchange post-induction to implement pseudo- perfusion, and feeding post-induction (henceforth referred to as "selected parameters").

The second set of experiments was designed to confirm these results and to compare once again the method in reaching HCD. The shake flasks were set up in triplicates for baseline parameters (referred to as LCD set) as previously defined for M1, selected TFDF parameters with one-step concentration as the method to reach HCD at the TOI (referred to as HCD-C set), and selected parameters with medium exchange pre-induction as the method to reach HCD at the TOI (referred to as HCD-ME set). Section B in Table 1 shows that, when compared to the average values of the baseline parameters (LCD set), the average values of the selected parameter sets: increase the TFP of the final product by 23- and 26-fold for HCD-C and HCD-ME, respectively; increase the TVP by 8.6- and 12-fold, respectively; and decrease the TVP/TFP by 2.7- and 2.0-fold, respectively.

For parameter confirmation in this second set of experiments, Figure 12C shows a similar decreasing trend in both the VCD and percent cell viability over the time course of LV production as seen in Figure 12A and Figure 12D confirms that implementing the tested parameters resulted in an increase of TFP and TVP. Taking a closer look, Figure 12D shows that the TFP of the final product of both selected parameter sets (average 1.52×10^{10} TFP for HCD-C set, average 1.71×10^{10} TFP for HCD-ME set) are 2 logs higher than the baseline parameter set (average 6.54×10^{8} TFP for LCD set). Figure 12D also shows an increasing trend in TVP, where the TVP of the final product of both selected parameter sets (average 3.33×10^{11} TVP for HCD-C set, average 4.81×10^{11} TVP for HCD-ME set) are 1 log higher than the baseline parameter set (average 3.89×10^{10} TVP for LCD set).

Ordinary one-way ANOVA was performed to compare the effect of the selected parameters on TFP and TVP. The statistical analysis revealed that there was a statistically significant difference in mean TFP (Figure 12E) between at least two groups ($F(2, 6) = 21.33$, $p = 0.0019$). Tukey's HSD Test for multiple comparisons found that the mean value of TFP was significantly different between the LCD set and HCD-C set ($p = 0.0045$) as well as between the LCD set and the HCD-ME set ($p = 0.0024$). There was no statistically significant difference in TFP between HCD-C and HCD-ME ($p = 0.7772$), which makes sense since the only experimental difference between these two groups is the method in reaching HCD (i.e., one-step concentration for HCD-C and daily medium exchange for HCD-ME). The statistical analysis also revealed that there was a statistically significant difference in mean TVP (Figure 12F) between at least two

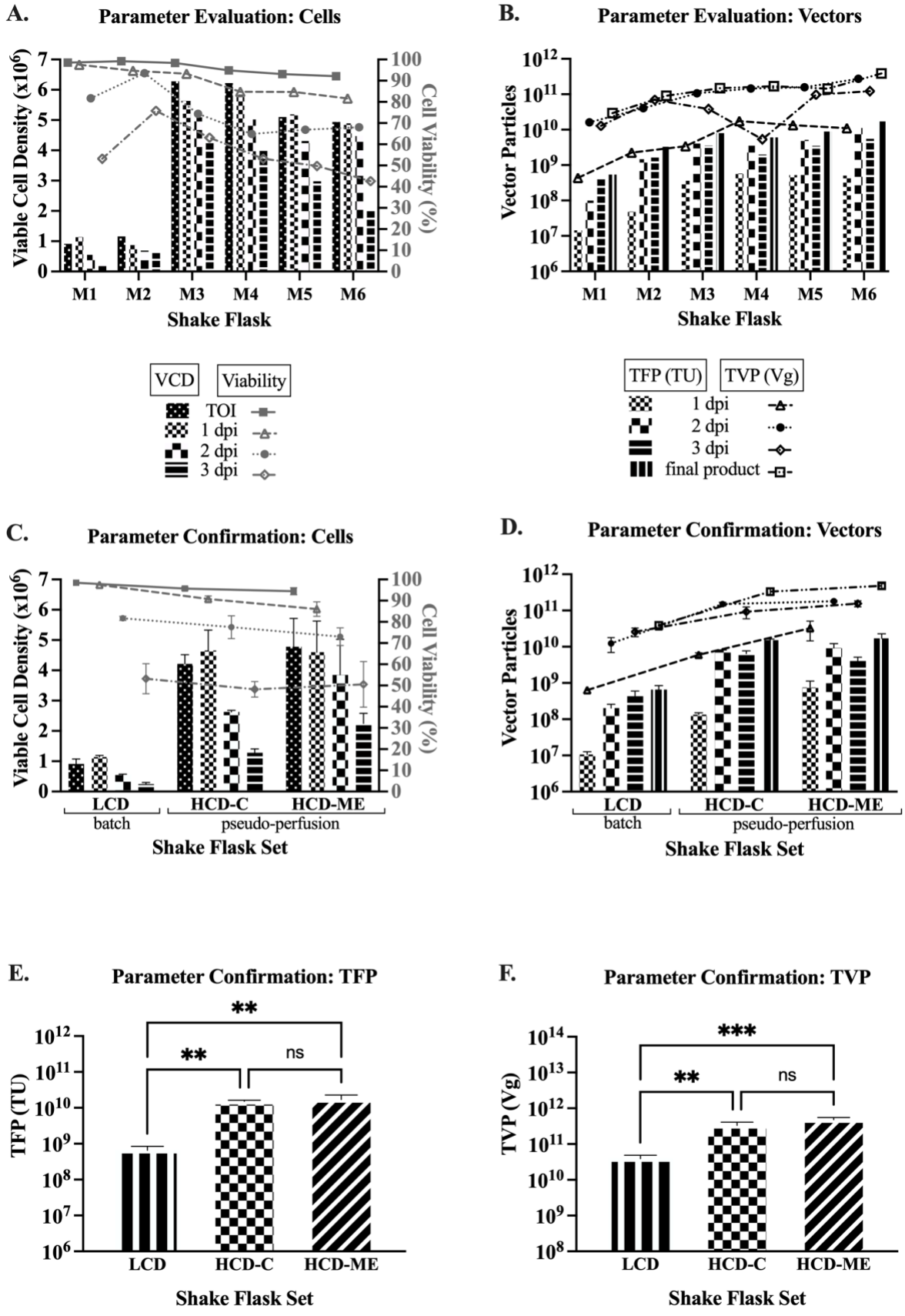
A.
Parameter Evaluation: Cells
Viable Cell Density (x10^6)
Cell Viability (%)
M1
M2
M3
M4
M5
M6
Shake Flask
VCD
Viability
TOI
1 dpi
2 dpi
3 dpi
B.
Parameter Evaluation: Vectors
Vector Particles
Shake Flask
TFP (TU)
TVP (Vg)
1 dpi
2 dpi
3 dpi
final product
C.
Parameter Confirmation: Cells
Viable Cell Density (x10^6)
Cell Viability (%)
LCD
HCD-C
HCD-ME
batch
pseudo-perfusion
Shake Flask Set
D.
Parameter Confirmation: Vectors
Vector Particles
Shake Flask Set
E.
Parameter Confirmation: TFP
TFP (TU)
**
ns
Shake Flask Set
F.
Parameter Confirmation: TVP
TVP (Vg)
***
Shake Flask Set

Figure 12. LV production at shake flask scale. VCD = viable cell density; TOI = time of induction; dpi = days post induction; LCD = low cell density at the TOI; HCD-C = high cell density at the TOI, obtained by one-step concentration; HCD-ME = high cell density at the TOI, obtained by daily medium exchange; pseudo-perfusion = daily medium exchange after induction to mimic perfusion at bioreactor scale; TFP = total functional particles; TVP = total vector particles; TU = transducing units; Vg = vector genome. 1, 2, and 3 dpi represent sample pools (e.g., 1 dpi includes LVs produced from 0 to 24 h post induction). (A) VCD and cell viability for parameter evaluation (6 single flasks: M1 = baseline conditions: LCD, batch, no feed; M2 = LCD, pseudo-perfusion; M3 = HCD-C, feed; M4 = HCD-ME, feed; M5 = HCD-ME, pseudo-perfusion; M6 = HCD-ME, pseudo-perfusion, feed). (B) TFP and TVP for parameter evaluation (flasks M1-M6). (C) VCD and cell viability for parameter confirmation (3 flasks per set x 3 sets: LCD baseline conditions; HCD-C + pseudo-perfusion + feed; HCD-ME + pseudo-perfusion + feed; values are shown as mean +SD). (D) TFP and TVP for parameter confirmation (n = 3 per set, values are shown as mean +SD). (E) Statistical analysis of TFP using one-way ANOVA–adjusted p-value for LCD vs. HCD-C is 0.0045, LCD vs. HCD-ME is 0.0024, and HCD-C vs. HCD-ME is 0.7772. (F) Statistical analysis of TVP using one-way ANOVA–adjusted p-value for LCD vs. HCD-C is 0.0024, LCD vs. HCD-ME is 0.0003, and HCD-C vs. HCD-ME is 0.0532.

groups ($F(2, 6) = 41.97$, $p = 0.0003$). Tukey's HSD Test for multiple comparisons found that the mean value of TVP was significantly different between LCD and HCD-C ($p = 0.0024$) as well as between LCD and HCD-ME ($p = 0.0003$). There was no statistically significant difference in TVP between HCD-C and HCD-ME ($p = 0.0532$).

The results from the second set of experiments confirmed the findings of improved yields for LV production using Clone 92 producer cells when operating under the parameters of HCD at the TOI, medium exchange post-induction to implement pseudo-perfusion, and feeding post-induction. The actual TFP and TVP values for both shake flask experiments are presented in Supplementary Table S4.

3.2 LV Production in Perfusion Mode Using TFDF

Two LV production runs in perfusion mode with TFDF as the cell retention device at 3L bioreactor scale were implemented. Clone 92 cells were inoculated at 0.35×10^6 cells/mL at 2 L working volume and the cells were grown in batch mode until 72 h after inoculation. Then, perfusion started at 0.5 VVD (vessel volume per day) for 3 days and ramped up to 0.75 and 1 VVD, respectively, for the following 2 days to support the HCD. At 176 h after inoculation, in which the VCD was 11.4×10^6 cells/mL for perfusion run 1 (P1) and 12.3×10^6 cells/mL for perfusion run 2 (P2), doxycycline and cumate were added for induction, and perfusion continued at 1 VVD for P1 and ramped up to 2 VVD for P2. The exchange rate for the LV production phase was ≤ 1.25 VVD for P1 and 2 VVD for P2. The inducers and basic feeding strategies of 6 g/L glucose and 3 mM glutamine were employed from the time of induction until the end of the run, which was 6 dpi for P1 and 4 dpi for P2. The total volume of media used for the LV production

phase was 16.3 L for P1 and 18 L for P2. A final harvest step, where the cell culture in the bioreactor was concentrated, diafiltered with 1x phosphate buffered saline, and concentrated again, was performed for P1 using the same TFDF filter utilized for the LV production phase in perfusion mode. The final harvest step was not performed for P2.

Figure 13A shows that the cell viability dropped steadily after induction, labeled as day 0 on the x-axis, whereas the total cell density and VCD increased at 1 dpi before dropping steadily. The perfusate was sampled at various time points to determine LV production kinetics, where the titers shown in Figure 13B represent a snapshot of the LV production at specific timepoints. As indicated in Figure 13B, there were some common and some different time points sampled between the two perfusion runs.

For P1, the functional titers for 1 hpi (hour post induction), 6 hpi, and 9 hpi were under the limit of detection of the GTA and the first detectable functional titer is 9.7×10^4 TU/mL at 13 hpi. The peak functional titer is 4.4×10^7 TU/mL at 72 hpi and the peak total titer is 3.6×10^9 Vg/mL at 84 hpi. For P2, the peak functional titer is 4.1×10^7 TU/mL at 72 hpi and the peak total titer is 4.5×10^9 Vg/mL at 92 hpi. Looking at the kinetics of TVP/TFP, Figure 13D shows the lowest ratios between 24 hpi and 75 hpi for P1 and between 24 hpi and 72 hpi for P2.

The bioreactor vessel was also sampled at every 24-h interval to capture the snapshot of LV production at those specific timepoints to compare to the perfusate samples, with the goal of assessing whether the virus is retained by the TFDF device, as shown in Figure 13C. Overall, both functional and total vector titers are comparable between the perfusate and bioreactor samples, which indicates that the LVs were not retained by the TFDF device. Figures 13B and 13C show that the functional vector titers are typically 2 logs lower than total vector titers, which is the same trend observed in past LV experiments conducted at our laboratory as well as some materials produced at the National Research Canada (Transfiguracion et al., 2020).

Figure 13E shows the cumulative vectors produced during the two perfusion runs – 3.3×10^{11} TFP and 1.8×10^{13} TVP over 6 days for P1; and 3.9×10^{11} TFP and 2.0×10^{13} TVP over 4 days for P2. Figure 13F shows a comparison of DNA content by the Picogreen assay of an early time point (48 hpi) and a late time point (96 hpi) between 3 sample types – perfusate and bioreactor samples that capture a snapshot of LV production at those time points, and harvest pool (i.e., 48 hpi includes LVs produced from 24 to 48 hpi, 96 hpi includes LVs produced from 72 to 96 hpi). Overall, the results show that DNA content is higher at the later stage of the perfusion bioreactor run.

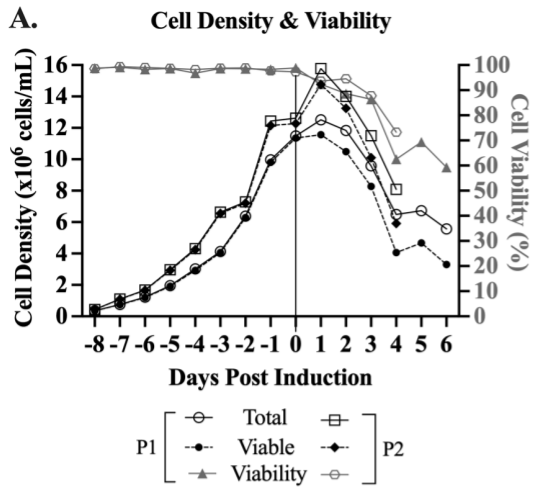
A.
Cell Density & Viability
Cell Density (x10^6 cells/mL)
Cell Viability (%)
Days Post Induction
P1
Total
Viable
Viability
P2

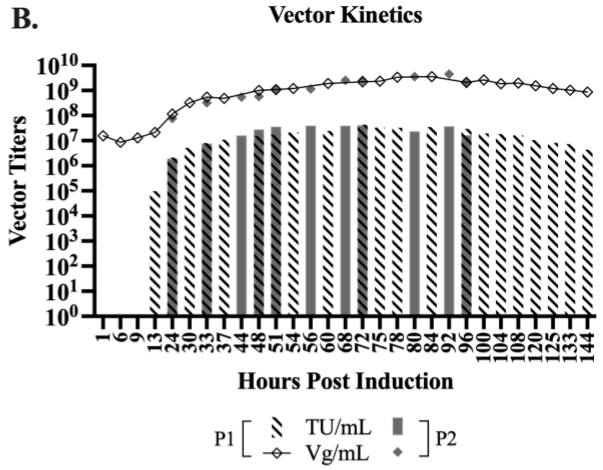
B.
Vector Kinetics
Vector Titers
Hours Post Induction
P1
TU/mL
Vg/mL
P2

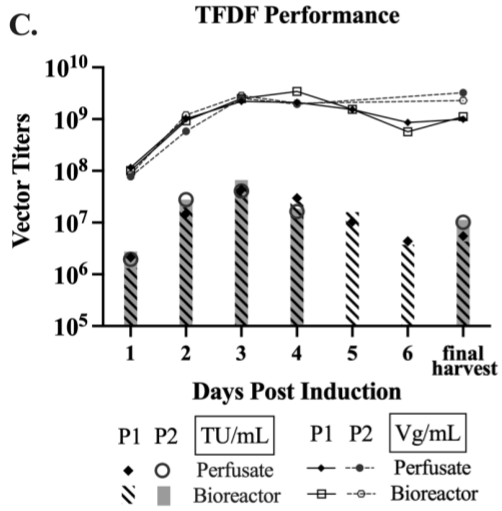
C.
TFDF Performance
Vector Titers
Days Post Induction
final harvest
P1 P2 TU/mL
Perfusate
Bioreactor
P1 P2 Vg/mL
Perfusate
Bioreactor

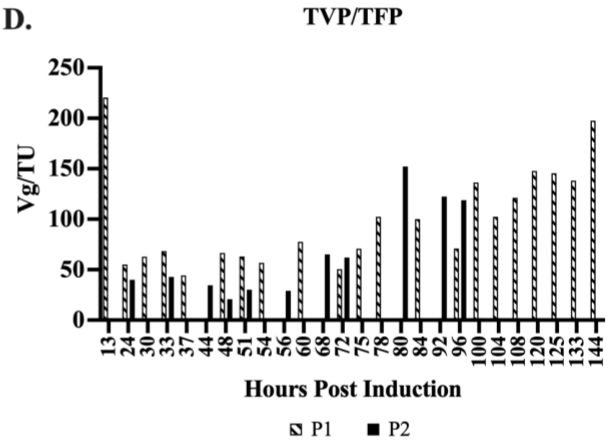
D.
TVP/TFP
Vg/TU
Hours Post Induction
P1
P2

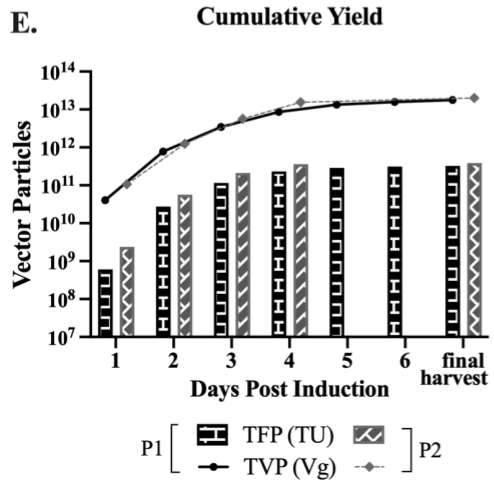
E.
Cumulative Yield
Vector Particles
Days Post Induction
final harvest
P1
TFP (TU)
TVP (Vg)
P2

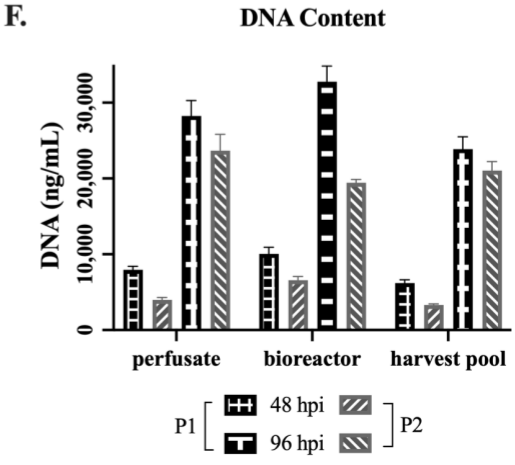
F.
DNA Content
DNA (ng/mL)
perfusate
bioreactor
harvest pool
P1
48 hpi
96 hpi
P2

Figure 13. LV production in perfusion mode using TFDF. TFDF = Tangential Flow Depth Filtration; P1 = perfusion run 1; P2 = perfusion run 2; TU = transducing units; Vg = vector genome; TFP = total functional particles; TVP = total vector particles. "Final harvest" refers to the material recovered from the final harvest step (i.e., concentration, diafiltration, final concentration) in P1 and the leftover material in the bioreactor in P2 at the end of the perfusion runs. (A) Cell density and cell viability data of perfusion runs (n = 2). (B) LV production kinetics in TU/mL and Vg/mL (some common and some different time points sampled between P1 and P2). (C) Perfusate and bioreactor samples in TU/mL and Vg/mL to assess whether the virus is retained by the TFDF device. (D) Ratio of TVP to TFP (some common and some different time points sampled between P1 and P2). (E) Cumulative vector yields for P1 (3.2×10^{11} TFP, 1.8×10^{13} TVP) over 6 days and for P2 (3.9×10^{11} TFP, 2.0×10^{13} TVP) over 4 days. (F) DNA content at an early time point (48 hpi) and late time point (96 hpi) of the perfusion runs (values are shown as mean + SD and refer to serial dilutions of the samples on the assay plate).

3.3 Improving TFP and TVP With TFDF Perfusion Bioreactors

Figure 14 compares the two 3L bioreactors that used the TFDF as a cell retention device (HCD of average 11.8×10^6 cells/mL at the TOI, perfusion mode, basic feeding of 6 g/L glucose and 3 mM glutamine, harvested at 6 dpi for run 1 and 4 dpi for run 2) and two 1L bioreactors at baseline parameters (LCD of average 1.42×10^6 cells/mL at the TOI, batch mode, no feeding, both harvested at 3 dpi). Figure 14A shows that the cell viability drops slower in the perfusion runs as compared to the batch runs. Figure 14B shows higher DNA content for the two perfusion runs as compared to the two bioreactor runs for the sample pool up to 3 dpi (i.e., includes LVs produced from 0 to 72 hpi).

Figure 14C recapitulates the TFP and TVP produced during each 24-h interval and shows higher values for perfusion. Comparing the first three sample pools, the average TFP for the perfusion runs is higher than the average TFP for the batch runs by 1 log for 1dpi (1.5×10^9 vs. 1.2×10^8), by 2 logs for 2dpi (4.1×10^{10} vs. 4.3×10^8), and by 2 logs for 3 dpi (1.2×10^{11} vs. 4.4×10^9). As for the TVP, the average for the perfusion runs is higher than the average TVP for the batch runs by 1 log for all three sample pools (7.4×10^{10} vs. 9.7×10^9 for 1 dpi, 9.4×10^{11} vs. 4.8×10^{10} for 2 dpi, and 3.5×10^{12} vs. 3.0×10^{11} for 3 dpi).

An unpaired t-test was performed to compare the TFP and TVP attained in perfusion mode and batch mode (Figure 14D). There was a significant difference in TFP between perfusion mode ($M = 5.1 \times 10^{10}$, $SD = 3.0 \times 10^9$) and batch mode ($M = 6.3 \times 10^9$, $SD = 2.5 \times 10^9$); $t(2) = 16.3$, $p = 0.0037$). Also, there was a significant difference in TVP between perfusion mode ($M = 1.4 \times 10^{12}$, $SD = 2.8 \times 10^{10}$) and batch mode ($M = 4.5 \times 10^{11}$, $SD = 1.4 \times 10^{11}$); $t(2) = 9.7$, $p = 0.0104$).

To facilitate a direct comparison between the perfusion and batch runs, the cumulative yields are normalized per liter of harvest. Figure 14E shows the normalized cumulative yields of average 5.1×10^{10} TU/L and average 1.4×10^{12} Vg/L for the perfusion runs and average 6.3×10^9

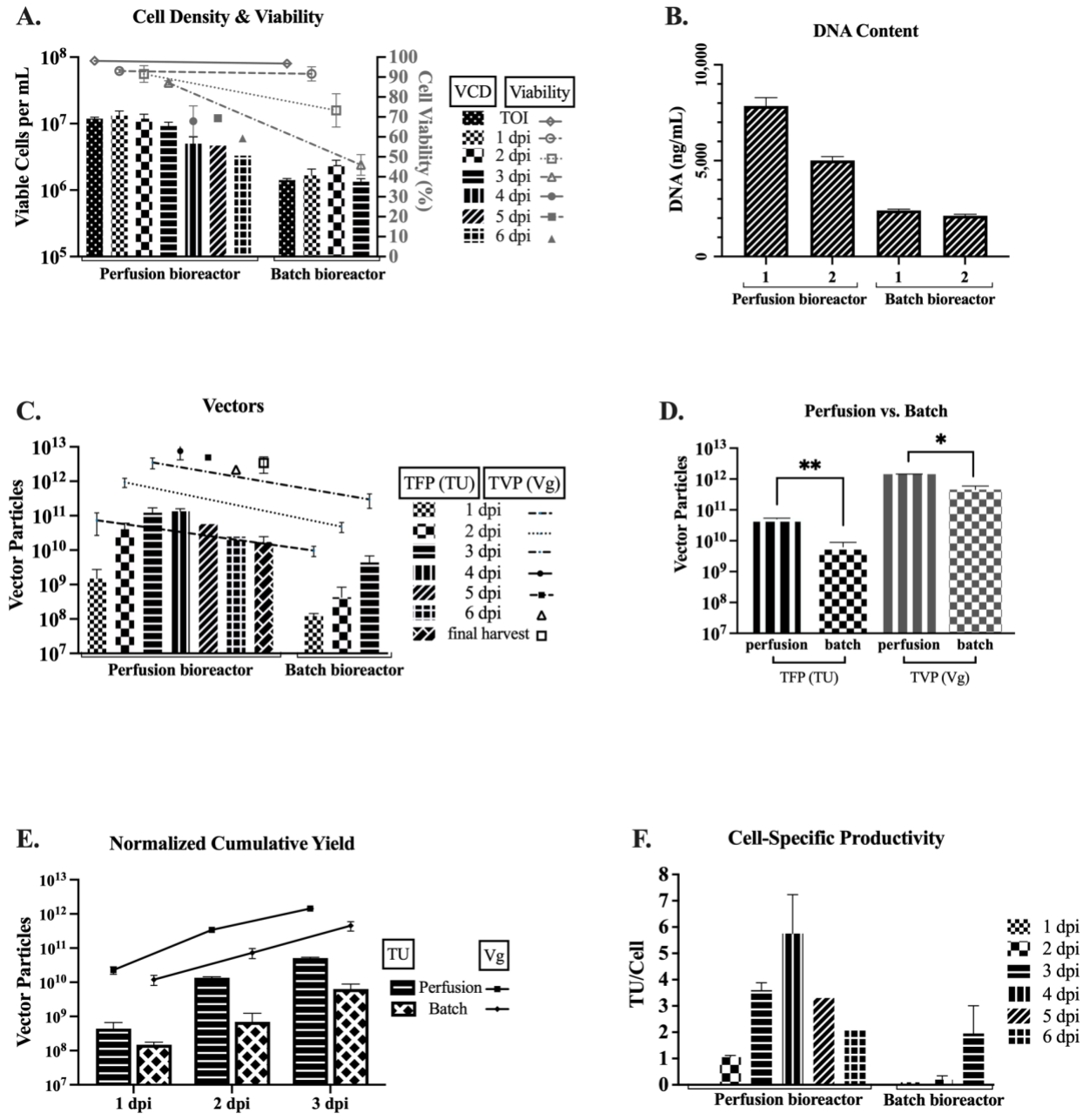

Figure 14. Improved TFP and TVP with TFDF perfusion bioreactors. TFDF = Tangential Flow Depth Filtration; VCD = viable cell density; TOI = time of induction; dpi = days post induction; TFP = total functional particles; TVP = total vector particles; TU = transducing units; Vg = vector genome. 1 dpi, 2 dpi, and 3 dpi represent sample pools (e.g., 2 dpi includes LVs produced from 24 to 48 h post induction). Values are shown as mean + SD (n = 2 for perfusion runs, n = 2 for bioreactor runs). (A) VCD and cell viability data. (B) DNA content for the sample pool up to 3 dpi (i.e., includes LVs produced from 0 to 72 h post induction; values shown as mean + SD refer to serial dilutions of the samples on the assay plate). (C) TFP and TVP data. (D) Statistical analysis using an unpaired t-test – adjusted p-value for TFP between perfusion vs. batch runs is 0.0037 and adjusted p-value for TVP between perfusion vs. batch runs is 0.0104. (E) Cumulative yields normalized per 1 L of harvest (at 3dpi - perfusion runs: average 5.1 x 10^{10} TU/L, average 1.4 x 10^{12} Vg/L; batch runs: average 6.3 x 10^{9} TU/L, average 4.5 x 10^{11} Vg/L). (F) Cell-specific productivity, calculated using the total cell density at each time point for each run (peak values: 7 TU/cell and 5 TU/cell for the 4 dpi pool for perfusion runs; 3 TU/cell and 1 TU/cell for the 3 dpi pool batch runs).

TU/L and average 4.5 x 10^{11} Vg/L for the bioreactor runs at 3 dpi. Overall, the perfusion runs outperformed the batch runs. Figure 14F shows the cell-specific productivity calculated using the total cell density at each time point for each run. The peak specific productivity for perfusion mode is 7 TU/cell for perfusion run 1 and 5 TU/cell for perfusion run 2 for the 4 dpi pool, and the peak specific productivity for batch mode is 3 TU/cell for batch run 1 and 1 TU/cell for batch run 2 for the 3 dpi pool.

4. Discussion

As the field of LVs is progressing towards large-scale manufacturing to generate sufficient material for treating patients, scalability, reproducibility, and robustness are three important aspects to consider. As such, the LV production method has shifted from transfecting multiple plasmids to transfecting packaging or inducing producer cell lines. To contribute to the efforts of shifting to a more scalable, reproducible, and robust method, we chose the Clone 92 stable producer cell line for our development work. Clone 92 produces LVs with a GFP transgene, which simplifies the analytical workflow by allowing us to take advantage of the GFP as the readout signal on the flow-cytometer to assess the functional vector particles in terms of transducibility using the gene transfer assay. In addition, early upstream work has been published for these producer cells with the acoustic filter by Manceur et al. (Manceur et al., 2017), which allows us to make comparisons with the TFDF.

By testing and evaluating basic parameters at shake flask scale, we were able to select those that lead to improved yields for LV production using Clone 92 producer cells. Instead of investing time and effort in additional cell culture strategies, we focused on implementing the perfusion bioreactor runs as soon as possible. As a proof of concept for using the TFDF as a cell retention device, we successfully demonstrated LV production in two 3L bioreactors in perfusion mode using Clone 92 at the high cell density of 11.4 x 10^6 cells/mL and 12.3 x 10^6 cells/mL at the time of induction. For perfusion run 1, 3.3 x 10^{11} TFP and 1.8 x 10^{13} TVP was attained over 6 days, and for perfusion run 2, 3.9 x 10^{11} TFP and 2.0 x 10^{13} TVP was attained over 4 days. We implemented a longer perfusion run 1 and sampled more aggressively in the interest of monitoring the vector kinetics in addition to testing the TFDF as a cell retention device. We chose to implement a shorter perfusion run 2 since our main goal was to confirm the utilization of the TFDF as a cell retention device.

To make a direct comparison with Manceur et al.'s highest cumulative titer from a perfusion run using the acoustic filter with the same cell line (Manceur et al., 2017), we calculated the normalized cumulative functional yield per 1 L of harvest at 5 dpi. Using the TFDF as the cell retention device, we achieved 1.2 x 10^{11} TU/L in perfusion run 1, which is 1.5-fold higher than Manceur et al.'s value of 8 x 10^{10} TU/L. We believe that there is potential for further improvements with the TFDF. Addressing the metabolic needs of the cells during cell growth and LV production phases should be achievable with further optimization in upstream conditions, which can directly result in an even higher increase of the cumulative functional vector yield.

The highest cell-specific productivity for our batch bioreactors is 3 TU/cell, which is slightly lower than Manceur et al.'s highest batch bioreactor value at 4.4 TU/cell, and the highest cell-specific productivity for our TFDF perfusion bioreactors is 7 TU/cell, which is lower than their highest perfusion bioreactor value at 11.5 TU/cell. We suspect that their defined upstream conditions might have an effect on the cell-specific productivity, since a small difference is observed in the batch bioreactor and that difference became much more observable in the perfusion bioreactor. However, overall, these values are in line with the 3-10 virus/cell produced for LVs and they are still far from the specific productivity that is typically attained by the wildtype HIV-1 virus, 10^3 virus/cell (Ramirez, 2018). This points to the complexity of the heavily modified and extremely labile nature of the HIV-1-based LV system.

Of the perfusate samples that were collected at various time points of the perfusion bioreactor runs, we observed that the peak functional titer, 4.4 x 10^7 TU/mL (run 1) and 4.1 x 10^7 TU/mL (run 2), is at 72 hpi and the peak total titer, 3.6 x 10^9 Vg/mL (run 1) and 4.5 x 10^9 Vg/mL (run 2), is at 84 hpi and 92 hpi, respectively (Figure 13B). The actual peaks may shift slightly if we were to collect the samples hourly between those time points. Furthermore, the kinetics of the ratio of total vector particles to total functional particles (TVP/TFP), as shown in Figure 13D, show lowest ratios between 24 hpi and 75 hpi, which is in line with previous reports that claimed 48 hpi to 72 hpi as the typical and ideal harvest times, as longer incubations lead to a significant decrease in LV functionality (Logan et al., 2004).

DNA content is shown to be higher in the later stage of LV production for the perfusion runs (Figure 13F), this makes sense as there is higher cell death as the LV production process continues. Another observation is that there seems to be lower DNA content in perfusion run 2 as compared to perfusion run 1. This might be attributed to the fact that a higher exchange rate was implemented, essentially clearing the waste quicker, and/or that the Prototype media (HyCell

TransFx-H modified SH31192) was used for the LV production phase for perfusion run 2, whereas the commercial HyCell TransFx-H medium was used perfusion run 1. In comparing the 3 dpi product, the DNA content is higher for the perfusion runs as compared to the bioreactor runs (Figure 14B), which is probably due to the fact that there is a much higher cell density in the perfusion runs. It would be a point of interest to evaluate how effectively the downstream processing steps can clear the DNA impurities along with other impurities such as host cell proteins.

Currently popular cell retention devices on the market such as the ATF (alternating tangential flow) and the acoustic filter have limitations. For example, enveloped viruses like LVs (>100 nm) stick to the ATF filter. Given the inherent fragile nature of LVs, having to find a way to remove the virus adds an additional challenge to the LV production process. The acoustic filter, on the other hand, does not promote sticking; however, it is not scalable because of heat exchange limitations. Ultimately, the TFDF performed well as a cell retention device for perfusion, as the LVs are not retained in the device (Figure 13C), and it has the scalability potential to support large-scale manufacturing of LVs.

In addition, the TFDF provides a few other advantages. For perfusion run 1, both the perfusion and final harvest operations were performed using the same filter, which provides an added benefit of a one-unit operation. No cell debris was observed in the harvest pools during the perfusion run (i.e., perfusate material), which can be an advantage as the starting material for downstream processing. Another point of observation is that the recirculation of the cell culture through the TFDF facilitates improved mixing of the cell culture, as the samples taken from the bottom of the bioreactor vessel appears to have fewer dead cells than in batch mode.

Stability is a big challenge in LV production, as LVs lose function over time and they are sensitive to environmental factors. Finding a way to produce LVs in perfusion mode at large scale would allow for the generation of more material and the usage of a cell retention device that is adapted to the fragility of the LVs would maintain a higher number of the produced functional vectors. The novelty in the work presented in this manuscript is demonstrating two successful operations of a cell retention device that can be scaled to industrial-size bioreactors. The future of this work would be an integrated continuous process, where the LVs are harvested continuously and passed onto the capture step of downstream purification, which would greatly reduce hold times, rendering less loss of LV functionality.

Data Availability Statement

The original contributions presented in the study are included in the article/Supplementary Material, further inquiries can be directed to the corresponding author.

Author Contributions

Conceptualization, MT and AK; Methodology, MT; Execution, MT, Writing – original draft, MT; writing – review and editing, MT and AK; Funding acquisition and resources, MT and AK.

Funding

MT is financially supported by a fellowship from the Faculty of Engineering at McGill University and a doctoral scholarship from Fonds de recherche – Nature et technologies Québec (FRQNT); AK is partially funded through Canada Research Chair CRC-240394.

Acknowledgements

The authors acknowledge Repligen Corp for lending the TFDF system and supplying consumables as well as providing technical support throughout the perfusion bioreactor runs; Cytiva for supplying the Prototype media (HyClone HyCell TransFx-H modified SH31192); National Research Council Canada, Montreal site for providing the lentivirus producing cell line; and Alina Venereo-Sanchez for general advising. A portion of this work has been captured in the form of an abstract (Tran and Kamen, 2021) published online for the 15th Protein Expression in Animal Cells Conference, held virtually on 13-16 September 2021.

Supplemental Information

The Supplementary Material for this article can be found online at:
https://www.frontiersin.org/articles/10.3389/fbioe.2022.887716/full#supplementary-material

References

Ansorge, S., Henry, O., and Kamen, A. (2010). Recent Progress in Lentiviral Vector Mass Production. *Biochemical Engineering Journal*, *48*(3), 362-377. https://doi.org/10.1016/j.bej.2009.10.017

Ansorge, S., Lanthier, S., Transfiguracion, J., Durocher, Y., Henry, O., and Kamen, A. (2009). Development of a Scalable Process for High-Yield Lentiviral Vector Production by Transient

Transfection of HEK293 Suspension Cultures. *Journal of Gene Medicine*, *11*(10), 868-876. https://doi.org/10.1002/jgm.1370

Broussau, S., Jabbour, N., Lachapelle, G., Durocher, Y., Tom, R., Transfiguracion, J., et al. (2008). Inducible Packaging Cells for Large-Scale Production of Lentiviral Vectors in Serum-free Suspension Culture. *Molecular Therapy*, *16*(3), 500-507. https://doi.org/10.1038/sj.mt.6300383

Chen, Y. H., Pallant, C., Sampson, C. J., Boiti, A., Johnson, S., Brazauskas, P., et al. (2020). Rapid Lentiviral Vector Producer Cell Line Generation Using a Single DNA Construct. *Molecular Therapy – Methods & Clinical Development*, *19*, 47-57. https://doi.org/10.1016/j.omtm.2020.08.011

Côté, J., Garnier, A., Massie, B., and Kamen, A. (1998). Serum-free Production of Recombinant Proteins and Adenoviral Vectors by 293SF-3F6 Cells. *Biotechnology and Bioengineering*, *59*(5), 567-575. https://doi.org/10.1002/(SICI)1097-0290(19980905)59:5<567::AID-BIT6>3.0.CO;2-8

Escors, D., Breckpot, K., Arce, F., Kochan, G., and Stephenson, H. (2012). Lentiviral Vectors and Gene Therapy. *Springer*. https://doi.org/10.1007/978-3-0348-0402-8

Gutiérrez-Granados, S., Gòdia, F., and Cervera, L. (2018). Continuous Manufacturing of Viral Particles. *Current Opinion in Chemical Engineering*, *22*, 107-114. https://doi.org/10.1016/j.coche.2018.09.009

Hu, P. R., Li, Y., Sands, M. S., McCown, T., and Kafri, T. (2015). Generation of a Stable Packaging Cell Line Producing High-Titer PPT-Deleted Integration-Deficient Lentiviral Vectors. *Molecular Therapy – Methods & Clinical Development*, *2*, 15025. https://doi.org/10.1038/mtm.2015.25

Kafri, T., van Praag, H., Ouyang, L., Gage, F. H., and Verma, I. M. (1999). A Packaging Cell Line for Lentivirus Vectors. *Journal of Virology*, *73*(1), 576-584. https://doi.org/10.1128/jvi.73.1.576-584.1999

Logan, A. C., Nightingale, S. J., Haas, D. L., Cho, G. J., Pepper, K. A., and Kohn, D. B. (2004). Factors Influencing the Titer and Infectivity of Lentiviral Vectors. *Human Gene Therapy*, *15*(10), 976-988. https://doi.org/10.1089/hum.2004.15.976

Manceur, A. P., Kim, H., Misic, V., Andreev, N., Dorion-Thibaudeau, J., Lanthier, S., et al. (2017). Scalable Lentiviral Vector Production Using Stable HEK293SF Producer Cell Lines. *Human Gene Therapy Methods*, *28*(6), 330-339. https://doi.org/10.1089/hgtb.2017.086

Martínez-Molina, E., Chocarro-Wrona, C., Martínez-Moreno, D., Marchal, J. A., and Boulaiz,

H. (2020). Large-Scale Production of Lentiviral Vectors: Current Perspectives and Challenges. *Pharmaceutics*, *12*(11), 1051. https://doi.org/10.3390/pharmaceutics12111051

McCarron, A., Donnelley, M., McIntyre, C., and Parsons, D. (2016). Challenges of Up-Scaling Lentivirus Production and Processing. *Journal of Biotechnology*, *240*, 23-30. https://doi.org/10.1016/j.jbiotec.2016.10.016

Merten, O.-W., Hebben, M., and Bovolenta, C. (2016). Production of Lentiviral Vectors. *Molecular Therapy – Methods & Clinical Development*, *3*, 16017. https://doi.org/10.1038/mtm.2016.17

Milone, M. C., and O'Doherty, U. (2018). Clinical Use of Lentiviral Vectors. *Leukemia*, *32*(7), 1529-1541. https://doi.org/10.1038/s41375-018-0106-0

Moleirinho, M. G., Silva, R. J. S., Alves, P. M., Carrondo, M. J. T., and Peixoto, C. (2020). Current Challenges in Biotherapeutic Particles Manufacturing. *Expert Opinion on Biological Therapy*, *20*(5), 451-465. https://doi.org/10.1080/14712598.2020.1693541

Moreira, A. S., Cavaco, D. G., Faria, T. Q., Alves, P. M., Carrondo, M. J. T., and Peixoto, C. (2021). Advances in Lentivirus Purification. *Biotechnology Journal*, *16*(1), e2000019. https://doi.org/10.1002/biot.202000019

Naldini, L., Trono, D., and Verma, I. M. (2016). Lentiviral Vectors, Two Decades Later. *Science*, *353*(6304), 1101-1102. https://doi.org/10.1126/science.aah6192

Perry, C., and Rayat, A. (2021). Lentiviral Vector Bioprocessing. *Viruses*, *13*(2), 268. https://doi.org/10.3390/v13020268

Ramirez, J. C. (2018). Lentiviral Vectors Come of Age? Hurdles and Challenges in Scaling up Manufacture. *Systems Biology, IntechOpen*. https://doi.org/10.5772/intechopen.81105

Sanber, K. S., Knight, S. B., Stephen, S. L., Bailey, R., Escors, D., Minshull, J., et al. (2015). Construction of Stable Packaging Cell Lines for Clinical Lentiviral Vector Production. *Scientific Reports*, *5*, 9021. https://doi.org/10.1038/srep09021

Schofield, M. (2018). Current State of the Art in Continuous Bioprocessing. *Biotechnology Letters*, *40*, 1303-1309. https://doi.org/10.1007/s10529-018-2593-5

Segura, M. M., Mangion, M., Gaillet, B., and Garnier, A. (2013). New Developments in Lentiviral Vector Design, Production and Purification. *Expert Opinion on Biological Therapy*, *13*(7), 987-1011. https://doi.org/10.1517/14712598.2013.779249

Sharon, D., and Kamen, A. (2018). Advancements in the Design and Scalable Production of Viral Gene Transfer Vectors. *Biotechnology and Bioengineering*, *115*(1), 25-40. https://doi.org/

10.1002/bit.26461

Tolmachov, O. E., Tolmachova, T., and Al-Allaf, F. A. (2011). Designing Lentiviral Gene Vectors. *Viral Gene Therapy, IntechOpen*, 263-284. https://doi.org/10.5772/17361

Tomás, H. A., Rodrigues, A. F., Carrondo, M. J. T., and Coroadinha, A. S. (2018). LentiPro26: Novel Stable Cell Lines for Constitutive Lentiviral Vector Production. *Scientific Reports*, *8*, 5271. https://doi.org/10.1038/s41598-018-23593-y

Tran, M. Y., and Kamen, A. (2021). Tangential Flow Depth Filtration to Support Effective Perfusion of Lentivirus Vector Production towards Continuous Manufacturing. *15th Protein Expression in Animal Cells Conference*. Virtual, Bioprocess Intensification Session, Abstract 218-gGSx-156. Available here.

Transfiguracion, J., Tran, M. Y., Lanthier, S., Tremblay, S., Coulombe, N., Acchione, M., et al. (2020). Rapid In-Process Monitoring of Lentiviral Vector Particles by High-Performance Liquid Chromatography. *Molecular Therapy – Methods & Clinical Development*, *18*, 803-810. https://doi.org/10.1016/j.omtm.2020.08.005

Williams, T., Goodyear, O., Davies, L., Knevelman, C., Bransby, M., Mitrophanous, K., et al. (2020). Lentiviral Vector Manufacturing Process Enhancement Utilizing TFDF Technology. *Cell & Gene Therapy Insights*, *6*(3), 455-467. https://doi.org/10.18609/cgti.2020.053

Zufferey, R., Donello, J. E., Trono, D., and Hope, T. J. (1999). Woodchuck Hepatitis Virus Posttranscriptional Regulatory Element Enhances Expression of Transgenes Delivered by Retroviral Vectors. *Journal of Virology*, *73*(4), 2886-2892. https://doi.org/10.1128/JVI.73.4.2886-2892.1999

Conflicts of Interest

The authors declare that the research was conducted in the absence of any commercial or financial relationships that could be construed as a potential conflict of interest.

Publisher's Note

All claims expressed in this article are solely those of the authors and do not necessarily represent those of their affiliated organizations, or those of the publisher, the editors and the reviewers. Any product that may be evaluated in this article, or claim that may be made by its manufacturer, is not guaranteed or endorsed by the publisher.

Copyright

Preface to Chapter 5

The submitted manuscript enclosed in Chapter 5 is in support of Objective 3, which is to *improve LV functional yield through integrated semi-continuous manufacturing*. This work is a direct continuation of the preceding chapter. The Introduction section of Chapter 4 discussed the appeal and importance of continuous processing for unstable products such as LVs. Furthermore, it pointed out that establishing an integrated continuous process would be an impactful strategy for process intensification. While Chapter 4 focuses on the process intensification of the upstream process (i.e., implementing a perfusion process with an effective cell retention device that allows for full recovery of the product of interest), Chapter 5 demonstrates the feasibility of combining the perfusion process from upstream with the capture step from downstream in a semi-continuous manner.

First, Chapter 5 discusses the establishment of a scalable anion exchange membrane chromatography method to be used as the capture step. Selecting and testing a method that has the scalability to support LV production at manufacturing-scale provides tangible potential to execute this in the industry. Next, Chapter 5 describes the implementation of a semi-continuous downstream process that includes nuclease treatment, clarification, and the capture step. In fact, the semi-continuous operation of the capture step in itself is a strategy for process intensification, as it is an improvement of the process at the unit operation by greatly reducing the processing time.

Then, Chapter 5 demonstrates the benefits of executing an integrated semi-continuous manufacturing process that bridges the upstream to the downstream. In combining the perfusion cell culture (i.e., process intensification of the upstream unit operation) and the semi-continuous downstream process (i.e., process intensification of the downstream unit operation), this integrated process works hand-in-hand to further improve the LV production and purification process. Lastly, Chapter 5 touches on the possibility of monitoring the LV transduction activity in HEK293SF cells using confocal microscopy. This has the potential to become an additional method in the analytical toolbox for assessing LV product quality and it is in support of Objective 1 of the thesis.

In the Discussion section of Chapter 4, it was stated that the DNA level is higher in the LV material produced from the perfusion runs as compared to the batch runs. Upon closer examination, I realized that I had assayed and compared LV material from the perfusion runs that was not yet treated with Benzonase with LV material from the batch runs which had been treated

with Benzonase. In reviewing my data, I observed a similar amount of DNA in the nuclease treated material in both the batch and perfusion runs. Therefore, the difference that I observed initially was refuted.

As a reminder, the gene transfer assay (GTA) and the digital droplet polymerase chain reaction (ddPCR) assay were the two main analytical tools used to support the quality assessment of LVs discussed in Chapters 4 and 5. The detailed GTA and ddPCR protocols are included in the Materials and Methods section of Chapter 4, the optimization of the GTA is described in Appendix 1, and the optimization of the ddPCR assay is described in Appendix 2.

Chapter 5: Integrated Semi-Continuous Manufacturing of Lentiviral Vectors Using a HEK-293 Producer Cell Line

Authors: **Michelle Yen Tran**, Shantoshini Dash, Zeyu Yang, and Amine A. Kamen

Author affiliation: Viral Vectors and Vaccine Bioprocessing Group, Bioengineering Department, McGill University, Montreal, Quebec, Canada

Status: Submitted for publication to *Molecular Therapy – Methods & Clinical Development* (Cell Press)

Abstract

There have been considerable efforts on improving the lentiviral vector (LV) system and their production. However, there remains the persisting challenge of producing a sufficient quantity of LVs at manufacturing scale to support treatments beyond early clinical trials. Furthermore, their innately labile nature poses an equally important obstacle in LV production. As LVs lose function over time and they are sensitive to environmental factors in each unit operation in the bioprocess workflow, integrated continuous manufacturing is an attractive strategy for process intensification. This manuscript describes the implementation of nuclease treatment, clarification, and capture step in a semi-continuous mode. Combining the clarification and loading of the capture step as well as operating those steps in parallel to the purification of the capture step expedite the processing time, reducing it by 4-fold as compared to processing the same volume in batch mode. This semi-continuous operation also improves the recoveries of functional vector particles and total vector particles by 26% and 18%, respectively, showing an added benefit in loading the capture membranes in series. Building on previously published upstream work using a scalable cell retention device in perfusion mode, this manuscript demonstrates the integration of upstream and downstream in a semi-continuous manner, reducing processing and hold times as well as showing improvements in LV product quality and recovery.

Keywords

Lentiviral vector, lentiviral vector production, lentiviral vector manufacturing, large-scale manufacturing, continuous manufacturing, integrated continuous manufacturing, membrane chromatography, stable producer cell line, perfusion, cell retention device.

1. Introduction

Lentiviral vectors (LVs) have become a prevailing gene delivery tool in cell and gene therapy in the past three decades (Escors et al., 2012; Naldini et al., 2016; Milone and O'Doherty, 2018). LVs are primarily used for *ex vivo* modifications, such as transduction of T-cells for expression of chimeric antigen receptor in CAR-T cell therapies, and they are gaining popularity in *in vivo* applications. With 6 approved *ex vivo* LV products and a rapidly growing number of LV clinical trials, there is an increased urgency in addressing the persisting challenge of producing LVs at manufacturing scale to support treatments beyond early clinical trials (Ansorge et al., 2009, 2010; Martínez-Molina et al., 2020). In addition to the challenge of generating a sufficient quantity

of LVs, their innately labile nature poses an equally important obstacle in LV production. As LVs lose function over time and they are sensitive to environmental factors in each unit operation in the bioprocess workflow (Ansorge et al., 2010; Merten et al., 2016; Transfiguracion et al., 2020), integrated continuous manufacturing is an attractive strategy for process intensification (McCarron et al., 2016; Gutiérrez-Granados et al., 2018; Moleirinho et al., 2020).

Continuous bioprocessing has the potential to address the current challenges of biomanufacturing technology, such as reducing cost, increasing flexibility and standardization, accelerating development and scaling times, and improving product quality. There have been many discussions about the impact of continuous bioprocessing (Konstantinov and Cooney, 2015; Croughan et al., 2015) and an integrated process (Zydney, 2015; Walther et al., 2015) that connects the upstream and downstream, especially for unstable products. The shift from batch to continuous bioprocessing for biopharmaceuticals has been realized in antibody production, and an end-to-end integrated continuous process has been reported (Godawat et al., 2015).

In the space of viral vectors, mentions of continuous manufacturing have typically referred to the continuous nature of the perfusion cell culture for the upstream process (Gutiérrez-Granados et al., 2018). Usually, the perfusion harvest is pooled and frozen every 24 hours, and the collected material is then processed downstream as a series of batches, where unit operations are performed and completed before the process stream moves to the next step. For the downstream process, there are two recent publications of continuous purification of Adeno-Associated Virus (Mendes et al., 2022) and hepatitis C virus-like particles (Silva et al., 2020) using multiple-column counter-current chromatography, utilizing upstream material produced in the batch format. Although there has been some development work in continuous manufacturing in either upstream or downstream, an integrated continuous bioprocess has yet to be reported.

Implementing the upstream process in perfusion mode increases productivity and continuously harvesting LVs from the bioreactor reduces the residence time, thus preserving their quality attributes. Executing this at manufacturing scale has been a challenge due to limitations of currently commercialized cell retention devices. To circumvent this, a scalable technology that can be used as a cell retention device that does not retain the product in perfusion mode for LV production using a stable producer cell line was demonstrated (Tran and Kamen, 2022), which serves as the first piece of an integrated continuous manufacturing process of LVs.

Building on that upstream work, this manuscript demonstrates (1) the implementation of a downstream process in semi-continuous mode and (2) the integration between the perfusion

culture from upstream to the capture step from downstream in a semi-continuous manner. The Mustang Q membrane, which has been reported to work well for purifying LVs (Moreira et al., 2021; Tinch et al., 2019), is chosen for the capture step for its attributes that are advantageous at manufacturing scale – high binding capacity, ability to handle high volumetric flow rates, and scalability.

To characterize the LV product quality, functional vector particles and total vector particles are analyzed to convey the potency aspect, and DNA and protein contents are analyzed to convey the purity aspect. The functional vector particles are reported as transducing units, assessed by a cell-based assay that measure the GFP-transgene expression in transduced target cells. The total vector particles are reported as vector genome units, assessed by a droplet digital PCR assay. Furthermore, the product quality of LVs produced by the integrated semi-continuous process is supported by an in-vitro validation using confocal microscopy.

2. Results

2.1 Establishing Mustang Q as the Capture Step

To establish run conditions, first, the loading flowrate (2.5 MV/min vs. 7 MV/min), the general flowrate (2.5 MV/min vs. 10 MV/min), and a quick verification of the load amount (100 vs. 600 MV, membrane volume) were tested in four purification runs (Figure 15) using LVs harvested from 72 to 96 hpi (hours post induction) from a perfusion run (referred to as P1 72-96 hpi LV). The amount of functional vectors, total vectors, DNA, and protein in the load material for the membrane, which had been nuclease treated and filtered, was defined as 100% and the amounts in the subsequent purification steps were calculated as percent recoveries.

Figures 15A and 15B show that there is no loss of functional vectors (represented by transducing units, TU) and total vectors (represented by vector genome units, Vg) in the flowthrough (FT) and wash steps for the three purification runs with 100 MV load (M1, M2, and M3). There is a loss of both TU and Vg in the FT, and a loss of Vg in the wash, for the purification run with 600 MV load (M4), suggesting an over-loaded membrane. The highest TU and Vg recoveries in the elution are 68% and 79%, respectively, for M3.

Overall, Mustang Q is effective at clearing DNA and protein, as shown by high percentages in the FT of all four runs (Figures 15C, 15D). The protein clearance for M4 is significantly higher than the other three runs, most likely due to loss in the FT. Between the three runs with 100 MV load, results show highest DNA clearance in M1 (86%), with a close second highest in M3 (84%),

and highest protein clearance in M3 (63%). Ultimately, the loading and general flowrates for M3 were selected.

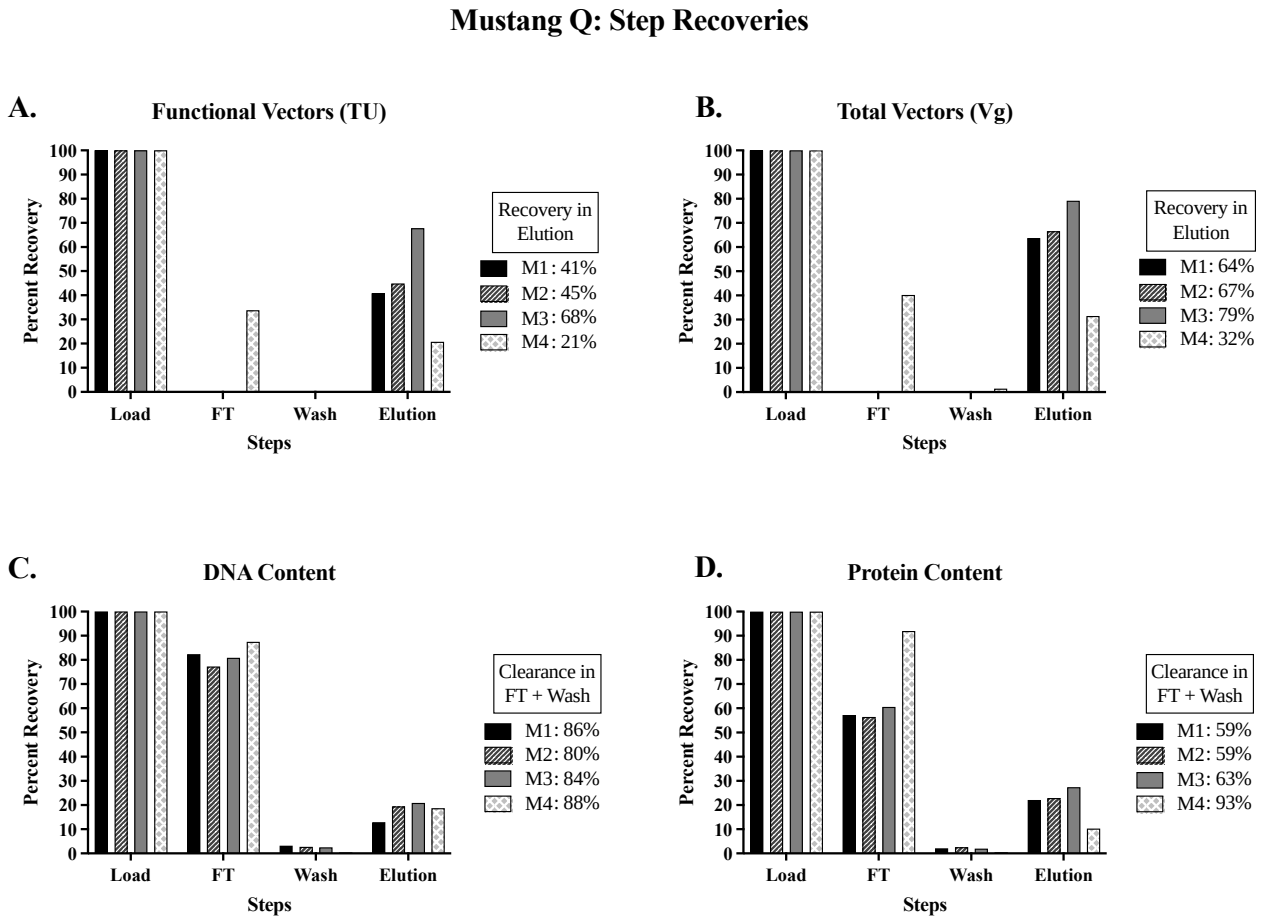

Purification Run	Load Amount (MV)	Loading FR (MV/min)	General FR (MV/min)
M1	100	2.5	2.5
M2	100	2.5	10.0
M3	100	7.0	10.0
M4	600	7.0	10.0

Figure 15. Percent recoveries in the Mustang Q capture step. The amount of functional vectors, total vectors, DNA, and protein in the load material for the membrane, which had been nuclease treated and filtered, was defined as 100% and the amounts in the subsequent purification steps were calculated as percent recoveries. TU = transducing units; Vg = vector genome units; FT = flowthrough; MV = membrane volume; FR = flowrate. (A) Functional vectors, represented by TU. (B) Total vectors, represented by Vg. (C) DNA content. (D) Protein content.

Next, 100 MV, 200 MV, and 300 MV loads were tested to fine-tune the load amount, using a different pool of LVs, harvested 0 to 72 hpi from the perfusion run (referred to as P1 0-72 hpi

LV). Aside from the difference in harvesting time, P1 0-72 hpi LV was held at 4ºC for 5 days before downstream processing whereas P1 72-96 hpi LV was processed upon thawing. Figure 16 shows TU recoveries for the Mustang Q step (from load to elution) and cumulatively (from thawed LV harvest to Mustang Q elution). For P1 0-72 hpi LV material, results show highest step and cumulative recoveries (58% and 43%, respectively) for 100 MV as compared to 200 and 300 MV.

Similar cumulative recoveries are observed for both 100 MV runs (43% for P1 0-72 hpi LV vs. 44% for P1 72-96 hpi LV), although the step recovery is higher for P1 72-96 hpi LV (68%) as compared to P1 0-72 hpi LV (58%). The difference in step recoveries can be explained by the 5-day hold time, although the cumulative recovery was not affected similarly. Given the highest step and cumulative recoveries of functional vectors were observed in both experiments, 100 MV load was selected.

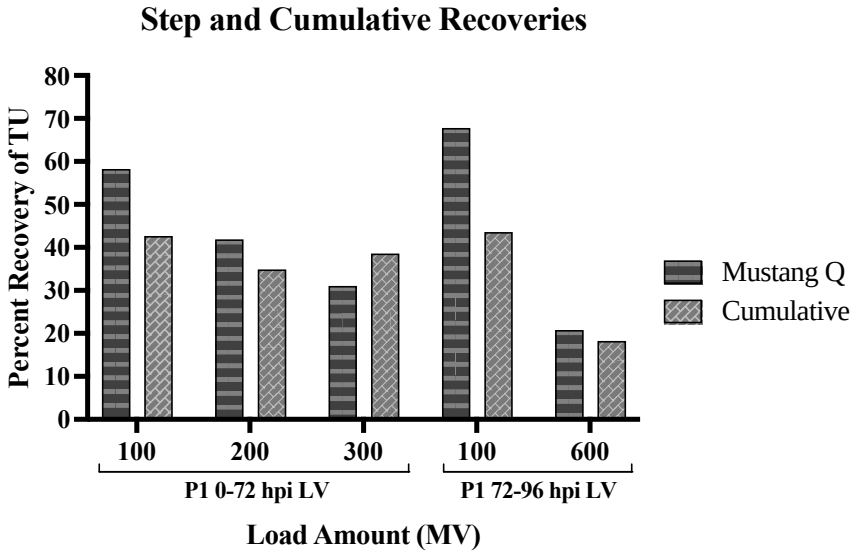

Figure 16. Step and cumulative recoveries of functional vectors, represented as TU. Mustang Q step recovery is calculated from membrane load to elution; cumulative recovery is calculated from thawed LV harvest material to Mustang Q elution. P1 0-72 hpi LV was held at 4ºC for 5 days before downstream processing, P1 72-96 hpi LV was processed upon thawing. TU = transducing units; MV = membrane volume.

2.2 Comparing Mustang Q to Sucrose Cushion

LV material from a batch bioreactor run harvested at 72 hpi was utilized in an experiment to compare Mustang Q purification to Sucrose Cushion (SC) ultra-centrifugation. The SC LV was concentrated by 100-fold. Overall, results show that Mustang Q LV has higher product quality. Figure 17A shows a higher percent recovery for TU (48% vs. 26%), a higher percent recovery for

Vg (82% vs. 36%), and a lower Vg/TU ratio (75 vs. 99) for Mustang Q LV as compared to SC LV. The ratio of Vg to TU is an indication of the potency aspect of LV product quality, where a smaller number indicates higher LV potency since it means that a higher percentage of the produced total vector particles have effectively transduced the host cells and delivered the genetic material to be integrated in the host cell genome, thus expressing the GFP transgene. Figure 17B shows that Mustang Q LV has lower DNA and protein concentrations.

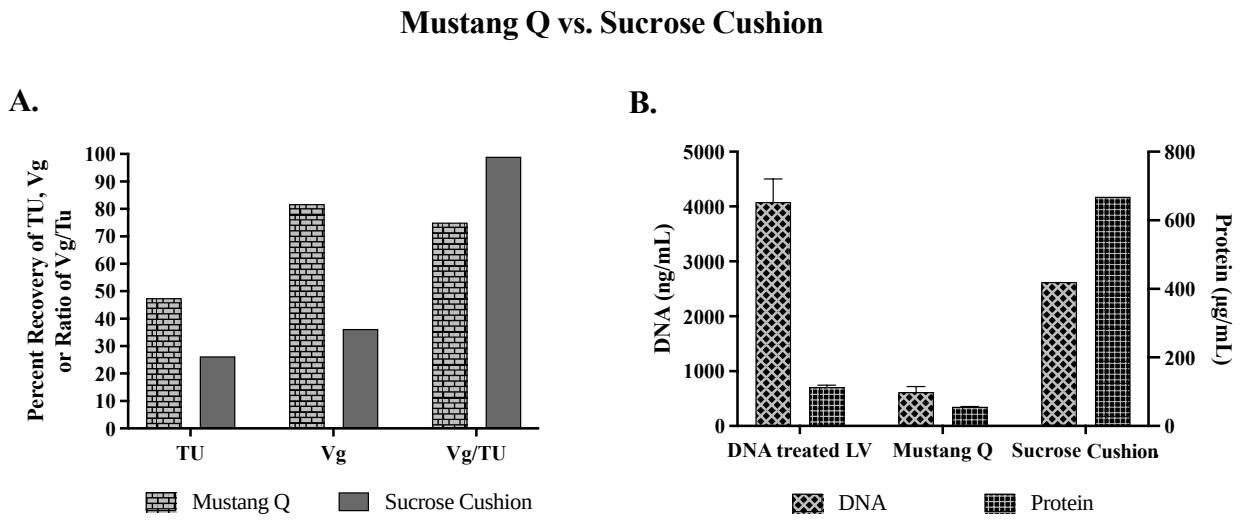

Figure 17. Comparison of Mustang Q purified LV and Sucrose Cushion ultra-centrifuged LV. The Sucrose Cushion ultra-centrifuged LV was concentrated by 100-fold. TU = transducing units; Vg = vector genome units; Vg/TU ratio indicates potency. (A) TU and Vg percent recoveries, and ratio of Vg/TU. (B) DNA and protein concentrations.

2.3 Semi-Continuous Downstream Process

Two systems operate concurrently in the semi-continuous downstream setup (Figure 18). In system 1, nuclease treated LV material is pumped through a depth filter before directly loading onto two Mustang Q membranes connected in series. While the clarification and loading processes occur in system 1, a third fully loaded membrane is subjected to wash, elution, and regeneration steps in system 2, the AKTA. The run time per cycle is similar on both systems (steps 2 through 6 in Figure 18), with 14m 20s for loading 100 MV at a flowrate of 7 MV/min in system 1 and 13m 24s for the rest of the purification steps at a flowrate of 10 MV/min in system 2. There is a time difference in step 1 due to filling the dead volume of the flow path in system 1, and in step 7 when the last membrane is purified in system 2 (Figure 18).

In this semi-continuous set up, the time for loading and eluting six Mustang Q membranes to process 516 mL of LV harvest is ~1.75 hr. Including the 30 min of nuclease treatment brings the total to ~2.25 hr. In contrast, processing the same amount in batch mode, where each cycle is nuclease treated, clarified, loaded, and purified in series, takes ~8.75 hr. Therefore, implementing these downstream steps in a semi-continuous mode expedites the process by almost 4-fold.

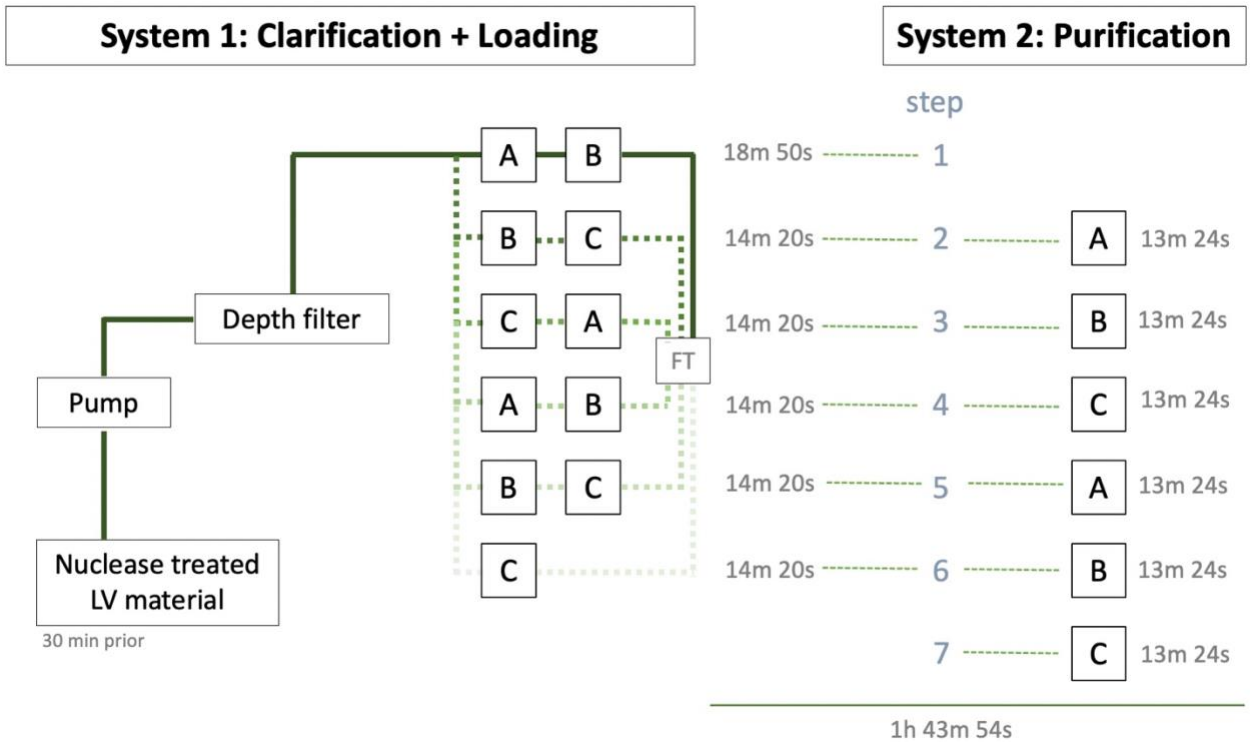

Figure 18. Semi-continuous downstream process set up. Three Mustang Q membranes are denoted as A, B, and C. Once A is fully loaded, it is removed from system 1 and transferred to system 2 (the AKTA), and C is then connected in series after B. While the clarification and loading processes continue in system 1 for B + C, A is subjected to wash, elution, and regeneration steps (i.e., strip, then equilibration) in system 2. Then, B is transferred to system 2 for purification and A is re-transferred to system 1 behind C. These steps are repeated until all three membranes go through two cycles each.

Figure 19A compares the recoveries of functional vectors, total vectors, DNA content, and protein content between semi-continuous and batch modes using LVs harvested from 0 to 72 hpi from the perfusion run (P1 0-72 hpi LV). Overall, results show advantages in implementing the downstream in semi-continuous mode. The semi-continuous operation improves the recoveries of functional vector particles by 26% (69% vs. 43%) and total vector particles by 18% (91% vs. 73%). The DNA clearance is similar in both modes, with 15% recovered in the Mustang Q elution for semi-continuous mode and 16% for batch mode. The protein clearance is higher for semi-

continuous mode, with 25% recovered in Mustang Q elution for semi-continuous mode and 31% for batch mode. Figure 19C shows that the Vg/Tu ratio is lower for the downstream process in semi-continuous mode (75) as compared to batch mode (119), indicating higher LV potency.

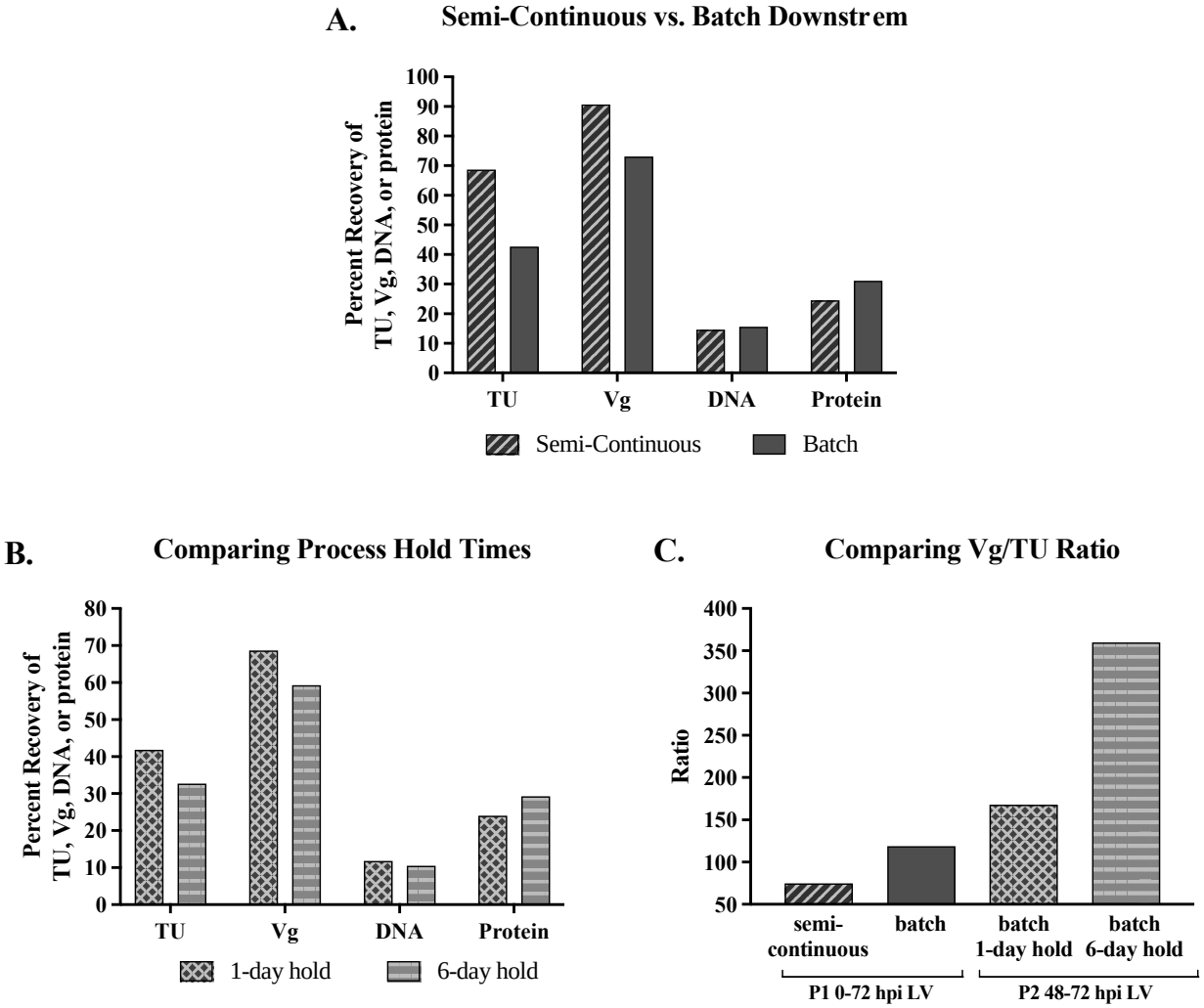

Figure 19. Semi-continuous downstream process. In semi-continuous mode, the clarification of nuclease treated LV material and loading of the Mustang Q capture step are combined, and they are operated in parallel to the purification steps of the capture step. In batch mode, nuclease treatment, clarification, loading, and purification for each cycle occurs in series. TU = transducing units; Vg = vector genome units; Vg/TU ratio indicates potency. 1-day and 6-day hold were implemented at 4ºC upon LV harvest thaw. (A) Comparing semi-continuous and batch downstream processes. (B) Comparing process hold times of the LV harvest. (C) Comparing Vg/TU ratio.

2.4 Integrated Semi-Continuous Process

To evaluate the effect of the process hold time for LV harvest before the capture step, LVs harvested from 48 to 72 hpi from another perfusion run (referred to as P2 48-72 hpi LV) was used for the downstream process in batch mode (Figure 19B). The LV material was held at 4°C for 1 day or 6 days before nuclease treatment, clarification, and purification over the Mustang Q capture step. A shorter process hold time shows a higher functional vector recovery (42% for 1-day hold vs. 33% for 6-day hold) and a higher total vector recovery (69% vs. 59%, respectively). The DNA clearance was similar in both purification runs, with 12% recovered in the elution for the 1-day hold and 11% for the 6-day hold. The protein clearance is higher for the 1-day hold, with 24% recovered in the elution for the 1-day hold and 29% for the 6-day hold. Figure 19C shows that the Vg/TU ratio is lower for the batch mode with 1-day hold (168) as compared to the batch mode with 6-day hold (360), indicating higher LV potency.

2.5 In-Vitro Validation of LVs Produced by the Integrated Semi-Continuous Process

Confocal microscopy was used to monitor LV transduction effectiveness in HEK293SF cells. Three samples were tested – LVs manufactured by the integrated semi-continuous process (ISC LV for short), in which LVs were produced in a perfusion bioreactor and processed downstream in semi-continuous mode; LV supernatant from a shake flask production; and supernatant from non-induced producer cells serving as the negative control.

Several rounds of live cell imaging HEK293SF cells transduced with both LV samples from 0 to 36 hours post transduction at 100x magnification reveal the earliest timepoint of GFP expression around 10 h and peak saturation around 20 h. In addition, images containing cells transduced with LV supernatant have a distinct background signal, which is not observed in images of cells transduced with ISC LV.

GFP expression is observed in cells transduced with ISC LV (Figure 20A) and LV supernatant (Figure 20B), with a sharper contrast for the former. The GFP signal intensity is comparable for both samples (Figure S5), which makes sense given the same multiplicity of infection was used. However, the error bar for the ISC LV is much tighter, which corroborates the sharper contrast observed in the microscopy images, implying the purification achieved in the capture step. Figure 20C shows that there is no GFP expression observed in the negative control and Figure S5 confirms no GFP signal.

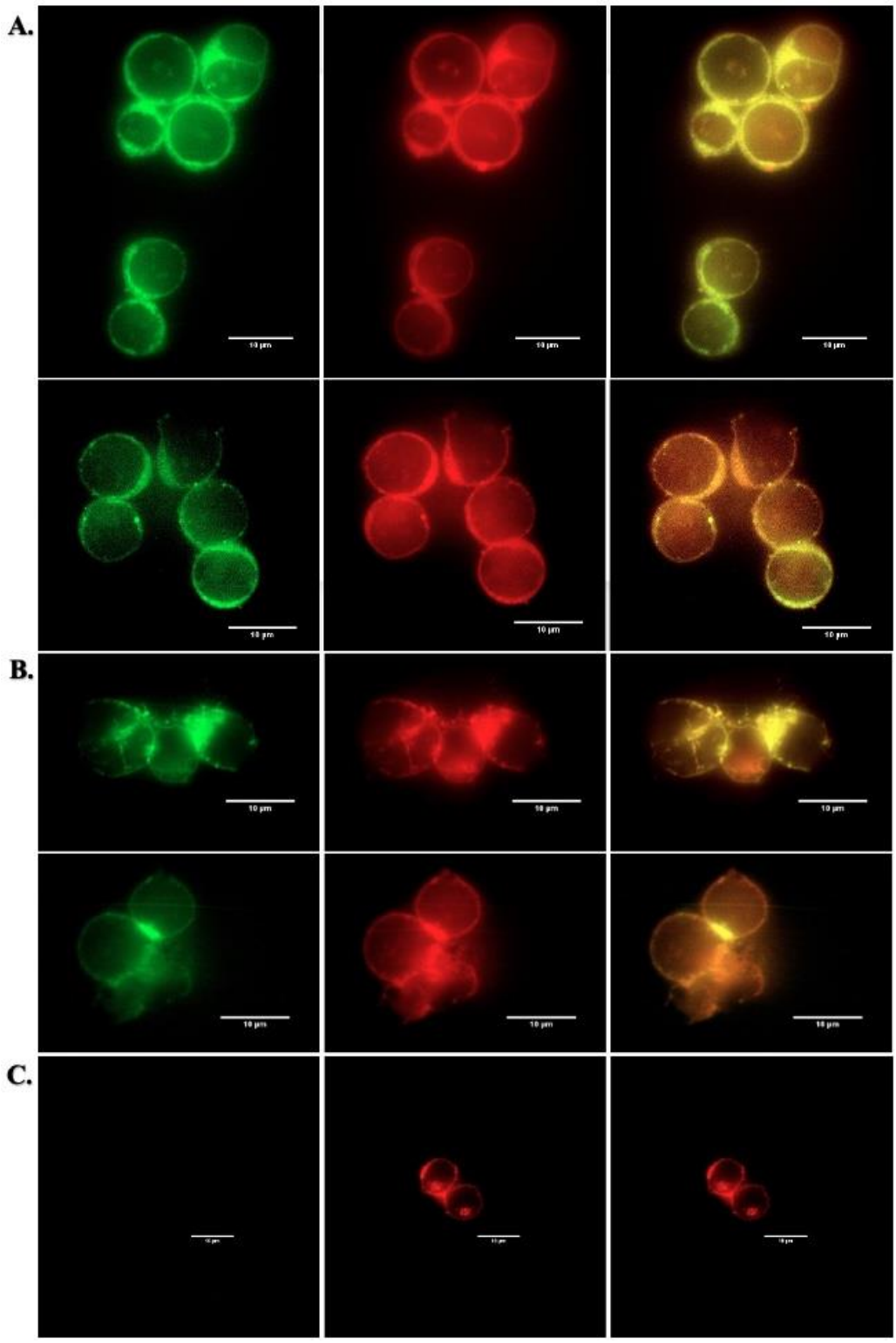

Figure 20: Confocal microscopy images of transduced HEK293SF cells. Cells were transduced with (A) LVs manufactured by the integrated semi-continuous process (i.e., LVs produced in perfusion bioreactor and processed downstream in semi-continuous mode), captured at 11 h 50 min post transduction. (B) LV supernatant from a shake flask production, captured at 15 h 10 min post transduction. (C) Supernatant from non-induced Clone 92 cells serving as the negative control. Left panel = GFP expression in green; Middle panel = plasma membrane stained in red; Right panel = merged. Scale bar corresponds to 10 µm.

2.6 A Case Study: Comparing Projected Processing Times and Functional Yields

To investigate the significance of a semi-continuous process, a comparison of projected processing times (Figure 21) and a comparison of projected recovered functional yields (Figure 22) were generated. The cases include batch upstream and batch downstream (Case I), perfusion upstream and batch downstream (Case II), and perfusion upstream and semi-continuous downstream (Case III).

To facilitate a direct comparison between the perfusion and batch bioreactor runs, the harvesting scheme for the perfusion bioreactor was normalized to 3 dpi (days post induction) and the functional yield (represented by total transducing units, TU) for the batch bioreactor was normalized to 2 L working volume. Using upstream data from the previously published work (Tran and Kamen, 2022), it is calculated that 2.13×10^{11} TU is achieved for the perfusion bioreactor and 1.62×10^{10} TU is achieved for the batch bioreactor. Assuming that the batch operation is reproducible with the same level of production, it would need to repeat 13 times in order to produce the same amount of functional vectors as in perfusion mode. In terms of harvest volume for the perfusion bioreactor, a 2 L working volume at an exchange rate of 1 vessel volume per day, harvested for 3 days, including a 20% increase of the working volume in a final harvest step, brings the total to 8.4 L.

In Case I with batch upstream and batch downstream (Figure 21A), the producer cells were grown for 2 days, induced for LV production, and harvested 3 dpi. Then, the downstream processing which includes nuclease treatment, clarification, and purification over the capture step for 2 L harvest takes ~1.5 days. Thus, the total time for one operation from inoculation of the batch bioreactor to purification over the capture step is 6.5 days. Using the assumption made above, where the batch upstream process is repeated 13 times, brings the projected processing time to 84.5 days.

In Case II with perfusion upstream and batch downstream (Figure 21B), the producer cells were grown for 9 days to reach high cell density, induced for LV production, and harvested continuously for 3 dpi, including a final harvest step. The downstream processing for 8.4 L takes ~6.25 days, which brings the projected processing time to 18.25 days.

In Case III with perfusion upstream and semi-continuous downstream (Figure 21C), the upstream process is the same as in Case II. Here, the downstream can initiate shortly after the producer cells are induced for LV production. Scenario 1 presents a timeline for LVs processed every 12 h of harvesting (denoted as DSP S1, Figure 21) and scenario 2 presents a processing

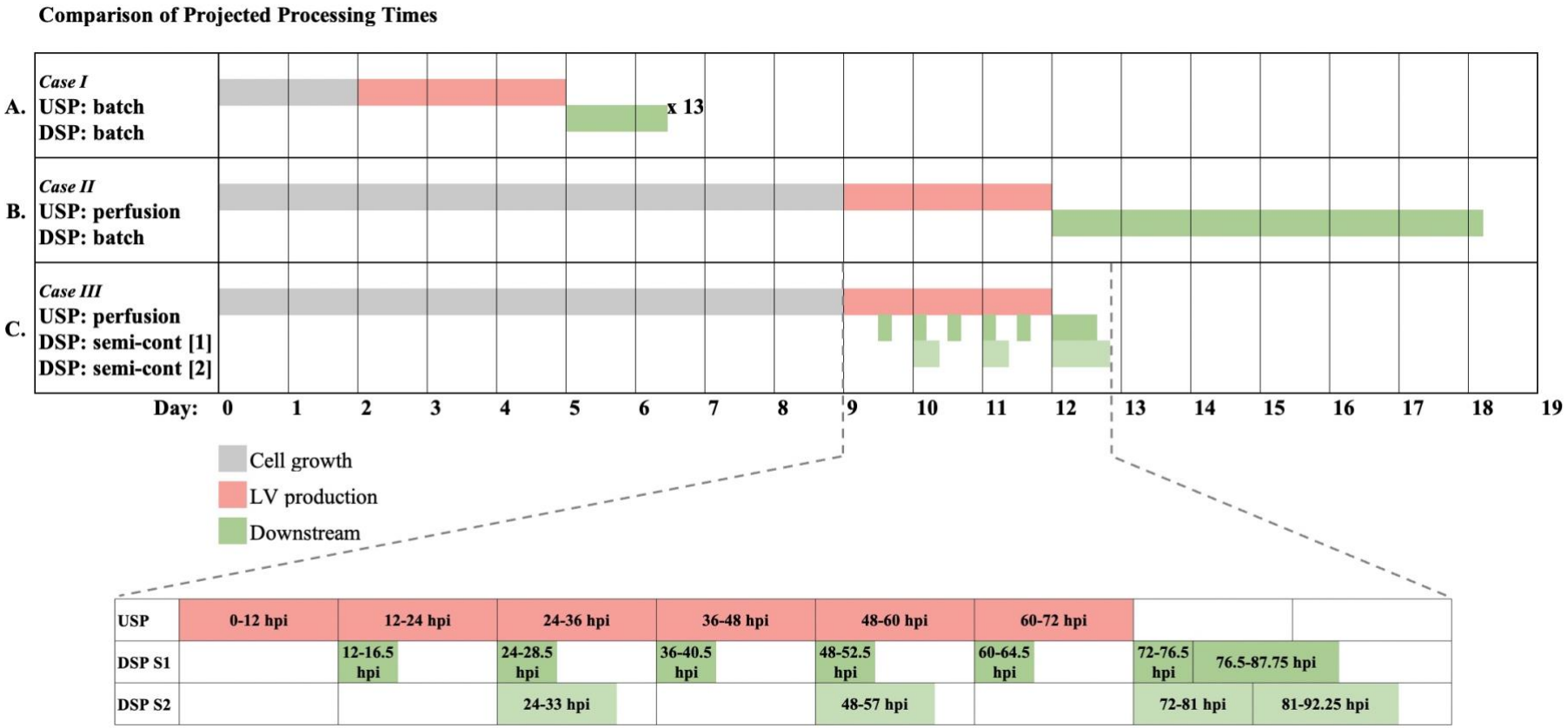

Figure 21: Comparison of projected processing times for batch versus semi-continuous manufacturing. USP = upstream processing; refers to LV production in cell culture. DSP = downstream processing; refers to nuclease treatment, clarification, and Mustang Q capture step. Calculations are made based on the 2 L working volume of the perfusion bioreactor with 1 vessel volume per day media exchange rate, resulting in 2 L of LV harvest per day over 3 days along with 2.4 L of the final harvest, rendering a total of 8.4 L of harvest material with a total of 2.13×10^{11} TU. The yield of functional vectors for the batch bioreactor is normalized to 2 L to facilitate comparison between the two modes of LV production, resulting in 1.62×10^{11} TU. Assuming that the batch operation is completely reproducible, this process in batch mode needs to be repeated 13 times to produce the same amount of functional vectors as compared to the perfusion upstream processes. (A) Batch upstream and batch downstream; 6.5 days of processing repeated 13 times to equal 84.5 days of manufacturing; this estimation does not take in account the necessary time for cleaning and set up between the batch operations. (B) Perfusion upstream and batch downstream; 18.25 days of manufacturing. (C) Perfusion upstream and semi-continuous downstream; average of 12.75 days of manufacturing, depending on the scenario of the downstream. Scenario 1 processes LV harvest every 12 hours, scenario 2 processes LV harvest every 24 hours.

timeline for every 24 h (denoted as DSP S2), and both scenarios bring the projected processing time to less than 13 days.

To speculate the recovered functional yields for each of the three cases, the percent recovery of TU achieved in previous downstream experiments were used. For Case I, using 48% TU recovery for batch upstream material processed downstream in batch mode (Figure 17A) results in 1.01 x 10^{11} TU. For Case II, using 43% for perfusion upstream and batch downstream (Figure 19A) results in 9.16 x 10^{10} TU. For Case III, using 69% for perfusion upstream and semi-continuous downstream (Figure 19A) results in 1.47 x 10^{11} TU.

Figure 22 shows the projected processing times and recovered functional yields to highlight the advantages of a semi-continuous process. Comparing Cases II and III, implementing just the downstream in a semi-continuous mode increases the functional yield by 1.6-fold while reducing 5.5 days in the manufacturing plant. Comparing Cases I and III, implementing an integrated semi-continuous process increases the functional yield by 1.5-fold while reducing 71.75 days in the manufacturing plant.

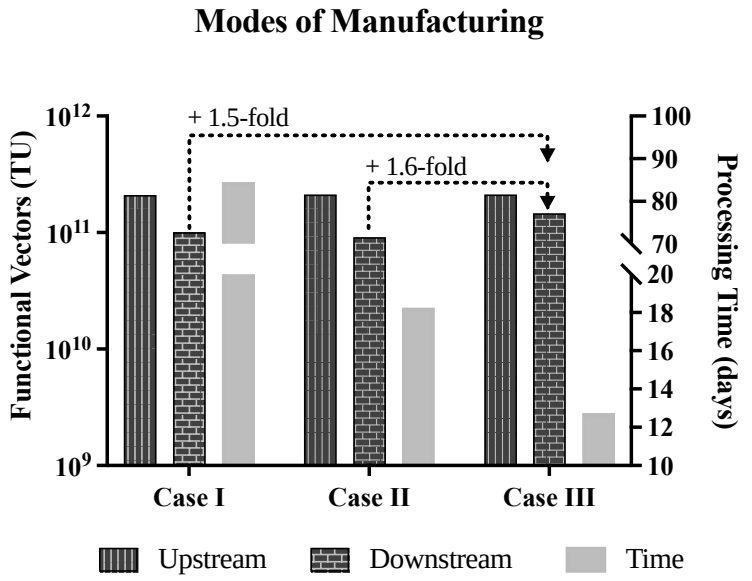

Figure 22: Comparison of projected processing times and functional recoveries for batch versus semi-continuous manufacturing. Case I = batch upstream + batch downstream. Case II = perfusion upstream + batch downstream. Case III = perfusion upstream + semi-continuous downstream; representative of an integrated semi-continuous manufacturing process. Upstream refers to LV production in cell culture. Downstream refers to nuclease treatment, clarification, and Mustang Q capture step; batch refers to each of these steps implemented in series; semi-continuous refers to these steps implemented in parallel, as described in Section 2.3. Total processing time for Case I repeated 13 times is assumed to produce the same amount of functional vectors as compared to Cases II and III is 84.5 days. Total processing time for Case II is 18.25 days and Case III is 12.75 days.

3. Discussion

With an increasing number of successful clinical trials utilizing LVs for cell and gene therapy treatments for various conditions, an integrated manufacturing process that connects the upstream to the downstream has become more frequently discussed in the field. Integrated continuous manufacturing is a powerful strategy that has the potential to address the persisting challenges of producing a sufficient amount of LVs at manufacturing scale to support treatments for patients as well as addressing the innately labile nature of LVs. In attempting to establish an integrated continuous process for LV production that has the capability to be implemented at manufacturing scale, the work was broken into two parts. First, a scalable technology that can be used as a cell retention device that does not retain the product in perfusion mode for LV production using a stable producer cell line was demonstrated in a recently published work (Tran and Kamen, 2022). Second, implementing the downstream process in a semi-continuous mode and then demonstrating the integration of the upstream and downstream, as discussed in this manuscript.

In the development of the Mustang Q capture step (Figures 15, 16), results show high step recoveries of functional vectors (represented by transducing units, TU) and total vectors (represented by vector genome units, Vg) at the higher tested loading (7 MV/min) and general (10 MV/min) flowrates. Results also show high DNA and protein clearance in the flowthrough, confirming that Mustang Q is an efficient capture step for LVs. Operating at high flowrates expedites the processing time, which poses as an asset at manufacturing scale, and doing so without compromising on product integrity is advantageous when purifying an unstable product. Further optimizing the Mustang Q capture step can potentially improve product recovery and quality.

In comparing Mustang Q purified LV with Sucrose Cushion (SC) ultra-centrifuged LV, better product recovery and quality are observed for the former – higher TU and Vg recoveries, lower Vg/TU ratio which indicating higher potency, and lower DNA and protein concentrations (Figure 17). Mustang Q has higher throughput due to its ability to process large harvest volumes and ease of operation, whereas SC is limiting in processing volume and more time-consuming to operate. In contrast, SC offers a concentration factor, whereas Mustang Q does not. Additionally, LVs are typically eluted in high salt from the Mustang Q membrane and an immediate dilution is necessary, further increasing the elution volume. Ultimately, even with the implication of having to process more volume in the following downstream steps, there are clear advantages to utilizing the Mustang Q for purification, especially for its scalability, making it a promising candidate to be used in large-scale manufacturing.

The load amount of 100 MV was selected due to high step and cumulative recoveries of TU and Vg (Figure 16). Fortuitously, the load time for 100 MV on the Mustang Q membrane lines up well with the time for the purification steps on the AKTA, allowing the two systems to run in parallel (Figure 18). Combining the clarification and loading of the capture step as well as operating those steps in parallel to the purification of the capture step expedited the processing time, reducing it by 4-fold as compared to processing the same volume in batch mode, where each unit operation is completed before moving onto the next step.

In addition to the time saved from running the downstream process in semi-continuous mode, improvement in product recovery is observed, with a 26% increase in the recovery of functional vectors and 18% increase in the recovery of total vectors (Figure 19A), and a lower Vg/TU ratio indicating higher potency (Figure 19C). These results show higher LV product quality for the semi-continuous process and suggest an added benefit in loading the membranes in series. There is a possibility of further improving the product quality by optimizing the nuclease treatment and clarification steps. For example, temperature and duration can be optimized for the nuclease treatment, and the depth filtration step might be further assessed for improved performance.

An additional characterization of the ISC LV (i.e., LVs manufactured by the integrated semi-continuous process) was implemented to assess product quality. The functionality of LVs is defined as their ability to transduce host cells to effectively deliver genetic material to be integrated in the host cell genome. Given that the transgene of the LVs in this work is GFP, it is possible to qualitatively assess the functionality in terms of GFP expression using confocal microscopy (Figure 20A). These results indicate the potential of leveraging imaging techniques as additional analytical tools for assessing the quality of LVs. For example, a validation assay to assess transduction effectiveness for LVs used in *ex vivo* applications.

In investigating the effect of process hold times, results show that perfusion LV harvest held at 4^{o}C for 6 days versus 1 day decreases the TU recovery by 9% and the Vg recovery by 10% (Figure 19B) and increases the Vg/TU ratio indicating lower potency (Figure 19C). These results support the implication that reducing process hold times can help in maintaining a higher number of the produced functional vectors. Thus, highlighting the relevance of integrating a continuous upstream process (i.e., perfusion) that increases LV productivity and a semi-continuous downstream process that preserves LV quality attributes by reducing both the processing time and processing hold times.

The presented case study demonstrates the feasibility and practicality of an integrated semi-continuous process for LV production and capture using upstream data from a previous publication (Tran and Kamen, 2022) and downstream data from this manuscript to generate projected processing times (Figure 21) and recovered functional yields (Figure 22). The assumption of repeating the batch bioreactor to produce the same amount of functional vectors as in one perfusion bioreactor is used for comparison with precaution. The projected processing time for the batch upstream and batch downstream process (Case I) is an underestimation, since it does not take in account the necessary time for cleaning and set up between batch operations. In addition, the need to operate multiple batch bioreactors increases the risk of contamination.

The case study shows reduced processing time and improved product recovery for both the semi-continuous downstream process (Case II) and the integrated semi-continuous manufacturing (Case III). The integrated semi-continuous process results in the shortest processing time for the highest amount of recovered functional vectors, which has great implications on reducing cost and increasing productivity of the manufacturing plant. Depending on the layout of the manufacturing plant, LVs harvested from the perfusion bioreactor can be processed downstream every 12 h or 24 h, which gives flexibility in operation.

In summary, an integrated semi-continuous process that has the capability to be implemented at manufacturing scale was demonstrated to address two notable challenges of LV production – generating a sufficient quantity for treatments and increasing the vector quality. In combining the perfusion cell culture in the upstream process, which generates a considerably higher amount of LVs and reduces their residence time in the bioreactor, with an expedited semi-continuous downstream process that offers high recovery of the LV product, the integrated semi-continuous process mitigates LV instability and improves product quality by slowing down the loss of functionality of LVs through reduced processing times and process hold times.

4. Materials and Methods

4.1 LV Starting Materials

The LV harvest materials used for the downstream work in this manuscript are previously described in detail (Tran and Kamen, 2022). In brief, LVs containing GFP as the transgene and VSV-G at the membrane surface were produced in batch (1 L bioreactor) and perfusion (3 L bioreactor) modes using a stable producer cell line HEK293SF-LVP-CMVGFPq-92 (Manceur et al., 2017) by inducing with doxycycline and cumate. Both inducers are required for LV production

in this double switch system to ensure tighter transcription regulation, as previously described (Broussau et al., 2008). In batch mode, the producer cells were inoculated at 0.35 x 10^6 cells/mL in Hyclone HyCell TransFx-H media, induced at 1 x 10^6 cells/mL 48 h (hours) after inoculation, and harvested at 3 dpi (days post induction).

In perfusion mode, the Tangential Flow Depth Filtration cartridge with 30 cm^2 surface area was used as the cell retention device. The producer cells were inoculated at 0.35 x 10^6 cells/mL, grown in batch mode until 72 h after inoculation, grown in perfusion mode from 0.5 to 1 VVD (vessel volume per day) until 176 h after inoculation, and then induced at 11.4 x 10^6 cells/mL for run 1 and 12.3 x 10^6 cells/mL for run 2. LVs were continuously harvested at around 1 VVD over 6 days for run 1 and at 2 VVD over 4 days for run 2. Hyclone HyCell TransFx-H media was used for the LV production phase of run 1 while Hyclone HyCell TransFx-H modified SH31192 media was used for the LV production phase of run 2, as well as for the cell growth phase in both perfusion runs.

4.2 Development of the Capture Step

Mustang Q XT Acrodisc Units (Pall Life Sciences) with a membrane volume of 0.86 mL were used for the capture step and an AKTA Avant (GE Healthcare) was used for chromatography purification. Three buffers were used: equilibration (EQ) contains 10 mM Histidine and 0.15 M Sodium Chloride (NaCl), elution A contains 20 mM Tris-HCl with 3% sucrose, and elution B contains 20 mM Tris-HCl and 1.6 M NaCl with 3% sucrose, all at pH 7.5.

The purification steps are as follows: equilibration for 25 membrane volumes (MV) with EQ buffer, LV load (variable, between 100 and 600 MV), wash for 60 MV with EQ buffer, elution 1 for 12 MV using 25% elution buffer B for 0.4 M NaCl, elution 2 for 12 MV using 75% elution buffer B for 1.2 M NaCl, and strip for 25 MV using 100% elution buffer B. Elution 2 fraction was immediately diluted with EQ buffer to achieve a lower salt concentration of 0.4 M NaCl. In this work, the combined elution fractions represent the Mustang Q elution.

The loading flowrate (2.5 MV/min vs. 7 MV/min) and general flowrate (2.5 MV/min vs. 10 MV/min) were tested in establishing Mustang Q run conditions. For the rest of the downstream work, the flowrates used were 7 MV/min for loading and 10 MV/min for the rest of the purification steps. The conversions from MV/min to mL/min are as follows: 2.5 MV/min = 2.15 mL/min, 7 MV/min = 6.02 mL/min, 10 MV/min = 8.60 mL/min. This work reports in the units of MV and MV/min.

4.3 Downstream Steps in Batch Mode

The LV materials from the perfusion bioreactor runs were processed by nuclease treatment using 50 U/mL Benzonase (MilliPore Sigma) and 2 mM $MgCl_2$ at 24ºC with 135 RPM shaking speed for 30 min, followed by clarification through a 0.45 µm syringe filter (MilliPore Sigma), and then purification on the AKTA for the Mustang Q capture step.

The LV materials from the batch bioreactor runs were previously treated with 20 U/mL Benzonase and 2 mM $MgCl_2$ at 27ºC for 60 min with 110 RPM mixing before harvesting by centrifuging at 2000 g for 15 min. Therefore, after thawing, these materials were clarified using a 0.45 µm syringe filter and then purified on the AKTA.

4.4 Downstream Steps in Semi-Continuous Mode

Two systems were used in the semi-continuous downstream set up. In system 1, nuclease treated material was pumped through a MD0HC23CL3 depth filter (Millipore Sigma) before being directly loaded onto 2 Mustang Q membranes, MA + MB, connected in series. Once MA was loaded to the targeted 86 mL, it was removed from system 1 and transferred to system 2 (the AKTA), and MC was then connected in series after MB. While the clarification and loading processes continued in system 1 for MB + MC, MA was subjected to wash, elution, and regeneration steps (i.e., strip, then EQ) in system 2. Then, MB was transferred to system 2 for purification and MA was re-transferred to system 1 behind MC. These steps were repeated until all three membranes went through two cycles each, totaling 516 mL of LV starting material.

Before commencing the semi-continuous operation, the depth filter was first flushed with milli-Q water and then with EQ buffer using the peristaltic pump in system 1, and the 3 Mustang Q membranes were equilibrated with EQ buffer using the AKTA in system 2.

4.5 Concentration of LVs by Ultracentrifugation in 25% Sucrose Cushion

LV harvest material from the batch bioreactor run was thawed, passed through a 0.45 µm filter, then 32.4 mL was pipetted into a polypropylene tube, followed by 3.6 mL underly of 25% sucrose cushion solution (25% sucrose in 20 mM Tris-HCl, pH 7.5). The sample was centrifuged at 37,000 x g (26,000 RPM) for 3 hours at 4ºC, using the Optima L-90K Ultracentrifuge (Beckman Coulter) with maximum acceleration and deceleration. The supernatant was discarded by pouring out slowly without disturbing the pellet. The tube was left upside down on to rest on a Kimwipe for 10 min to dry. Once dried, 324 µL of 20 mM Tris-HCl with 5% sucrose and 2 mM $MgCl_2$

solution at pH 7.5 was added for a 100x concentration factor, ensuring that the pellet was covered completely by the solution. The suspension was kept overnight at 4°C and then frozen before analytics. The SWTI-32 rotor (Beckman Coulter) and polypropylene tube (Beckman Coulter) were cooled in 4°C the night prior to sample loading and centrifugation.

4.6 Gene Transfer Assay for Functional LV Quantification

A flow cytometry-based gene transfer assay was used to determine functional vector titer in transducing units per milliliter (TU/mL), as previously described in detail (Tran and Kamen, 2022). In brief, suspension HEK293SF cells were inoculated in 24-well suspension plates at 0.5 x 10^6 cells/mL in HyCell TransFx-H media, supplemented with 8 ng/µL final concentration of polybrene, and transduced with 50 µL neat or diluted LV samples for a final of 500 µL per well. After 72 h of incubation at 37°C and 135 RPM shaking speed, the transduced cells were pelleted, fixed with 2% paraformaldehyde in 1x phosphate buffered saline (PBS) for 30 min, and re-suspended in 1x PBS before reading for GFP expression on the flow cytometer. The titer in TU/mL was calculated using the following equation: (GFP percentage) / 100 x total cells x dilution factor x 1000 / (volume of LVs). Downstream samples were filtered using a 0.45 µm filter and 1% Penicillin-Streptomycin was added to their respective wells to avoid contamination.

4.7 Droplet Digital Polymerase Chain Reaction Assay for Total LV Quantification

A QX200™ Droplet Digital PCR (ddPCR) system was used to determine total vector titer in vector genome units per milliliter (Vg/mL), as previously described in detail (Tran and Kamen, 2022). In brief, RNA content was extracted from LV samples and 10 ng RNA was reverse transcribed into cDNA before running the samples on the ddPCR system. Each PCR reaction contained EvaGreen Supermix, woodchuck hepatitis virus posttranscriptional regulatory element primer set, milli-Q water, and neat or diluted cDNA samples. The PCR reactions went through droplet generation, amplification in a thermo-cycler, and analysis by the droplet reader.

4.8 Picogreen Assay for DNA Quantification

The Quant-iT PicoGreen dsDNA Assay kit (Invitrogen) was used to quantify DNA in LV samples, as previously described in detail (Tran and Kamen, 2022).

4.9 RC DC Assay for Protein Quantification

The RC DC Protein Assay Kit (Bio-Rad) was used to quantify protein content in LV samples, following the manufacturer's protocol.

4.10 Confocal Microscopy

HEK293SF cells were plated onto 35mm coverglass bottom dishes (MatTek) and 24 h later were either transduced with LVs manufactured by the integrated semi-continuous process, LV supernatant produced in a shake flask, or non-induced Clone 92 cell supernatant serving as the negative control at MOI of 1. Just prior to imaging, the cells were stained with Deep Red CellMask plasma membrane stain (Invitrogen). Dishes were placed onto the stage of a IX83-DSU Olympus microscope and maintained at 37°C and 5% CO_2 in a stage-top incubator. The labelling of the cell membrane was performed as per the manufacturer's instructions. All images were acquired at 100X (oil immersion) UPLANO objectives with 1000-ms exposure uniformly for all image acquisition using the Metamorph Advanced Olympus software. The acquired images were post-processed using ImageJ FIJI v1.53. The built-in fluorescence intensity per unit area plugins were used for all the analysis.

Acknowledgements

M.Y.T. is financially supported by a fellowship from the Faculty of Engineering at McGill University and a doctoral scholarship from Fonds de recherche - Nature et technologies Québec (FRQNT); A.A.K. is partially funded through Canada Research Chair CRC-2021-00032.

Author Contributions

Conceptualization, M.Y.T. and A.A.K.; Methodology, M.Y.T.; Execution, M.Y.T., S.D., and Z.Y.; Writing – Original Draft, M.Y.T.; Writing – Review & Editing, M.Y.T. and A.A.K.; Funding Acquisition & Resources, A.A.K.

Conflicts of Interest

The authors declare that the research was conducted in the absence of any commercial or financial relationships that could be construed as a potential conflict of interest.

References

Ansorge, S., Henry, O., and Kamen, A. (2010). Recent Progress in Lentiviral Vector Mass Production. *Biochemical Engineering Journal*, *48*(3), 362-377. https://doi.org/10.1016/j.bej.2009.10.017

Ansorge, S., Lanthier, S., Transfiguracion, J., Durocher, Y., Henry, O., and Kamen, A. (2009). Development of a Scalable Process for High-Yield Lentiviral Vector Production by Transient Transfection of HEK293 Suspension Cultures. *Journal of Gene Medicine*, *11*(10), 868-876. https://doi.org/10.1002/jgm.1370

Broussau, S., Jabbour, N., Lachapelle, G., Durocher, Y., Tom, R., Transfiguracion, J., et al. (2008). Inducible Packaging Cells for Large-Scale Production of Lentiviral Vectors in Serum-free Suspension Culture. *Molecular Therapy*, *16*(3), 500-507. https://doi.org/10.1038/sj.mt.6300383

Croughan, M. S., Konstantinov, K. B., and Cooney, C. (2015). The future of industrial bioprocessing: batch or continuous? *Biotechnology and Bioengineering*, *112*(4), 648-651. http://dx.doi.org/10.1002/bit.25529

Escors, D., Breckpot, K., Arce, F., Kochan, G., and Stephenson, H. (2012). Lentiviral Vectors and Gene Therapy. *Springer*. https://doi.org/10.1007/978-3-0348-0402-8

Godawat, R., Konstantinov, K., Rohani, M., and Warikoo, V. (2015). End-to-end integrated fully continuous production of recombinant monoclonal antibodies. *Journal of Biotechnology*, *213*(suppl C), 13-19. http://dx.doi.org/10.1016/j.jbiotec.2015.06.393

Gutiérrez-Granados, S., Gòdia, F., and Cervera, L. (2018). Continuous Manufacturing of Viral Particles. *Current Opinion in Chemical Engineering*, *22*, 107-114. https://doi.org/10.1016/j.coche.2018.09.009

Konstantinov, K., and Cooney, C. (2015). White Paper on Continuous Bioprocessing May 20-21, 2014, Continuous Manufacturing Symposium. *Journal of Pharmaceutical Sciences*, *104*(3), 813-820. https://doi.org/10.1002/jps.24268

Manceur, A. P., Kim, H., Misic, V., Andreev, N., Dorion-Thibaudeau, J., Lanthier, S., et al. (2017). Scalable Lentiviral Vector Production Using Stable HEK293SF Producer Cell Lines. *Human Gene Therapy Methods*, *28*(6), 330-339. https://doi.org/10.1089/hgtb.2017.086

Martínez-Molina, E., Chocarro-Wrona, C., Martínez-Moreno, D., Marchal, J. A., and Boulaiz, H. (2020). Large-Scale Production of Lentiviral Vectors: Current Perspectives and Challenges. *Pharmaceutics*, *12*(11), 1051. https://doi.org/10.3390/pharmaceutics12111051

McCarron, A., Donnelley, M., McIntyre, C., and Parsons, D. (2016). Challenges of Up-Scaling

Lentivirus Production and Processing. *Journal of Biotechnology, 240*, 23-30. https://doi.org/10.1016/j.jbiotec.2016.10.016

Mendes, J. P., Bergman, M., Solbrand, A., Peixoto, C., Carrondo, M. J. T., and Silva, R. J. S. (2022). Continuous Affinity Purification of Adeno-Associated Virus Using Periodic Counter-Current Chromatography. *Pharmaceutics*, *14*(7), 1346. http://dx.doi.org/10.3390/pharmaceutics14071346

Merten, O.-W., Hebben, M., and Bovolenta, C. (2016). Production of Lentiviral Vectors. *Molecular Therapy – Methods & Clinical Development, 3*, 16017. https://doi.org/10.1038/mtm.2016.17

Milone, M. C., and O'Doherty, U. (2018). Clinical Use of Lentiviral Vectors. *Leukemia, 32*(7), 1529-1541. https://doi.org/10.1038/s41375-018-0106-0

Moleirinho, M. G., Silva, R. J. S., Alves, P. M., Carrondo, M. J. T., and Peixoto, C. (2020). Current Challenges in Biotherapeutic Particles Manufacturing. *Expert Opinion on Biological Therapy*, *20*(5), 451-465. https://doi.org/10.1080/14712598.2020.1693541

Moreira, A. S., Faria, T. Q., Oliveira, J. G., Kavara, A., Schofield, M., Sanderson, T., Peixoto, C., et al. (2021). Enhancing the purification of Lentiviral vectors for clinical applications. *Separation and Purification Technology, 274*. http://dx.doi.org/10.1016/j.seppur.2021.118598

Naldini, L., Trono, D., and Verma, I. M. (2016). Lentiviral Vectors, Two Decades Later. *Science, 353*(6304), 1101-1102. https://doi.org/10.1126/science.aah6192

Silva, R. J. S., Mendes, J. P., Carrondo, M. J. T., Marques, P. M., and Peixoto, C. (2020). Continuous Chromatography Purification of Virus-Based Biopharmaceuticals: A Shortcut Design Method. *Animal Cell Biotechnology: Methods in Molecular Biology*, chapter 21, 367-384. New York, NY: Springer US. http://dx.doi.org/10.1007/978-1-0716-0191-4_21

Tinch, S., Szczur, K., Swaney, W., Reeves, L., and Witting, S. R. (2019). A scalable lentiviral vector production and purification method using mustang Q chromatography and tangential flow filtration. *Viral Vectors for Gene Therapy: Methods in Molecular Biology*, chapter 8, 135-153. Springer. http://dx.doi.org/10.1007/978-1-4939-9065-8_8

Tran, M. Y., and Kamen, A. A. (2022). Production of Lentiviral Vectors Using a HEK-293 Producer Cell Line and Advanced Perfusion Processing. *Frontiers in Bioengineering and Biotechnology*, 10. http://dx.doi.org/10.3389/fbioe.2022.887716

Transfiguracion, J., Tran, M. Y., Lanthier, S., Tremblay, S., Coulombe, N., Acchione, M., et al. (2020). Rapid In-Process Monitoring of Lentiviral Vector Particles by High-Performance

Liquid Chromatography. *Molecular Therapy – Methods & Clinical Development*, *18*, 803-810. https://doi.org/10.1016/j.omtm.2020.08.005

Walther, J., Godawat, R., Hwang, C., Abe, Y., Sinclair, A., and Konstantinov, K. (2015). The business impact of an integrated continuous biomanufacturing platform for recombinant protein production. *Journal of Biotechnology*, *213*, 3-12. http://dx.doi.org/10.1016/j.jbiotec.2015.05.010

Zydney, A. L. (2015). Perspectives on integrated continuous bioprocessing – opportunities and challenges. *Current Opinion in Chemical Engineering*, *10*, 8-13. http://dx.doi.org/10.1016/j.coche.2015.07.005

Chapter 6: General Discussion

The work presented in this thesis has contributed to the field of LV production for cell and gene therapy, specifically to be used in the *ex vivo* transduction of T-cells for expression of chimeric antigen receptor in CAR-T cell therapies for cancer treatment, and it has the potential to be applied towards LVs used in *in vivo* applications. The main goals of this thesis are to increase the LV product yield to support the treatment of patients beyond early phase clinical trials and improving the LV functional yield by mitigating their instability throughout the production process, with the underlying context of large-scale manufacturing. As such, the work was conducted with the perspective of investigating practical and scalable methods that can be implemented in the industry-scale manufacturing. To support my investigations, I also contributed to optimizing analytical methods for making the quality assessment of LVs.

The hypothesis of my thesis is that an integrated semi-continuous manufacturing process can increase LV production and improve functional yield for LVs by slowing down the loss of functionality that is typically caused during processing times and process hold times of the production and purification processes. To achieve this, first I implemented the process intensification of the upstream process (Chapter 4), then I implemented the downstream process in a semi-continuous mode (Chapter 5), and finally demonstrated the integration of the upstream to the downstream in a semi-continuous manner (Chapter 5).

In the case of LVs, the reference to the continuous nature in terms of integrating the upstream and downstream steps depicts the desire to retrieve the LV product as soon as it is released in the supernatant, rather than letting the LV product accumulate over time prior to harvesting. Since LVs are unstable with a short half-life at 37^{o}C that is typical of their cell culture environment, continuously harvesting LVs reduces the residence time in the bioreactor, which limits the loss of functionality. In addition, since LVs have a high sensitivity to environmental pH, salt concentration, and shear stress during downstream processing, reducing the downstream processing time to 1 day instead of 3-4 days can limit loss of functionality.

The Clone 92 stable producer cell line was chosen as the production method since producer cells have the potential to generate more consistent harvest titers and higher quality material, with lower running costs and simpler downstream steps due to the elimination of DNA plasmids as required in transient transfection. In terms of the duration of LV production, a similarity was observed between the inducible stable producer cell line method and the transient transfection

method due to the detrimental effect of LVs budding out of the producer cells and the cytotoxicity effects from viral components (Comisel et al., 2021). Even though the Clone 92 producer cell line is under a double switch inducible system, which provides a tighter transcription regulation by expressing viral proteins only at the time of LV production, cell viability dropped from 86.4% at 72 hpi (hours post induction) to 62.5% at 96 hpi for perfusion run 1 and from 87.8% to 73.3% for perfusion run 2, as shown in Figure 13A.

In addition, the vector kinetics graph in Figure 13B shows that the functional vector titer drops as the production process continues, whereas the total vector titer maintains the same level. The lowest ratio of total vector particles to total functional parties in the two perfusion runs were between 24 and 75 hpi, which is in line with previous reports that claimed 48 hpi to 72 hpi as the typical and ideal harvest times since longer incubation times lead to a significant decrease in LV functionality (Logan et al., 2004). Even though this is the case, the work in Chapter 4 shows value in implementing a short perfusion process. For example, running a perfusion cell culture for just 3 days can surpass the productivity of a batch cell culture. Comparing the pooled material up to 72 hpi between perfusion and batch processes shows much higher product yield and improved product quality in the perfusion process. Looking at the cumulative yield at 72 hpi, there is a 52-fold increase for the TFP (batch: average of 5.41×10^9 TFP, perfusion: average 2.79×10^{11} TFP) and 13-fold increase for the TVP (batch: average of 3.54×10^{11} TFP, perfusion: average 4.55×10^{12} TFP). Normalizing the cumulative yields per 1 L of harvest at 72 hpi shows an 8-fold increase for the functional vector particles (batch: average 6.3×10^9 TU/L, perfusion: average 5.1×10^{10} TU/L) and 3-fold increase for the total vector particles (batch: average 4.5×10^{11} Vg/L, average 1.4×10^{12} Vg/L).

The investigation of the TFDF technology resulted in demonstrating its effectiveness to be used as a cell retention device in perfusion mode. Figure 13C demonstrates the TFDF performance in two perfusion runs, showing that the device allows for full recovery of the LV product, which is a significant contribution to the field since existing commercial cell retention devices tend to retain enveloped viruses or they are not scalable. Another benefit to using the Clone 92 stable producer cell line is the ability to make direct comparisons with previously published work using the same cell line with the acoustic filter, further highlighting the potential of the TFDF as a cell retention device.

There are more improvements that can be implemented for the current upstream process with the TFDF as the cell retention device in perfusion mode. An important area of investigation

is the cell health and metabolism during the cell growth and LV production stages. To make a bigger impact on the product yield and quality, it would be worthwhile to look closely at the LV producing cell line and testing additional feeding strategies such as lipid supplementation in order to cater to the specific needs of each cell line for a particular transgene, especially since it is investigated and discussed in the literature that the difference in transgene can have an effect on the production and purification processes.

Following the upstream work, the Mustang Q was established as the capture step and implemented in a semi-continuous mode with the nuclease treatment and clarification step. The Mustang Q membrane was chosen for its scalability, as membrane chromatography are 20 to 50 times faster than conventional chromatography sorbents. The comparison between Mustang Q purified LV and sucrose cushion ultracentrifugation (Figure 17) shows that better LV product quality for the Mustang Q, in terms of percent recovery of TU and Vg as well as the ratio of Vg/TU. The Mustang Q has been tested by a few other groups and have also shown positive data (Moreira, Faria et al., 2021; Tinch et al., 2019), making it a promising candidate to be used in large-scale manufacturing.

In addition to the time saved from running the process in semi-continuous mode as opposed to in batch mode, there was an improvement in the recoveries of the functional vector particles and the total vector particles (Figure 19) for the semi-continuous downstream process, which shows an added benefit in loading the Mustang Q membrane in series. This is in support of my overall hypothesis for the thesis, since there is an improvement in the recovery of functional yield. In comparing the hold time of the LV harvest at 4^{o}C, the data shows a benefit in processing the material quickly, which can be achieved by implementing the integrated semi-continuous method with the perfusion culture. This is also in support of my overall hypothesis for the thesis, since there is an improvement in the recovery of functional yield in reducing the process hold time.

The three cases presented in Chapter 5 showed improved processing time (Figure 21) and improved product recovery (Figure 22) and for both the semi-continuous downstream process and the integrated semi-continuous manufacturing, which has great implications on cost and productivity of the manufacturing plant. The processing time can further be shortened by optimizing the upstream process, such as inoculating the bioreactor with higher cell density or improving feeding strategies that can promote better cell health during the growth phase and the LV production phase.

The comparison of modes of manufacturing (Figure 22) contributes to the overall hypothesis for the thesis. The functional yield for the integrated semi-continuous process is the highest out of three cases, since the percent recovery for LV harvest from perfusion run purified over the Mustang Q membrane in a semi-continuous mode show the highest cumulative yield of 69% TU, as compared to 43% TU for perfusion upstream material being processed downstream in batch mode and 48% for batch upstream material being processed downstream in batch mode. The total processing time is reduced by 66.25 days in implementing only the upstream in a continuous mode (i.e., perfusion culture) and reduced by 71.75 days in implementing the integrated semi-continuous mode. Implementing just the downstream in semi-continuous mode reduces the processing time by 5.5 days. The calculations and the assumptions made were explained in the results section of Chapter 5.

Until other limitations have been addressed, such as hardware and software integration, the direct link between the bioreactor and the capture step cannot be made. However, by showing a proof-of-concept for the workflow in a semi-continuous manner, I was able to investigate whether implementing such strategy would be successful in maintaining the LV functionality of LVs produced in the bioreactor in perfusion mode. Ultimately, the work in this thesis shows that there is an advantage to implementing an integrated semi-continuous manufacturing process for LV production.

The main analytical methods used for characterization of the work presented in both Chapter 4 and Chapter 5 are to quantify the functional vector titer and total vector titer since potency is the aspect of product quality that is necessary to be improved in order to support the overall research hypothesis. In future work, characterization using the p24 ELISA to measure total particles can be a useful additional analytical method to add more information on the potency for the downstream samples. In addition, aggregation of LVs can occur throughout the downstream processing steps, therefore it would also be useful to characterize in future work.

The identity of the LVs produced by this producer cell line has already been characterized in Chapter 3 using SDS-PAGE, western blot, and negative stain electron microscopy (Figure 7). Safety is typically addressed further in the downstream steps and more applicable when the material is assessed to be released for clinical trials. Typically, recombinant competent lentiviruses, adventitious agents, mycoplasma, endotoxin, and sterility are tested to assess the safety of the final LV product (Figure 6).

The purity of the LVs is assessed using the total DNA and total protein quantification. Since the work is on process robustness and looking at the effectiveness of the downstream process, observing the clearance of total protein is sufficient. For a more polished material, it would be useful to use the ELISA for host cell protein quantification. However, in the case of LVs, there may be a challenge since LVs take parts of the cell membrane, thus some of the LVs might be included in the measuring of the host cell protein.

Since LV production by the Clone 92 stable producer cell line is initiated by two inducers, it would be important to check for their removal from the final product. While cumate is non-cytotoxis, doxycycline is an antibiotic of the tetracycline class that can pose an issue for people with tetracycline allergies if traces are present in the final product.

In optimizing analytical methods to support the quality assessment of LVs. The gene transfer assay (GTA), which measures the transgene expression of LVs in transduced host cells to report the functional vector titer, was successfully adapted to and optimized for suspension HEK293SF cells in a 24-well plate format. Building on an assay that traditionally uses adherent cells, the optimization simplified the analytical workload and increased assay throughput. For future work, the assay can be transferred to a 96-well format to further increase assay throughput. For the droplet digital polymerase chain reaction (ddPCR) method that is used to quantify the viral genome in LV samples to report total vector titer, an important observation was made regarding the additional sample preparations of RNA extraction and cDNA synthesis before executing the ddPCR. Through thorough investigation, it was determined that the amount of RNA used in cDNA synthesis has an effect on the viral genome titer obtained from the ddPCR. This important finding led to the establishment of a normalization step to target the same amount of RNA used in cDNA synthesis to minimize assay variability and increase confidence in comparing samples.

Another contribution to optimizing analytical methods is the high-performance liquid chromatography (HPLC) method that measures total vector particles, as discussed in Chapter 3. This method is suitable for all in-process samples from LV supernatants to final purified products, making it ideal for routine in-process monitoring of LV quality and extremely useful in accelerating the development of LV processes. In addition, this HPLC method has the potential to be an in-line monitoring technique that can be implemented at large-scale and eventually support the realization of integrated continuous manufacturing.

Monitoring the LV transduction of HEK293SF cells using a confocal microscopy method demonstrates the possibility of leveraging imaging techniques as additional analytical tools for LV

transduction effectiveness. Microscopy data shows peak GFP signal saturation around 20 hours post transduction. Perhaps it would be possible to shorten the GTA, as currently the transduced cells are harvested at 72 hpt, which would further increase the assay throughput.

Possible work in the future is to monitor the production of LVs from a producer cell line. It has been observed in the field, and also shown in this work, that as the time of LV production proceeds, there is a "loss" of the functional vectors whereas the number of total vectors is maintained (Figure 13B). It has been speculated in the field that as LVs are produced, a big number of them re-infect the cells. However, it is unclear if the LVs are sticking on the cell membrane, re-attaching, or re-entering the cells, as this process is not well characterized. Using microscopy to monitor the LV production process might contribute to shedding light on the mechanism, which can help to elucidate this additional challenge in the production of LVs.

Chapter 7: Summary of Observations and Final Conclusion

Objective 1 of the thesis, which is to *optimize analytical methods to support the quality assessment of LVs*, was fulfilled in three parts. First, two analytical methods were optimized in order to support the quality assessment of LVs obtained from the lab scale experiments of this PhD thesis and the protocols are included in the published manuscript enclosed in Chapter 4 – the gene transfer assay (GTA) that measures the transgene expression of LVs in transduced host cells to report the functional vector titer and the droplet digital polymerase chain reaction (ddPCR) method that is used to quantify the viral genome in LV samples to report total vector titer. Second, a high-performance liquid chromatography (HPLC) method that measures total vector particles was presented in the published manuscript enclosed in Chapter 3, which has the potential to be an in-line monitoring technique that can be implemented at large-scale manufacturing. Third, a confocal microscopy method that qualitatively monitor the LV transduction effectiveness of HEK293SF cells was presented in the submitted manuscript enclosed in Chapter 5, which demonstrates the possibility of leveraging imaging techniques as additional analytical tools for LVs.

Objective 2 of the thesis, which is to *improve LV productivity through process intensification of the upstream process*, was fulfilled by demonstrating a scalable technology that can be used as a cell retention device that does not retain the LV product in perfusion mode for LV production using a stable producer cell line in the published manuscript enclosed in Chapter 4. The work in Chapter 4 demonstrates improved total functional particles as well as total vector particles through the process intensification of the upstream process in perfusion mode.

Objective 3 of the thesis, which is to *improve LV functional yield through integrated semi-continuous manufacturing*, was fulfilled by implementing the downstream process in semi-continuous mode and integrating the upstream to the downstream in Chapter 5. The work shown in Chapter 5 confirms the hypothesis of my thesis, which is that an integrated semi-continuous manufacturing process can increase LV production and improve functional yield for LVs by slowing down the loss of functionality that is typically caused during processing times and process hold times of the production and purification processes.

In conclusion, this Ph.D. thesis builds on analytical tools and establishes process intensification strategies that increase yield and improve product quality, advancing the large-scale manufacturing of LVs intended for gene delivery that can be applied to both *ex vivo* and *in vivo* applications.

References

Ansorge, S., Henry, O., and Kamen, A. (2010). Recent Progress in Lentiviral Vector Mass Production. *Biochemical Engineering Journal, 48*(3), 362-377. https://doi.org/10.1016/j.bej.2009.10.017

Ansorge, S., Lanthier, S., Transfiguracion, J., Durocher, Y., Henry, O., and Kamen, A. (2009). Development of a Scalable Process for High-Yield Lentiviral Vector Production by Transient Transfection of HEK293 Suspension Cultures. *Journal of Gene Medicine, 11*(10), 868-876. https://doi.org/10.1002/jgm.1370

Arabi, F., Mansouri, V., and Ahmadbeigi, N. (2022). Gene therapy clinical trials, where do we go? An overview. *Biomedicine & Pharmacotherapy*, *153*. http://dx.doi.org/10.1016/j.biopha.2022.113324

Bauler, M., Roberts, J. K., Wu, C. C., Fan, B. C., Ferrara, F., Yip, B. H., Throm, R. E., et al. (2020). Production of Lentiviral Vectors Using Suspension Cells Grown in Serum-free Media. *Molecular Therapy – Methods & Clinical Development, 17,* 58-68. http://dx.doi.org/10.1016/j.omtm.2019.11.011

Broussau, S., Jabbour, N., Lachapelle, G., Durocher, Y., Tom, R., Transfiguracion, J., et al. (2008). Inducible Packaging Cells for Large-Scale Production of Lentiviral Vectors in Serum-free Suspension Culture. Molecular Therapy, 16(3), 500-507. https://doi.org/10.1038/sj.mt.6300383

Castella, M., Caballero-Baños, M., Ortiz-Maldonado, V., González-Navarro, E. A., Suñé, G., Antoñana-Vidósola, A., Juan, M., et al. (2020). Point-Of-Care CAR T-Cell Production (ARI-0001) Using a Closed Semi-automatic Bioreactor: Experience from an Academic Phase I Clinical Trial. *Frontiers in Immunology*, *11*. http://dx.doi.org/10.3389/fimmu.2020.00482

Comisel, R. M., Kara, B., Fiesser, F. H., and Farid, S. S. (2021). Lentiviral vector bioprocess economics for cell and gene therapy commercialization. *Biochemical Engineering Journal, 167*. http://dx.doi.org/10.1016/j.bej.2020.107868

Croughan, M. S., Konstantinov, K. B., and Cooney, C. (2015). The future of industrial bioprocessing: batch or continuous? *Biotechnology and Bioengineering, 112*(4), 648-651. http://dx.doi.org/10.1002/bit.25529

Do Minh, A., Star, A. T., Stupak, J., Fulton, K. M., Haqqani, A. S., Gélinas, J.-F., Kamen, A. A., et al. (2021). Characterization of Extracellular Vesicles Secreted in Lentiviral Producing HEK293SF Cell Cultures. *Viruses, 13*(5), 797. http://dx.doi.org/10.3390/v13050797

Escors, D., Breckpot, K., Arce, F., Kochan, G., and Stephenson, H. (2012). Lentiviral Vectors

and Gene Therapy. *Springer*. https://doi.org/10.1007/978-3-0348-0402-8

Greene, M. R., Lockey, T., Mehta, P. K., Kim, Y. S., Eldridge, P. W., Gray, J. T., and Sorrentino, B. P. (2012). Transduction of human CD34+ repopulating cells with a self-inactivating lentiviral vector for SCID-X1 produced at clinical scale by a stable cell line. *Human Gene Therapy Methods, 23*(5), 297–308. http://dx.doi.org/10.1089/hgtb.2012.150

Gutiérrez-Granados, S., Gòdia, F., and Cervera, L. (2018). Continuous Manufacturing of Viral Particles. *Current Opinion in Chemical Engineering, 22,* 107-114. https://doi.org/10.1016/j.coche.2018.09.009

Konstantinov, K., and Cooney, C. (2015). White Paper on Continuous Bioprocessing May 20-21, 2014, Continuous Manufacturing Symposium. *Journal of Pharmaceutical Sciences*, *104*(3), 813-820. https://doi.org/10.1002/jps.24268

Manceur, A. P., Kim, H., Misic, V., Andreev, N., Dorion-Thibaudeau, J., Lanthier, S., et al. (2017). Scalable Lentiviral Vector Production Using Stable HEK293SF Producer Cell Lines. *Human Gene Therapy Methods, 28*(6), 330-339. https://doi.org/10.1089/hgtb.2017.086

McCarron, A., Donnelley, M., McIntyre, C., and Parsons, D. (2016). Challenges of Up-Scaling Lentivirus Production and Processing. *Journal of Biotechnology, 240,* 23-30. https://doi.org/10.1016/j.jbiotec.2016.10.016

Merten, O.-W., Hebben, M., and Bovolenta, C. (2016). Production of Lentiviral Vectors. *Molecular Therapy – Methods & Clinical Development, 3,* 16017. https://doi.org/10.1038/mtm.2016.17

Milone, M. C., and O'Doherty, U. (2018). Clinical Use of Lentiviral Vectors. *Leukemia, 32*(7), 1529-1541. https://doi.org/10.1038/s41375-018-0106-0

Mitchell, R. S., Beitzel, B. F., Schroder, A. R. W., Shinn, P., Chen, H. M., Berry, C. C., Bushman, F. D., et al. (2004). Retroviral DNA integration: ASLV, HIV, and MLV show distinct target site preferences. *PloS Biology, 2*(8), 1127-1137. http://dx.doi.org/10.1371/journal.pbio.0020234

Moreira, A. S., Cavaco, D. G., Faria, T. Q., Alves, P. M., Carrondo, M. J. T., and Peixoto, C. (2021). Advances in Lentivirus Purification. *Biotechnology Journal, 16*(1), e2000019. https://doi.org/10.1002/biot.202000019

Moreira, A. S., Faria, T. Q., Oliveira, J. G., Kavara, A., Schofield, M., Sanderson, T., Peixoto, C., et al. (2021). Enhancing the purification of Lentiviral vectors for clinical applications. *Separation and Purification Technology, 274*. http://dx.doi.org/10.1016/j.seppur.2021.118598

Naldini, L., Trono, D., and Verma, I. M. (2016). Lentiviral Vectors, Two Decades Later.

Science, 353(6304), 1101-1102. https://doi.org/10.1126/science.aah6192

National Cancer Institute. (Last update 01 April 2022, accessed 11 December 2022). *T-Cell Transfer Therapy*. https://www.cancer.gov/about-cancer/treatment/types/immunotherapy/t-cell-transfer-therapy

National Cancer Institute. (Last update 10 March 2022, accessed 11 December 2022). *CAR T Cells: Engineering Patients' Immune Cells to Treat Their Cancers*. https://www.cancer.gov/about-cancer/treatment/research/car-t-cells

OHSU Knight Cancer Institute. (Accessed 11 December 2022). CAR T-Cell Therapy for Cancer. https://www.ohsu.edu/knight-cancer-institute/car-t-cell-therapy-cancer

Petiot, E., Cuperlovic-Culf, M., Shen, C. F., and Kamen, A. (2015). Influence of HEK293 metabolism on the production of viral vectors and vaccine. *Vaccine, 33*(44), 5974-5981. http://dx.doi.org/10.1016/j.vaccine.2015.05.097

Sanber, K. S., Knight, S. B., Stephen, S. L., Bailey, R., Escors, D., Minshull, J., et al. (2015). Construction of Stable Packaging Cell Lines for Clinical Lentiviral Vector Production. *Scientific Reports, 5*, 9021. https://doi.org/10.1038/srep09021

Schweizer, M., and Merten, O. W. (2010). Large-Scale Production Means for the Manufacturing of Lentiviral Vectors. *Current Gene Therapy, 10*(6), 474-486. http://dx.doi.org/10.2174/156652310793797748

Sharon, D., and Kamen, A. (2018). Advancements in the Design and Scalable Production of Viral Gene Transfer Vectors. *Biotechnology and Bioengineering, 115*(1), 25-40. https://doi.org/10.1002/bit.26461

Soldi, M., Sergi, L. S., Unali, G., Kerzel, T., Cuccovillo, I., Capasso, P., Kajaste-Rudnitski, A., et al. (2020). Laboratory-Scale Lentiviral Vector Production and Purification for Enhanced Ex Vivo and In Vivo Genetic Engineering. *Molecular Therapy – Methods & Clinical Development, 19*, 411-425. http://dx.doi.org/10.1016/j.omtm.2020.10.009

Sung, H., Ferlay, J., Siegel, R. L., Laversanne, M., Soerjomataram, I., Jemal, A., and Bray, F. (2021). Global Cancer Statistics 2020: GLOBOCAN Estimates of Incidence and Mortality Worldwide for 36 Cancers in 185 Countries. *CA: A Cancer Journal for Clinicians, 71*(3), 209-249. http://dx.doi.org/10.3322/caac.21660

Suzuki, Y. and Suzuki, Y. (2011). Gene Regulatable Lentiviral Vector System. *Viral Gene Therapy*. IntechOpen. http://dx.doi.org/10.5772/18155

Tapia, F., Vazquez-Ramirez, D., Genzel, Y., and Reichl, U. (2016). Bioreactors for high cell density and continuous multi-stage cultivations: options for process intensification in cell culture-

based viral vaccine production. *Applied Microbiology and Biotechnology, 100*(5), 2121-2132. http://dx.doi.org/10.1007/s00253-015-7267-9

Tinch, S., Szczur, K., Swaney, W., Reeves, L., and Witting, S. R. (2019). A scalable lentiviral vector production and purification method using mustang Q chromatography and tangential flow filtration. *Viral Vectors for Gene Therapy: Methods in Molecular Biology*, chapter 8, 135-153. Springer. http://dx.doi.org/10.1007/978-1-4939-9065-8_8

Tolmachov, O.E., Tolmachova, T., and Al-Allaf, F.A. (2011). Designing lentiviral gene vectors. *Viral Gene Therapy*, 263-284. https://doi.org/10.5772/17361

Walther, J., Godawat, R., Hwang, C., Abe, Y., Sinclair, A., and Konstantinov, K. (2015). The business impact of an integrated continuous biomanufacturing platform for recombinant protein production. *Journal of Biotechnology*, *213*, 3-12. http://dx.doi.org/10.1016/j.jbiotec.2015.05.010

World Health Organization. (03 February 2022, accessed 11 December 2022). *Cancer*. https://www.who.int/news-room/fact-sheets/detail/cancer

Wu, X., Li, Y., Crise, B., and Burgess, S. M. (2003). Transcription start regions in the human genome are favored targets for MLV integration. *Science, 300*(5626), 1749-1751. http://dx.doi.org/10.1126/science.1083413

Zydney, A. L. (2015). Perspectives on integrated continuous bioprocessing – opportunities and challenges. *Current Opinion in Chemical Engineering*, *10*, 8-13. http://dx.doi.org/10.1016/j.coche.2015.07.005

Appendix 1: Optimization of the Gene Transfer Assay

Summary

The gene transfer assay (GTA) is a cell-based analytical method that measures the transgene expression in transduced host cells. In this Ph.D. thesis, the LVs produced by the Clone 92 stable producer cell line contain green fluorescent protein (GFP) as the transgene, which can be easily detected by flow-cytometry. The GFP read-out is used to calculate for the titer of functional vector particles in transducing units per milliliter (TU/mL). Accepted GFP values range between 2-20% fluorescent cells to avoid signal due to super transduction.

Adherent cells are traditionally used for this method; however, adapting the method to suspension cells improved assay throughput by using 5-fold higher cell density for transduction, eliminating the cell attachment and detachment steps, and cutting down on assay preparation and incubation times. The GTA was successfully adapted to and optimized for suspension HEK293SF cells in a 24-well plate format. The detailed protocol can be found in the Materials and Methods section in Chapter 4.

Details

The adherent HEK293A cells were cultured in Dulbecco's modified Eagle's medium (DMEM) containing 5% FBS and 2 mM of L-glutamine. Each well of a 24-well plate was seeded with 1 x 10^5 cells. After leaving the cells adhere to the plate for 5 h, medium was removed. LV samples were serially diluted in DMEM supplemented with 8 µg/mL of polybrene and incubated at 37°C for 30 min. 200 µL of diluted LV sample were then added to the cells for transduction and the plates were incubated overnight at 37°C before adding 800 µL of fresh culture medium in each well the next day. The cells were harvested three days post-transduction (i.e., 48h after medium addition). The suspension HEK293SF cells were seeded in 24-well plates with 5x10^5 cells per well and transduced with neat or diluted LVs. The plates are incubated at 37ºC with shaking speed of 110 RPM for 72 h, then harvested. The protocol for suspension HEK293SF cells eliminates the cell attachment and detachment steps, which cuts down the assay preparation and incubation times significantly.

In starting out, I adapted an existing protocol for adherent cells that used 1% BSA (bovine serum albumin) and 1 mM EDTA (etheylenediaminetetraacetic acid) along with 2%

paraformaldehyde (PFA) in 1x phosphate buffered saline (PBS) for fixing the transduced cells upon harvesting and resuspension. After the first few rounds of experiments testing both adherent HEK293A and suspension HEK293SF cells, I simplified the buffers to 2% paraformaldehyde (PFA) in 1x phosphate buffered saline (PBS) for cell fixing after harvesting the transduced cells and 1x PBS for cell resuspension before reading them on the flow-cytometer. Streamlining the buffers reduced the assay preparation time and it had resolved some cell clumping issues that I observed with the original buffers.

Five different GTA protocols were then tested, altering parameters such as adherent versus suspension cells, treated versus non-treated plates, and the incorporation of spinoculation, a method reported in the literature to improve the transducibility of the LVs. Figure 23 shows comparable results between the five different GTA protocols for three tested samples – LV Control, Benzonase treated LV (abbreviated as Benz LV), and sucrose cushion purified LV (abbreviated as SC LV) – with acceptable percent coefficient of variation (CV) of 12.1%, 10.9%, and 10.8%, respectively. Therefore, the protocol with suspension HEK293SF cells using non-treated plates without the use of spinoculation was selected for future assays since this is the least laborious to implement and has higher throughput.

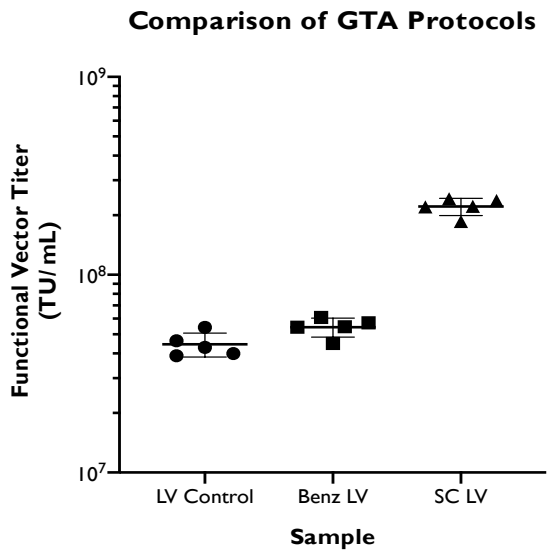

Figure 23: Functional vector particles reported as transducing units per milliliter (TU/mL) measured by five GTA protocols to test different parameters (adherent vs. suspension cells, treated vs. non-treated plates, +/- spinoculation) for three samples – LV Control, Benz LV (Benzonase treated LV), and SC LV (sucrose cushion purified LV).

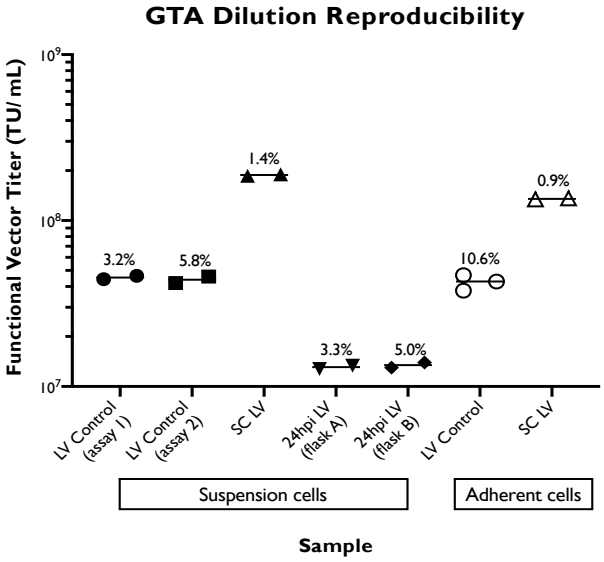

Figure 24: Functional vector particles reported as transducing units per milliliter (TU/mL) measured by the GTA to test varying dilutions of LV samples in the transduction of suspension and adherent cells. Percentages shown represent percent CV between tested dilutions. Samples: LV Control, SC LV (sucrose cushion purified LV), and 24 hpi (hours post induction) LV

To evaluate assay reproducibility for the selected protocol with suspension HEK293SF cells, three samples were tested in varying dilutions – SC LV, 24 hpi (hours post induction) LV (flask A), and 24 hpi LV (flask B). Results show 1.4%, 3.3%, and 5.0% CV, respectively, indicating reproducibility (Figure 24). In addition, the LV Control was tested in varying dilutions on two separate assays and showed 3.2% and 5.8% CV. In comparison, testing the LV control in varying dilutions using adherent cells show 10.6% CV, which indicates higher variability. This can suggest that the protocol using suspension cells is more reproducible. However, given that the GTA assay generally has high variability, perhaps a better conclusion that can be drawn from these data is that the reported functional vector titer for both the LV Control and SC LV samples between the two protocols are comparable. Therefore, this supports the selection of the simpler and higher throughput protocol.

Appendix 2: Optimization of the Droplet Digital Polymerase Chain Reaction Assay

Summary

The droplet digital polymerase chain reaction (ddPCR) assay is a physical-based direct method that quantifies the viral genome in samples. In this Ph.D. thesis, the LVs produced by the Clone 92 stable producer cell line contain the WPRE (woodchuck hepatitis virus posttranscriptional regulatory element) sequence in the transgene. WPRE is commonly included in viral vector design because it is known to stabilize the transgene mRNA and therefore enhance transgene expression delivered by LVs. Consequently, the use of the WPRE primer set (forward 5'-GTC CTT TCC ATG GCT GCT C-3', reverse 5'-CCG AAG GGA CGT AGC AGA-3') detects the presence of the viral genome, which is used to report total vector particles in LV samples.

The ddPCR method is based on water-oil emulsion droplet formation, where a sample is split into 20,000 droplets, and then PCR amplification of the template molecules would occur in each individual droplet. The ddPCR is more robust and has higher throughput than the gold standard PCR since it provides absolute quantification with higher sensitivity, omits the use of a standard, and requires less sample volume.

Although the ddPCR has many advantages over the qPCR method, additional sample preparations before executing the ddPCR pose as sources of variability. Since the LV genome consists of RNA, LV samples must go through RNA extraction and cDNA synthesis before ddPCR. Through experimentation, it was discovered that the total amount of RNA material used in cDNA synthesis has a strange correlation to the vector genome titer obtained from ddPCR. Therefore, it is crucial to normalize the amount of RNA used in the cDNA synthesis step to minimize variability and increase the confidence when making comparisons between samples. The detailed protocol can be found in the Materials and Methods section in Chapter 4.

Details

The ddPCR was quickly established and showed good assay reproducibility. Figure 25 shows that assaying three samples repeatedly in different ddPCR assays resulted in 2.4%, 7.8%, and 4.1% CV (coefficient of variation). In addition, in-house WPRE primers were compared with primers from a collaborator and showed comparable results, which further indicate assay robustness (data not shown).

Taking a closer look, the sample denoted as Extraction 1 in Figure 25 has an average of 1.88 x 10^8 vector genome per milliliter (Vg/mL). For this sample, the workflow included RNA extraction of the LV Control, then 13 µL of the RNA material was used in the cDNA synthesis step, and the same amount of cDNA was used in each of the ddPCR assays. When more cDNA material was needed for additional ddPCR assays, I continued to use 13 µL of the existing RNA material for the cDNA synthesis step. The amount of 13 µL is the maximum volume of RNA material that can be used in the cDNA synthesis, as indicated by the assay kit protocol. An issue was detected when I made another RNA extraction of the LV Control (sample denoted as Extraction 2 (3336 ng RNA) in Figure 25) and obtained an average result of 3.48 x 10^7 Vg/mL, which is 5.4-fold lower than Extraction 1.

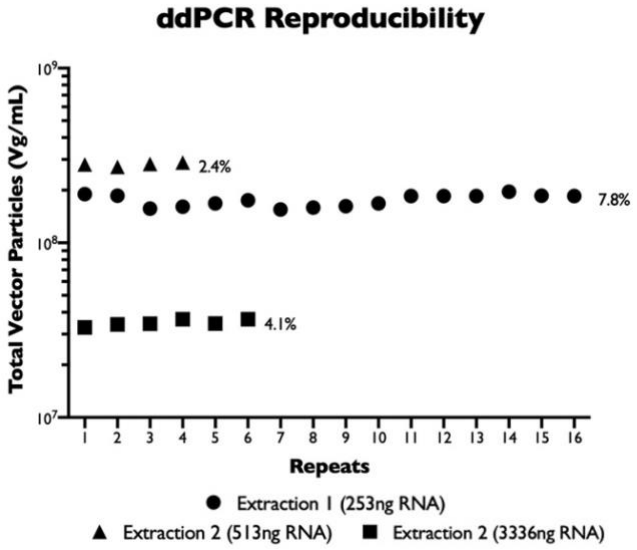

Figure 25: Total vector particles reported as vector genome per milliliter (Vg/mL) measured by ddPCR of an LV Control undergoing two different nucleic acid extractions and using varying total RNA amount in the cDNA synthesis step. Percentages shown represent %CV between ddPCR assays for each sample.

Reading the two RNA samples on the NanoDrop instrument showed 18.1 ng/µL for Extraction 1 and 256.6 ng/µL for Extraction 2. The reason for the big difference can be due to the efficiency of the RNA extraction kit, even though the kit protocol is followed exactly the same every time. Since 13 µL of RNA was used in the cDNA synthesis step, this means 235.3 ng RNA for the Extraction 1 sample and 3335.8 ng RNA for the Extraction 2 sample. A formed hypothesis after observing this was that higher total RNA used in the cDNA synthesis step leads to less efficient cDNA synthesis, thus affecting the viral genome titer. However, when I performed the cDNA synthesis step for the Extraction 2 sample using 2 µL, which is the minimum volume of

RNA material that can be used as indicated by the assay kit protocol, the obtained titer of 2.83 x 10^7 Vg/mL for this sample (denoted as Extraction 2 (513 ng RNA) in Figure 25) did not align with this trend.

Through a lot of experimentation, it was observed that the total amount of RNA material used in cDNA synthesis has a strange correlation to the viral genome titer obtained from ddPCR, as shown in Figure 26. Although the cDNA synthesis kit states that 1 pg to 1 µg of total RNA can be accommodated in the cDNA prep, results show that either extreme give falsely elevated vector genome titer. These results suggest that both low and high ends of the RNA range lead to less efficient cDNA synthesis; however, it is strange that 1 pg total RNA amount would give a falsely elevated Vg/mL similar to 1 µg total RNA. Given that the results show similar titers for RNA extractions for the LV Control using 1E-9 g and 1E-8 g of RNA in the cDNA synthesis step, it is reasonable to target this range for the normalization step. I had chosen to target 10 ng (i.e., 1E-8 g) RNA in the cDNA synthesis step for all my thesis work to ensure that I am making fair comparisons between samples.

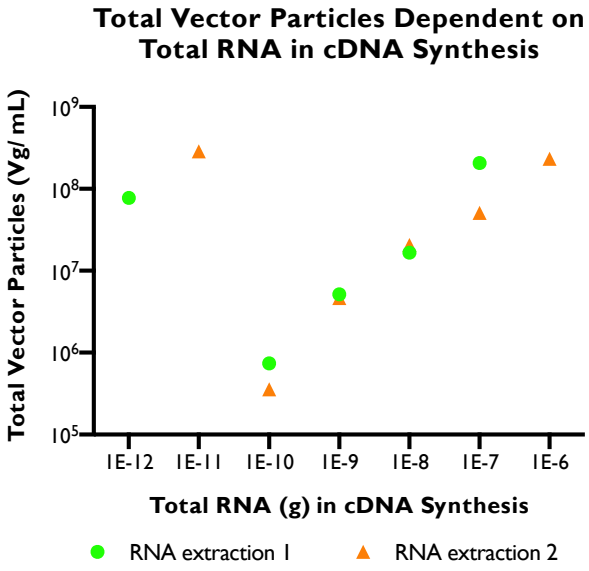

Figure 26: Total vector particles reported as vector genome per milliliter (Vg/mL) measured by ddPCR of an LV control sample undergoing two different nucleic acid extractions to test the effect of varying amounts of total RNA used in the cDNA synthesis step.

In conclusion, the ddPCR assay is reproducible, as suggested by the low % CV values in Figure 25, and reliable as long as the same amount of RNA is used in the cDNA synthesis step prior to ddPCR. Since the RNA extraction step can fail somewhere along the protocol, a verification of the RNA content is helpful in indication a successful extraction.

Appendix 3: Supplemental Information for Chapter 3

Figure S1

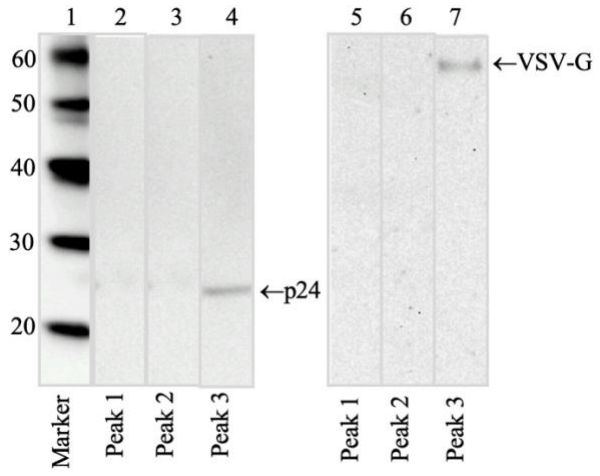

Characterization of HPLC peaks from the in-house LV standard, SC-LV, by western blot against p24 capsid and VSV-G envelope. Lane 1: protein molecular weight markers. Lanes 2, 3, and 4: peaks 1, 2, and 3, respectively, against p24 capsid. Lanes 5, 6, and 7: peaks 1, 2, and 3, respectively, against VSV-G envelope. Peak 3 is the only peak with the presence of p24 capsid and VSV-G envelope bands. Note that peak 4 was not collected and, thus, not analyzed.

Figure S2

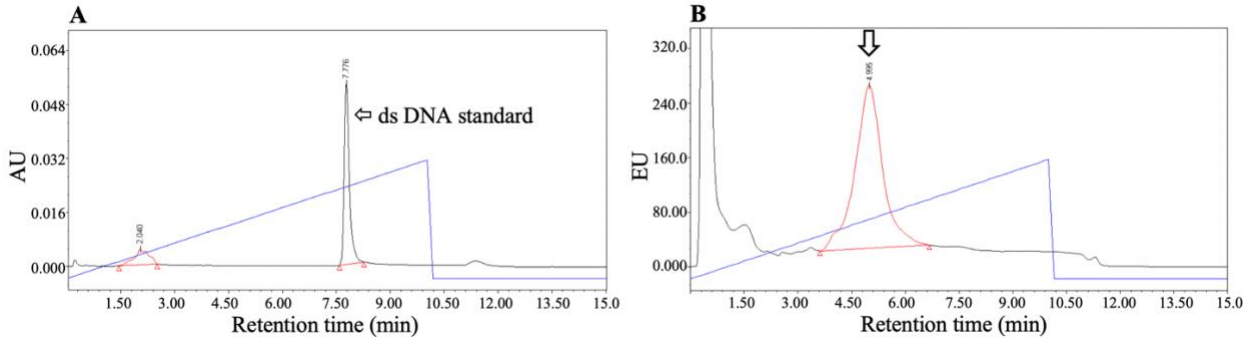

Chromatographic profiles of peaks 4 and 3, respectively, of the in-house LV standard, SC-LV, during HPLC method development. **A)** Double stranded (ds) DNA standard detected by absorbance at 260 nm (OD260). The ds DNA standard was eluted at 777 mM NaCl, which is the same salt elution as peak 4 in Figure 2A. Generally, DNA is strong negatively charged molecules that bind tightly to anion exchange columns and resins, which results in requiring high salt concentrations for elution. The small peak area of peak 4 in Figure 2A suggests that the SC-LV sample has an insignificant presence of residual DNA. **B)** Fluorescence (FL) detection of the SC-LV sample at excitation and emission wavelengths of 290 nm and 335 nm, respectively. The LV peak (indicated by an arrow) corresponds to peak 3 of the OD260 profile in Figure 2A. The FL profile shows a significantly higher LV peak than the OD260 profile; thus, chromatograms monitored by FL were used for the remainder of the HPLC method development.

Figure S3

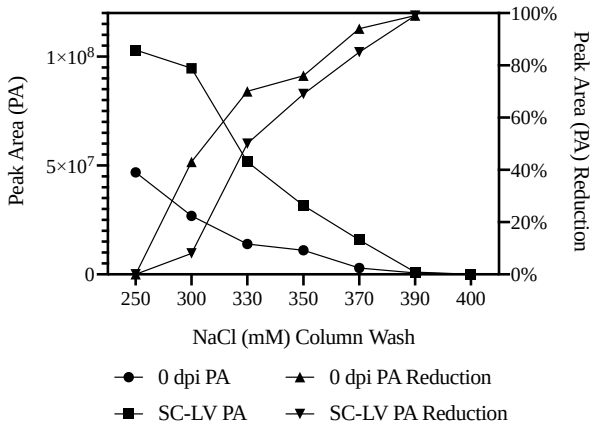

NaCl step gradient column wash, from 250 mM to 400 mM, post sample injection to minimize co-eluting EVs. Figure S3 shows a similar gradual reduction pattern of the peak area (PA) for both SC-LV and 0dpi as the concentration of NaCl column wash post sample injection was increased, with the highest peak area reduction at 370 mM NaCl column wash of 85% for SC-LV and 94% for 0dpi samples.

Figure S4

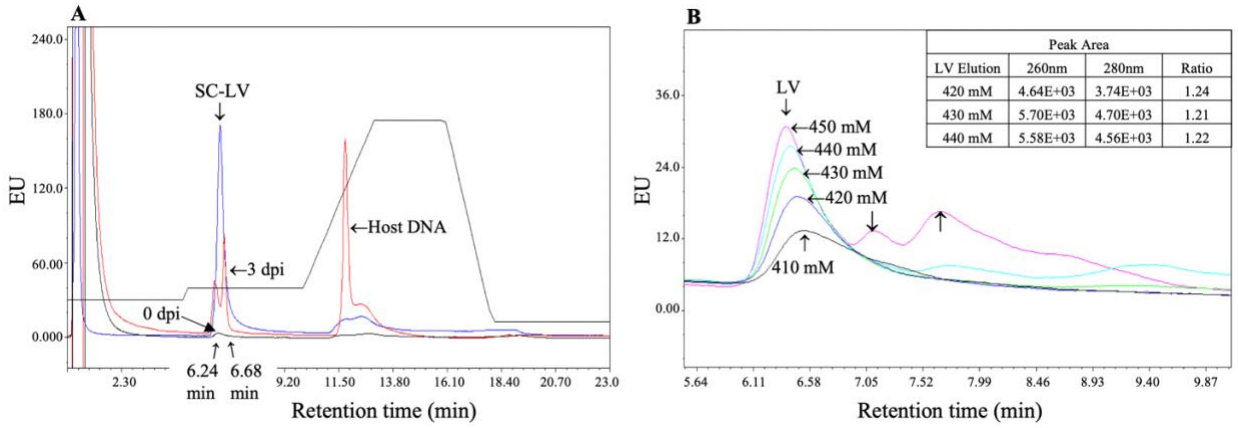

Chromatographic profiles of SC-LV, 3dpi, and 0dpi samples as well as optimization of LV peak elution. **A)** 370 mM NaCl column wash with 500 mM NaCl elution conditions tested on SC-LV, 3dpi, 0dpi samples; chromatogram shows a split peak with retention times of 6.24 min and 6.68 min in the 3dpi sample. **B)** 410 mM to 450 mM NaCl step elution to resolve the split peak found in the LV peak shown in the 3dpi sample in A). Lowering the NaCl gradient elution to 450 mM elution resulted in the appearance of 2 peaks that were eluted later than the original LV peak (indicated by arrows). These 2 peaks gradually disappeared with 440 mM, 430 mM, and 420 mM NaCl. The 410 mM eluted peak was significantly lower than the other eluted peaks and it was assumed that this NaCl concentration was not sufficient to elute all LV particles. The OD260/280 ratio of the 420 mM, 430 mM and 440 mM elutions was determined to be 1.22, 1.21, and 1.24, respectively (inset figure of Figure S4-B). Although the ratios were similar, it was observed that the LV PA at 420 mM and 430 mM elutions was lower than at 440 mM elution. Likewise, it was assumed that not all LV particles were eluted at these concentrations; thus, 440 mM was selected for the NaCl step gradient elution.

Table S1

Sample	RFU
SC-LV	554.8
3dpi	434.7
0dpi	281.6

Acetylcholinesterase activity results for SC-LV, 3dpi, and 0dpi samples. The relative fluorescence units (RFU) is the fluorescence intensity of a thiol probe provided in the assay kit that quantifies the thiocholine produced from the hydrolysis of acetylthiocholine by acetylcholinesterase (AChE) in samples, indicating the presence of EVs. RFU as low as 5 can be detected with 20 minutes of incubation.

Table S2

NaCl Column Wash (mM)	SC-LV Sample			0dpi Sample		
	OD260 PA	OD280 PA	Ratio	OD260 PA	OD280 PA	Ratio
250	1.63E+05	1.50E+05	1.09	2.51E+04	2.96E+04	0.85
300	1.34E+05	1.30E+05	1.03	7.83E+03	1.07E+04	0.73
330	7.44E+04	7.14E+04	1.04	6.35E+03	7.56E+03	0.84
350	4.18E+04	3.82E+04	1.10	3.07E+03	4.22E+03	0.73
370	3.59E+04	2.90E+04	1.24	Not detectable		NA
390	2.19E+04	1.77E+04	1.24	Not detectable		NA
400	Not detectable		NA	Not detectable		NA

Minimization of co-eluting EVs in HPLC method development. For the SC-LV sample, the OD260/280 ratios obtained were similar for 250 mM to 350 mM NaCl washes and increased to 1.24 for 370 mM and 390 mM NaCl washes. Noticeably, for 370 mM and 390 mM NaCl washes, although the OD260/280 ratio did not change, the PA for 390 mM NaCl wash showed a slight reduction as compared to 370 mM NaCl wash with both 260 nm and 280 nm absorbances (results not shown), which is an indication that at the 390 mM NaCl concentration, some of the LV particles were eluted in the flow-through. For 0dpi, the OD260/280 ratios obtained for 250 mM to 350 mM NaCl washes were <1.0 and the peak was no longer detectable from 370 mM to 400 mM NaCl washes. Thus, 370 mM was selected for the NaCl step gradient column wash post sample injection.

Table S3

	Mean LP/mL			
	SC-LV	**UFDF Product**	**Supernatant A**	**Supernatant B**
Tris Buffer	6.69E+09	4.00E+09	1.42E+09	1.90E+09
SFM4Transfx-293	1.18E+09	5.55E+08	5.27E+09	7.41E+09
Increase in Titer	82%	86%	63%	61%

p-24 ELISA method optimization. Four LV samples were diluted in Tris buffer (20 mM Tris-HCl, pH 7.5) and SFM4Transfx-293 medium for comparison. Titers, in LV particle concentration per milliliter (LP/mL), were 82% higher for SC-LV, 86% higher for UFDF Product, 63% higher for Supernatant A, and 61% higher for Supernatant B when using Tris buffer as the diluent as compared to cell culture medium. Thus, Tris buffer was established to be used as the diluent for this assay.

Appendix 4: Supplemental Information for Chapter 4

Table S4: TFP and TVP values for LV production at shake flask scale. TFP = total functional particles; TVP = total vector particles; TU = transducing units; Vg = vector genome; dpi = days post induction; LCD = low cell density; HCD-C = high cell density at the TOI, obtained by one-step concentration; HCD-ME = high cell density at the TOI, obtained by daily medium exchange; pseudo-perfusion = daily medium exchange after induction to mimic perfusion at bioreactor scale; feed = 6 g/L glucose and 3 mM glutamine daily. Parameter evaluation was implemented in single flasks (M1 through M6) to explore different parameters (inducing at HCD, pseudo-perfusion, and feeding) to select the best ones leading to improved yields for LV production using Clone 92 producer cells. Parameter confirmation was implemented in triplicate flasks (M17 through M25) for 3 sets (LCD baseline conditions; HCD-C + pseudo-perfusion + feed; HCD-ME + pseudo-perfusion + feed) to confirm results.

Shake Flask	Parameters	TFP = total functional particles (in transducing units, TU)				TVP = total vector particles (in vector genome copies, Vg)			
		1 dpi	2 dpi	3 dpi	Final product	1 dpi	2 dpi	3 dpi	Final product
A1. Parameter evaluation:									
M1	Baseline conditions: LCD, batch, no feed	1.43×10^{7}	9.97×10^{7}	4.25×10^{8}	5.39×10^{8}	4.36×10^{8}	1.62×10^{10}	1.28×10^{10}	2.94×10^{10}
M2	LCD Pseudo-perfusion	4.88×10^{7}	1.47×10^{9}	1.64×10^{9}	3.31×10^{9}	2.25×10^{9}	4.03×10^{10}	6.94×10^{10}	9.02×10^{10}
M3	HCD-C Feed	3.61×10^{8}	4.05×10^{9}	3.58×10^{9}	7.99×10^{9}	3.41×10^{9}	1.07×10^{11}	3.84×10^{10}	1.49×10^{11}
M4	HCD-ME Feed	5.81×10^{8}	3.53×10^{9}	1.98×10^{9}	6.09×10^{9}	1.75×10^{10}	1.46×10^{11}	5.32×10^{9}	1.69×10^{11}
M5	HCD-ME Pseudo-perfusion	5.21×10^{8}	5.16×10^{9}	3.48×10^{9}	8.91×10^{9}	1.34×10^{10}	1.58×10^{11}	9.72×10^{10}	1.43×10^{11}
M6	HCD-ME Pseudo-perfusion Feed	5.05×10^{8}	1.11×10^{10}	5.52×10^{9}	1.70×10^{10}	1.10×10^{10}	2.73×10^{11}	1.23×10^{11}	3.85×10^{11}
B. Triplicates:									
M17	Baseline conditions: LCD, batch, no feed	1.29×10^{7}	1.89×10^{8}	5.94×10^{8}	7.95×10^{8}	5.86×10^{8}	1.13×10^{10}	3.34×10^{10}	4.52×10^{10}
M18		9.19×10^{6}	1.53×10^{8}	2.77×10^{8}	4.39×10^{8}	6.49×10^{8}	7.58×10^{9}	1.93×10^{10}	2.75×10^{10}
M19		9.85×10^{6}	2.65×10^{8}	4.53×10^{8}	7.28×10^{8}	6.69×10^{8}	1.83×10^{10}	2.51×10^{10}	4.41×10^{10}
average		*1.06×10^{7}*	*2.02×10^{8}*	*4.41×10^{8}*	*6.54×10^{8}*	*6.35×10^{8}*	*1.24×10^{10}*	*2.59×10^{10}*	*3.90×10^{10}*
M20	HCD-C Pseudo-perfusion Feed	1.16×10^{8}	7.89×10^{9}	7.67×10^{9}	1.57×10^{10}	5.11×10^{9}	1.71×10^{11}	5.68×10^{10}	3.00×10^{11}
M21		1.46×10^{8}	8.10×10^{9}	6.49×10^{9}	1.59×10^{10}	6.69×10^{9}	1.44×10^{11}	9.76×10^{10}	2.80×10^{11}
M22		1.41×10^{8}	8.18×10^{9}	5.28×10^{9}	1.39×10^{10}	6.26×10^{9}	1.38×10^{11}	1.23×10^{11}	4.19×10^{11}
average		*1.34×10^{8}*	*8.06×10^{9}*	*6.48×10^{9}*	*1.52×10^{10}*	*6.02×10^{9}*	*1.51×10^{11}*	*9.25×10^{10}*	*3.33×10^{11}*
M23	HCD-ME Pseudo-perfusion Feed	9.47×10^{8}	1.07×10^{10}	4.55×10^{9}	2.10×10^{10}	3.06×10^{10}	1.82×10^{11}	1.47×10^{11}	5.29×10^{11}
M24		1.00×10^{9}	1.13×10^{10}	4.84×10^{9}	1.97×10^{10}	5.19×10^{10}	1.88×10^{11}	1.89×10^{11}	5.16×10^{11}
M25		3.28×10^{8}	5.92×10^{9}	2.84×10^{9}	1.05×10^{10}	1.57×10^{10}	1.71×10^{11}	1.32×10^{11}	3.99×10^{11}
average		*7.58×10^{8}*	*9.29×10^{9}*	*4.08×10^{9}*	*1.71×10^{10}*	*3.27×10^{10}*	*1.80×10^{11}*	*1.56×10^{11}*	*4.81×10^{11}*

Appendix 5: Supplemental Information for Chapter 5

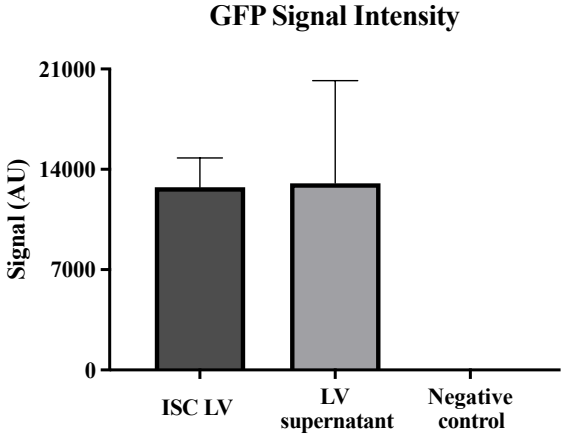

Figure S5: GFP signal intensity for transduced HEK293SF cells. ISC LV refer to LVs manufactured by the integrated semi-continuous process (i.e., LVs produced in perfusion bioreactor and processed downstream in semi-continuous mode); LV supernatant is from a shake flask production; negative control is the supernatant from non-induced Clone 92 cells used to transduce HEK293SF cells; GFP signal is in arbitrary units.